c. 2

THE VERIFICATION OF RELATIONSHIPS FOR EFFECTIVE STRESS METHOD TO EVALUATE LIQUEFACTION POTENTIAL OF SATURATED SANDS

by

SHOBHA K. BHATIA

B.E., University of Roorkee, Roorkee, India, 1971

A THESIS SUBMITTED IN PARTIAL FULFILLMENT OF
THE REQUIREMENTS FOR THE DEGREE OF
DOCTOR OF PHILOSOPHY

in the

Department of Civil Engineering
Faculty of Applied Science

We accept this thesis as conforming to the
required standards

THE UNIVERSITY OF BRITISH COLUMBIA

November 1982

Department of Civil Engineering

The University of British Columbia
1956 Main Mall
Vancouver, Canada
V6T 1Y3

Date 28th November, 1982

THE VERIFICATION OF RELATIONSHIPS FOR EFFECTIVE STRESS METHOD TO EVALUATE LIQUEFACTION POTENTIAL OF SATURATED SANDS

ABSTRACT

The constitutive relationships proposed by Finn, Lee and Martin (1977) for the effective stress analysis of saturated sands during earthquakes are studied. The basic assumptions of their porewater pressure model appears to be well founded. There is a strong verification of a unique relationship between volumetric strain in drained tests and porewater pressures in undrained tests for both normally and overconsolidated sands. An important point to emerge from this study is that the rebound modulus used in converting the volumetric strains to porewater pressures should be measured under dynamic conditions. The porewater pressure model predicts successfully the porewater pressure response under undrained conditions for uniform and irregular cyclic strain and stress histories.

When the porewater pressure model is coupled with a non-linear stress-strain relationship in effective stress analysis, it predicts realistic porewater pressure response in undrained tests for cyclic stress histories representative of earthquake loading. Results suggest that strain-hardening effects do not occur unless the sand is allowed to drain.

A new porewater pressure model based on endochronic theory is presented in which the porewater pressures are directly related to dynamic response parameters. This approach bypasses the need for converting volumetric strains to porewater pressures. The proposed formulation relates porewater pressure to a single monotonically increasing function of a damage parameter. This parameter allows the data from constant strain or stress cyclic loading tests to be applied directly to predict the porewater pressure generated in the field by irregular stress or strain histories due to earthquakes. This formulation is an extremely efficient way of representing a large amount of data and can be easily coupled with dynamic response

analysis to perform effective stress analysis.

This study is based on extensive experimental data on Ottawa sand, crystal silica sand and Toyoura sand. In total, one hundred and fifty tests were performed for this study. The tests were performed under cyclic simple shear conditions using Roscoe type simple shear apparatus. Dry sand was used for both the drained and constant volume tests conducted for this study. The tests were performed under both stress controlled and strain controlled conditions.

W.D. Liam Finn,
Thesis Supervisor.

TABLE OF CONTENTS

PAGE

LIST OF TABLES

LIST OF FIGURES

FIGURE		PAGE

LIST OF PLATES

LIST OF SYMBOLS

a,b,c	=	constants
a,b,c,d,e,τ_d	=	constants used by Bazant and Krizek (1976)
A,B	=	endochronic constants for pore pressure
$\bar{A},\bar{B},\bar{C},\bar{D}$	=	endochronic constants for pore pressure
A_1,A_2,A_3	=	hardening constants
A_1,B_1,C_1,D_1	=	endochronic constants for pore pressure
B_1,B_2,B_3	=	hardening constants
C_1,C_2,C_3,C_4	=	volume change constants
C_b	=	bulk compressibility of soil skeleton
$1/C_c$	=	secant constrained modulus
D_r	=	relative density
e	=	void ratio
de_{ij}	=	deviatoric shear strain
$(\bar{E}_r)_{dynamic}$	=	dynamic rebound modulus
$\bar{E}_\gamma$	=	tangent modulus of the one-dimensional unloading curve
G	=	secant shear modulus
G_{mo}	=	initial shear modulus
G_{mm}	=	maximum shear modulus in n^{th} cycle
H_1,H_2,H_3,H_4	=	hardening constants
Hz	=	cycles per second
k_2,m,n	=	rebound modulus constants
k_o	=	ratio of lateral effective stress to vertical effective stress
k_w	=	bulk modulus of water
$L(\sigma'_{vo}-\sigma')$	=	correction coefficient of Bazant and Krizek (1976)
n	=	porosity

N	=	number of cycles
OCR	=	overconsolidation ratio
p'	=	mean effective normal stress
PI	=	plasticity index
q	=	deviatoric stress
R	=	shape factor
u	=	porewater pressure
Δu	=	incremental pore pressure
u/σ'_{vo}	=	porewater pressure ratio
α	=	constant
γ	=	shear strain
γ_o	=	shear strain amplitude
γ_{max}	=	maximum shear strain
γ^p	=	plastic shear strain
γ_r	=	shear strain at reversal point
ε_{vd}	=	volumetric strain / cummulative volumetric strain
ε_{vro}	=	total recoverable strain due to unloading
ε_{vso}	=	non-recoverable strain due to interparticle slip
$\Delta\varepsilon_{vd}$	=	incremental volumetric strain
$\Delta\varepsilon_{vr}$	=	incremental recoverable strain
ζ	=	densification variable of Cuellar et al (1977)
η	=	distortion variable
$d\eta$	=	incremental length of stress path
κ	=	damage parameter
λ	=	material parameter of Ghaboussi and Dikmen (1978)
λ	=	transformation factor
ξ	=	rearrangement measure or length of strain path

$d\xi$	=	incremental length of strain path
δ_{ij}	=	deviatoric stress
σ'_v	=	vertical effective stress
σ'_{vo}	=	initial vertical effective stress
$\bar{\sigma}_z$	=	effective stress
τ	=	shear stress
τ/σ'_{mo}	=	ratio of cyclic shear stress to initial mean effective stress
τ/σ'_{vo}	=	shear stress ratio
τ_o	=	shear stress amplitude
τ_{hv}	=	shear stress
τ_{mo}	=	maximum shear stress
τ_{mn}	=	maximum shear stress in n^{th} cycle
τ_r	=	shear stress at reversal point
ϕ'	=	effective angle of shearing resistance
∂_w/∂_z	=	constrained strain level

ACKNOWLEDGEMENTS

I wish to record my deepest appreciation of the guidance and encouragement offered by Professor W.D. Liam Finn throughout this research, and to his many helpful suggestions in writing this manuscript. I am also grateful to Dr. P.M. Byrne, Dr. R.G. Campanella and Dr. N.D. Nathan for their encouragement and advice and to Dr. Y.P. Vaid and Dr. M.K. Lee for their generous help and invaluable discussions.

During my studies Mr. Y. Koga and Mr. Bill Deacon took personal interest in my progress and were always ready with their unselfish help. Ms. Desirée Cheung not only typed the manuscript but was a best friend to me in time of need. Ms. Monica Gutierrez showed everlasting patience while drafting the figures.

Mr. Fred Zurkichen and Mr. Wolfram Schmitt from the Civil Engineering workshop provided invaluable assistance with the equipment.

Finally, I would like to express my very special thanks to my husband for his support and constant encouragement.

The financial support by the Canadian Commonwealth Scholarship and Fellowship Committee is acknowledged.

CHAPTER 1

INTRODUCTION

In 1964 a violent earthquake hit Niigata and Yamagata prefectures in Japan inflicting damage on the city of Niigata far out of proportion of the magnitude (7.5) of the earthquake. In Niigata city, where sand deposits in the lowland areas are widespread, the damage was primarily associated with liquefaction of loose sand deposits. Buildings not embedded deep in firm strata sank and tilted. Underground structures, such as manholes, sewage conduits and septic and storage tanks floated up a meter or two above ground level. On level ground, sand flows and mud volcanoes ejected water and sand 2 to 3 minutes after the earthquake. Sand deposits 20-30 cm thick covered the entire city as if the whole area had been devastated by a sand flood (Kawasumi, 1964).

In the same year, an earthquake of magnitude 8.3 occurred in southern Alaska. This city is located on a delta composed of silt and fine sand occurring as beds and stringers within coarser sand and gravel deposits which liquefied and resulted in a massive slide involving approximately 18,000,000 cubic yards of material extending inland above 500 ft from the coast line and destroying the harbour and nearshore facilities. Several similar case histories where liquefaction has been the central factor in large landslides have been documented by Seed (1968).

In 1936, A. Casagrande explained for the first time the phenomenon of liquefaction induced by static loading, enabling engineers to understand the massive Fort Peck Dam slide of 1936. Florin and Ivanov

(1961) presented results obtained in shaking table experiments where the increase of porewater pressure due to the cyclic loading in saturated sands was demonstrated. But it was not until 1964 and the event at Niigata and Alaska that the process of liquefaction due to cyclic loading gained widespread attention. Since this time engineers' spontaneous interest in the process has been increased by the need to assess the safety of foundations of critical structures such as nuclear power plants and pipelines which are typically located in soils which are susceptible to liquefaction.

Study of the liquefaction process has yielded several methods of evaluating liquefaction potential. These fall into two groups: the empirical methods and the analytical methods.

Empirical methods are based on observations of the performance of sand deposits in locations where earthquakes have taken place. For example, relationships like those proposed by Kishida (1966) and Ohsaki (1966) are based on the Standard Penetration Resistance of the sand deposits in the Niigata area. Such relationships, however, cannot be applied to other sites, where shaking intensity or water tables may be at different depths than that in the Niigata area. More recently, Seed et al. (1975) have presented a correlation where the values of shear stress ratio known to be asosciated with liquefaction or no liquefaction in the field are plotted as a function of the corrected average Standard Penetration Resistance of the soil deposit involved. The shear stresses at any depth produced during earthquakes are estimated by the method proposed by Seed and Idriss (1967).

Observation of the conditions under which liquefaction has occurred in previous earthquakes will always be valuable when predicting the probable performance of a saturated sand deposit during earthquakes. However, it is limited in three ways:

1. Very meagre information is available on liquefaction occurring during any earthquake;

2. The method of observation cannot accommodate factors such as the duration of the earthquake or the possibility of drainage and redistribution of pore water pressure; and

3. The Standard Penetration Resistance of soil is not always reliably determined in the field. Its values may vary due to boring and sampling conditions.

Available analytical methods can be grouped into total stress methods and effective stress methods. The important difference between the two types of methods is that total stress methods do not take explicit account of change in porewater pressure. The total stress analysis performed to evaluate liquefaction involves two independent determinations: 1) an evaluation of the cyclic stresses induced in the field in the sand deposit by the earthquake, and 2) a laboratory investigation to determine the cyclic stress ratio which will cause liquefaction. Evaluation of liquefaction potential is based on the comparison of cyclic stresses induced in the field with the cyclic stresses required to cause liquefaction in the laboratory.

In 1967, Seed and Idriss presented a method to perform dynamic response analysis for calculating cyclic stresses occurring in the field. Schnabel et al. (1972), in their method for response analysis treated soil as an equivalent linear elastic material and this method is used to calculate cyclic stresses induced in the field. The irregular cyclic history obtained by dynamic response analysis at a given depth is converted to an equivalent number, Neq, of uniform shear stress, τ_{ave}. The converted uniform shear stress, τ_{ave}, is compared with uniform cyclic shear stress, τ or $\sigma_d/2$, required to cause liquefaction of the sample in cyclic triaxial conditions, where the sample is consolidated under the same all-round confining pressure as in the field, in Neq cycles. However, it should be noted that the stress conditions in cyclic triaxial are different than those existing in the field during an earthquake.

There are two limitations to this method. First, treating soil as an equivalent linear elastic material may overestimate the seismic response due to pseudo-resonance at periods corresponding to the strain compatible stiffnesses used in the elastic dynamic response analysis as shown by Finn et al. (1978). Second, the conversion of non-uniform stress cycles to equivalent uniform stress cycles as suggested by Seed et al. (1975) and Lee and Chan (1976), is computationally inefficient and the development of porewater pressures at levels below liquefaction may not be predicted with sufficient accuracy as pointed by Finn (1980), since the equivalence can be defined at only one point on the porewater pressure curve. In addition, total stress methods cannot predict permanent deformation which occur during seismic loading.

The limitations as outlined above for the total stress method, treating soil as an equivalent linear elastic material, are overcome by development of effective stress method used in conjunction with nonlinear stress-strain laws. Streeter et al. (1974) proposed the first true nonlinear analysis where a Ramberg-Osgood representation of the stress-strain behaviour of soil was used. But, it was not until 1975 when Martin et al. presented a fundamental model for predicting the porewater pressure in cyclic loading, coupled later with dynamic response analysis (Lee, 1975, Finn et al., 1977) that a realistic nonlinear effective stress method emerged. This dynamic effective stress analysis is able to include the nonlinear stress-strain law along with pore pressure generation and dissipation, while allowing for continuous modification of soil properties with increasing pore pressure.

In recent years, many other methods both effective and total stress dynamic analysis have been developed. Some of them are quite noticeable because of their potential for two- or three-dimensional analyses such as proposed by Zienkiewicz et al. (1978). Aspects of some of these methods are discussed in Chapter II.

1.1 Scope of this Research

The pore pressure model presented by Martin et al. (1975) later coupled with appropriate constitutive relationships for methods of dynamic analysis by Finn et al. (1977) accounts for the most essential elements of effective stress analysis, such as the nonlinear hysteretic behaviour of soil under cyclic loading, concurrent generation and dissipation of porewater pressure, and continuous modification of soil properties with increasing porewater pressure. However, at the time the model was proposed it was based on very limited experimental data and contained some crucial assumptions that had not been verified. This thesis undertakes to verify the most important assumptions made in the model to check whether the model can make any useful pore pressure predictions for general loading conditions.

In the effective stress analysis by Finn et al. (1977) volumetric strains are related with dynamic response parameters and by relating the unloading characteristics of sand with volumetric strain, the porewater pressure are calcualted. However, a more efficient way will be to directly relate porewater pressure with dynamic response parameters. In this thesis, a simple formulation based on the endochronic theory is presented where the porewater pressure are related with dynamic response parameters. This simple formulation is a very efficient way of representing large amounts of porewater pressure data and can easily be coupled with dynamic analysis to perform effective stress analysis.

In Chapter II the constitutive relationships proposed by various investigators for their effective stress analysis are briefly discussed. In Chapter III the pore pressure model proposed by Martin et al. (1975) is discussed emphasizing the most crucial assumptions. Chapter IV undertakes the verification of basic assumptions, providing adequate and experimentally based answers to several questions raised in Chapter III. Verification of the model in Chapter IV involves measurement of each variable in the model, prediction of pore pressure by these measured variables and comparison of computed pore pressure with experimental results. Detailed investigation of stress-strain relations is also performed and the pore pressure prediction capacity of the model is checked for sands with stress histories.

In Chapter V the predictive capacity of the model is checked for overconsolidated sands. The volumetric strains and rebound modulus parameters used for the model are discussed with respective comparison to normally consolidated sand. Lastly, in Chapter VI, the endochronic theory is invoked to relate porewater pressure with dynamic response parameters. A simple formulation is presented where porewater pressures are presented as a function of a single variable. This approach bypasses the measurement of soil parameters (volume change constants, rebound modulus constants) as required by Martin et al. (1975). The main advantages of the endochronic formulation are discussed with suggestions for incorporating it in dynamic effective stress analysis.

This research is based on extensive experimental data obtained in cyclic simple shear apparatus on Ottawa sand under strain and stress controlled drained and undrained conditions. In Chapter 6 experimental data for Toyoura and Crystal Silica sand is also presented.

Chapter 7 includes a brief summary of each chapter with suggestions for future research work.

CHAPTER 2

REVIEW OF CONSTITUTIVE RELATIONSHIPS USED FOR VARIOUS EFFECTIVE STRESS ANALYSIS

Effective stress methods of evaluating the liquefaction of sand deposits require realistic constitutive relationships to describe nonlinear hysteretic behaviour, porewater pressure generation and dissipation and continuous modification of soil properties with increasing pore pressure in a realistic manner. A method cannot be seen as reliable unless the set of constitutive relationships used in the model are thoroughly verified. This thesis undertakes to verify the constitutive relationships used for the effective stress model of Finn et al. (1977, 1978). By way of introduction, several recent methods of effective stress analysis are discussed and a critical review of the constitutive relationships used in each model is presented. Recently available, they are broadly classified into groups based on their most prominent characteristics and one model from each section is discussed in such a way that the most essential features of the constitutive laws used for models in that category are highlighted.

2.1 CRITICAL REVIEW OF CONSTITUTIVE RELATIONSHIPS

Several models developed since 1974 to predict pore pressure development for saturated sand under cyclic loading can broadly be classified as follows:

1. Stress Path Models - Ishihara et al. (1975), Ghaboussi and Dikmen (1978).

2. Volumetric Strain Models - Martin et al. (1975), Liou et al. (1977).

3. Endochronic Models - Bazant and Krizek (1976), Zienkiewicz et al. (1978).

4. Kinematic Hardening Models - Mroz et al. (1979).

5. Empirical Models - Ishibashi et al. (1977) Martin and Seed (1978), etc.

Salient features of the constitutive laws for a model in each of these categories will be critically discussed.

2.1.1 Stress Path Models

Ishihara et al. (1975) presented the first stress path model, later adopted and slightly modified by Ghaboussi and Dikmen (1978) and coupled with dynamic response analysis. The model used by Ghaboussi and Dikmen (1978) is based on the assumption that the effective stress path during the unloading condition can be established with sufficient accuracy.

In this model, the residual pore pressures are developed due to plastic deformations which occur whenever a stress path penetrates a current yield locus established by previous loading. The soil is treated as a two-phase solid-fluid media where the nonlinear stress-strain behaviour of the solid phase is idealised by a hyperbolic stress-strain relationship (Fig. 2.1A) for loading and unloading is assumed to be elastic with an initial shear modulus, G_o (Fig. 2.1B).

However, the shape of the hyperbolic form is not changed with increasing pore pressure, which is at variance with experimental observations by Hardin and Drnevich (1972). It is assumed that the shear

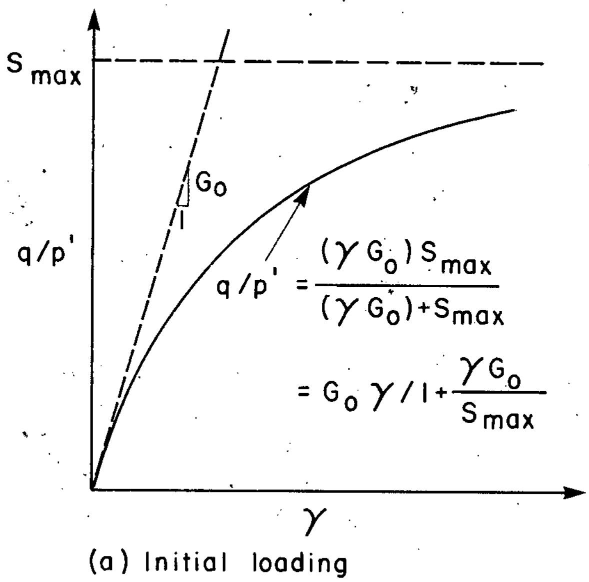

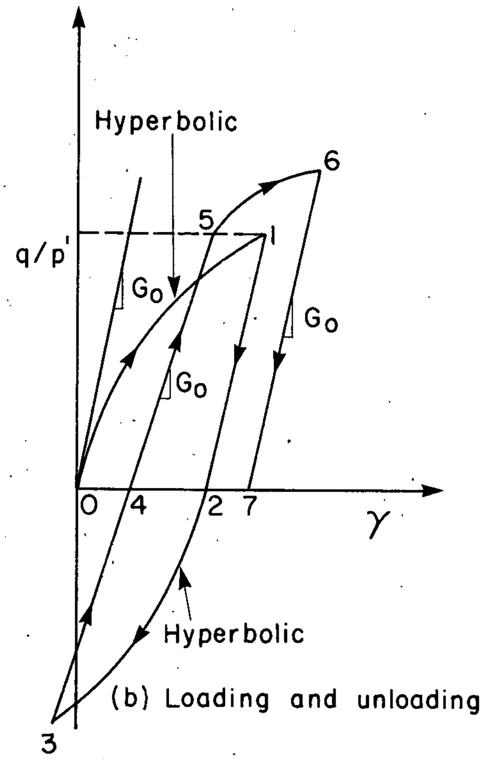

FIG. 2.1 Stress-Strain Relationship for Sand.

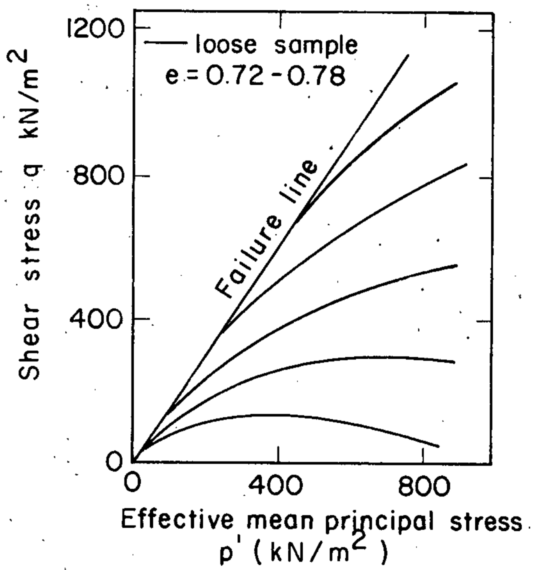

FIG. 2.2 Yield Loci for Loose Sand (After Ishihara et al, 1975).

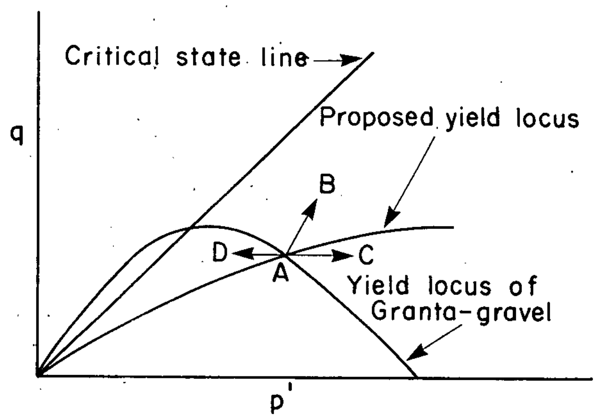

FIG. 2.3 Comparison of Two Kinds of Yield Loci (After Ishihara et al, 1974).

yield loci take the form of straight lines radiating from the origin in the q-p' plane, where q is the deviatoric shear stress and p' is the mean normal confining pressure. These shear yield loci are also considered to be lines of equal shear strain. This observation is based on the experimental data of Poorooshasb et al. (1971) and Tatsuoka and Ishihara (1974). A typical set of yield loci established by Ishihara et al. (1975) is shown in Fig. 2.2 for Fuji river sand. The plotted curves in Fig. 2.2 clearly show that the assumption of yield loci as straight lines radiating from the origin holds good only for mean effective stresses below 2.0 kN/m^2. At higher values of effective stress the yield loci approach a state parallel to p'-axis. Moreover, as Tatsuoka and Ishihara (1974) point out, the assumption of yield loci as radiating lines from the origin in the p-q' plane is in direct conflict with the critical state model presented by Schofield and Wroth (1968) for Granta Gravel. Two concepts of yielding are shown in Fig. 2.3 and direct contradiction between them is most clearly demonstrated by stress paths AB and AC.

Ghäboussi and Dikmen (1978) considered the effective stress-path for undrained loading to be a quarter of an ellipse (Fig. 2.4) with the ratio of the major to minor axes of the ellipse being a function of relative density and sand grain shape. In addition, they indicated that A, which governs the porewater response, is higher for angular particle sand than round particle sand for the same relative density as shown in Fig. 2.5. From Fig. 2.5, the pore pressure response of angular sand at a relative density of 20% would correspond to the pore pressure response of round particle sand at a relative density of 79%. This suggests that the particle shape has a significant influence on the development of pore pressure, hence, liquefaction.

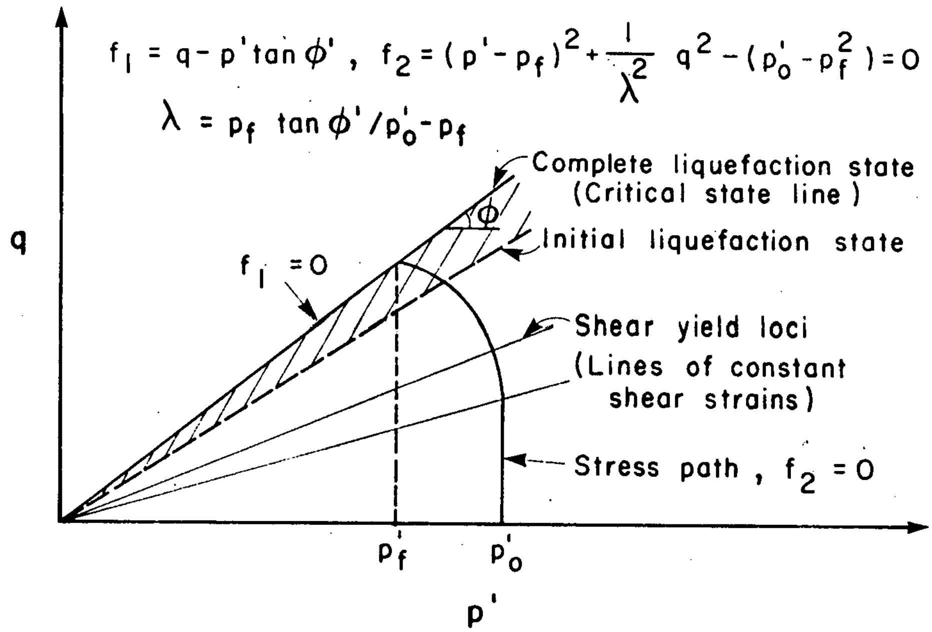

FIG. 2.4 Elliptical Stress Path for Undrained Loading Test (After Ghaboussi and Dikmen, 1978).

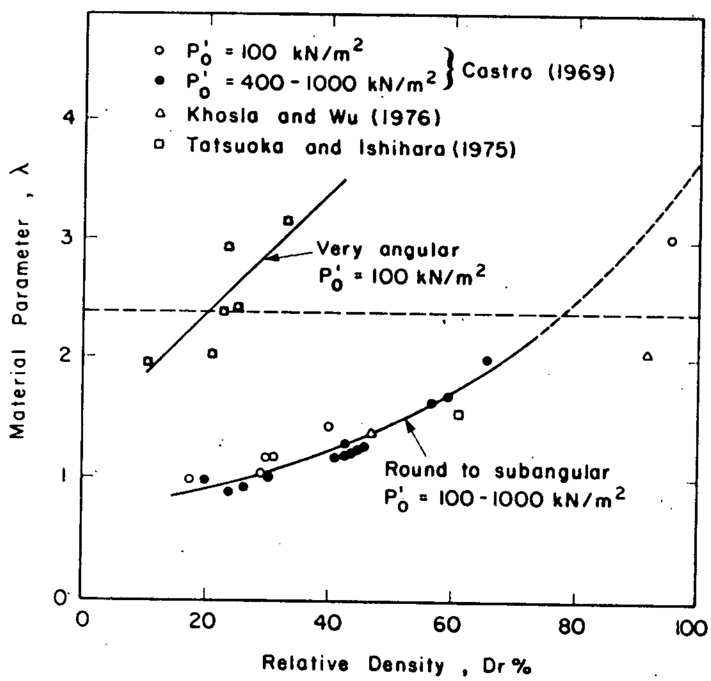

FIG. 2.5 Relationship Between Material Parameter λ and Relative Density (After Ghaboussi and Dikmen, 1978).

The most critical handicap of the present stress path models as discussed by Finn (1979) is the assumption of yield loci and lines of constant shear strain radiating from the origin. This assumption implies that the stress path during a strain controlled cyclic loading test (except for the first half cycle in contraction and extension) will establish the two limits of yield loci, while further application of cycles of constant strain would move the effective stress path in a vertical direction without any additional pore pressure generation. This behaviour of the model is caused by the assumption that isotropic hardening behaviour is applicable for sand under cyclic loading. Since experimental results contradict this prediction of the model, the assumption on which the model is based is in need of a complete review.

2.1.2 Volumetric Strain Models

Martin et al. (1975) presented the first fundamental porewater pressure model, later substantiated by Lee (1975), that accounts for the nonlinear hysteretic behaviour of sand during cyclic loading. This model will be discussed in detail in Chapter III.

Liou et al. (1977) proposed a model where soil is again treated as a two phase material. The nonlinear, strain dependent hysteretic behaviour of soil is accounted for by a shear wave sub-model. This shear wave sub-model uses the modified Ramberg-Osgood stress-strain relationship, where initial shear modulus and maximum shear strength is given by Hardin and Drnevich (1972). The pressure wave sub-model relates pore pressure to the bulk compressibility of water, secant constrained modulus of solid skeleton and porosity. The pore pressure model is given by

$$-\bar{\sigma}_z = \frac{1}{C_c}\frac{\partial w}{\partial z} \qquad (2.1)$$

where $$\frac{1}{C_c} = \frac{4}{3} G + \frac{1}{C_b} \qquad (2.2)$$

in which $\bar{\sigma}_z$ is effective stress, $\frac{1}{C_c}$ is secant constrained modulus of the soil skeleton, $\frac{\partial w}{\partial z}$ is the constrained strain level, G is the secant shear modulus and C_b is the bulk compressibility of the soil skeleton. Further, it is assumed that C_b remains constant during shearing. Thus, any change in C_c is directly attributed to a change in G. Since the secant shear modulus decreases with increasing shearing amplitude, C_c would increase with increasing shear strain and any change in C_c will calculate the change in effective stress by equation (2.1).

The pore pressure prediction by this model, in its simplest form, depends on the relationship (equation 2.2) which is true in the range of strain where soil behaves as an elastic material. However, beyond this range of strain the application of this relationship is questionable. In addition, Finn (1979) points out that changes in G with strain are recoverable on stress reversal, whereas changes in C_c are assumed to be permanent and cumulative which suggests that the relationship (equation 2.2) should not be assumed to hold for soil.

2.1.3 Endochronic Models

The endochronic theory was proposed by Valanis (1971) for metals to describe nonlinear stress-strain law, strain hardening behaviour and contraction of hysteresis loops with cyclic straining. The potential of this theory for saturated sands was first realised by Bazant and Krizek (1976). In the constitutive laws proposed for the pore pressure model of Bazant and Krizek, soil is treated as a two-phase porous media where inelastic and elastic behaviour are considered separately. The constitutive equations proposed by Biot (1956,1957) for elastic behaviour of the two-phase media were extended to include inelastic volumetric strain in 1975 and used for a pore pressure model. Bazant and Krizek assumed that the deviatoric stress-strain relationships for the inelastic isotropic two-phase media have the same form as that of a solid phase alone (i.e., dry sand). In addition, they assumed that in the undrained condition the presence of porewater in porespace produces viscous and inertial forces which oppose the relative movement of sand particles. They further postulated that intergranular stresses, σ', serve the purpose of overcoming the microscopic viscous and inertial forces. Hence, the actual extent of densification which is realised under undrained conditions is a function of intergranular stress σ'. Based on this concept, the actual densification which is responsible for pore pressure generation under undrained conditions is related with densification in drained conditions for the same strain history as given by Bazant and Krizek.

$$(\varepsilon_{vd})_{\substack{\text{Potential Volumetric} \\ \text{Strain in Undrained}}} = L(\sigma'_{vo}-\sigma')(\varepsilon_{vd})_{\text{Drained}} \tag{2.3}$$

where

$L(\sigma'_{vo}-\sigma')$ is a correction coefficient whose value is arbitrarily assigned.

σ'_{vo} is the initial vertical confining stress and σ' is the intergranular stress at a particular instant during cyclic loading.

The proposed porewater pressure model under undrained conditions and constant overburden stress, σ'_{vo}, is given as

$$d\sigma' = -\frac{(\varepsilon_{vd})_{\text{Drained}} \cdot L(\sigma'_{vo}-\sigma')}{C_b} \tag{2.4}$$

in which $d\sigma'$ is the change in effective stress and C_b is bulk compressibility of drained sand. It is not clear from the literature whether C_b is assumed constant or a function of intergranular stress.

To describe densification and hysteretic behaviour of drained sand under cyclic loading, the endochronic theory was applied. The only independent variable for these formulations is a scalar which characterizes the accumulation of total shear strain in time which is called the rearrangement measure ξ. Since both inelastic volumetric strains (densification) and inelastic shear strains are mainly due to rearrangement of sand particles under cyclic loading, they are considered to be related to ξ. For this purpose the following two variables are proposed by Bazant and Krizek.

1) Densification variable (ζ)[1] which relates densification, ε_{vd} with ξ.

2) Distorsion variable (η) which relates inelastic shear strain, γ^p with .

The following relationship is proposed by Bazant and Krizek for densification under cyclic loading which accounts for strain hardening and softening behaviour

$$\varepsilon_{vd} = \frac{1}{\alpha} L_n (1 + \alpha\zeta) \tag{2.5}$$

and for constant strain cyclic shear condition

$$\zeta = \gamma_o{}^q N \tag{2.6}$$

where γ_o is shear strain amplitude, N is the cycles of constant shear strain and α and q are soil constants which depend on the relative density. In Fig. 2.6, volumetric strain (densification) is plotted against the number of cycles of constant shear strain amplitude for D_r = 45% and 65%, where the solid curve represents experimental data and the dotted curve shows the analytical data. Figure 2.6 shows that the analytical and

---

[1]For the same variable Bazant and Krizek (1976) used the symbol, κ.

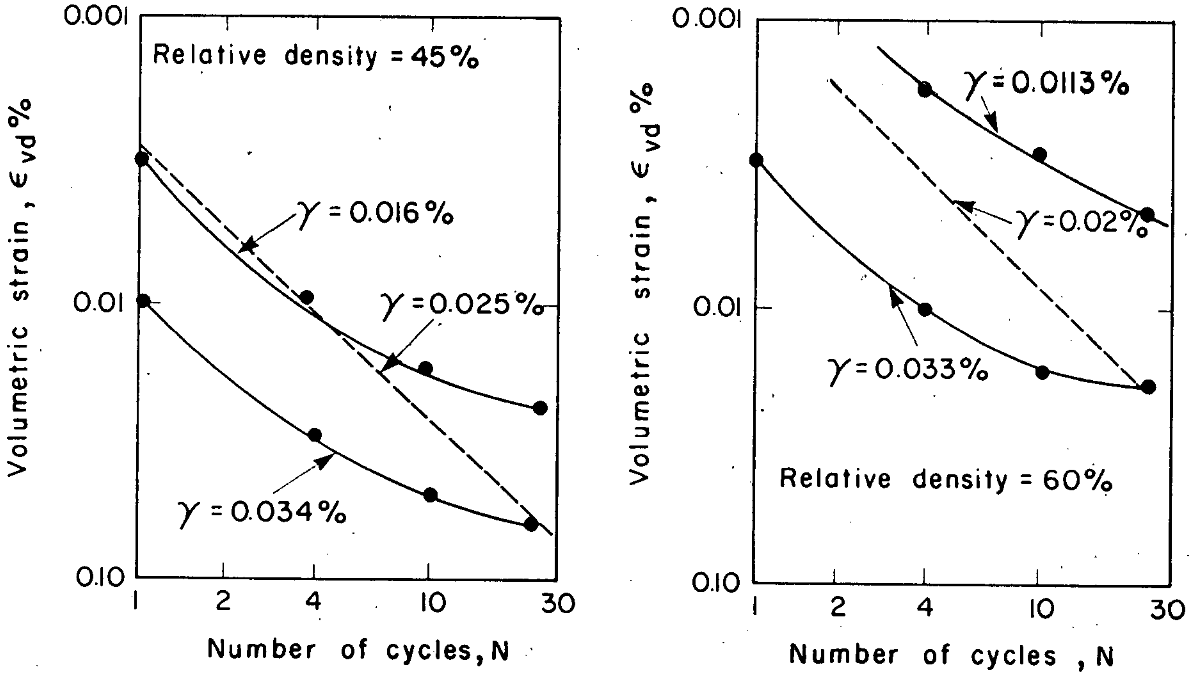

FIG. 2.6 Volumetric Strain vs. Number of Cycles for Crystal Silica Sand (After Cuellar et al, 1977).

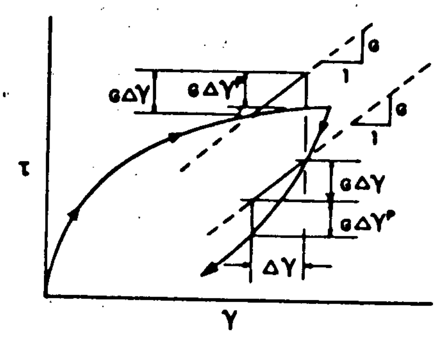

FIG. 2.7 Elastic and Inelastic Stress Increment (After Bazant and Krizek, 1976).

experimental data do not match very well. The analytical curves (double dotted) overpredicts the volumetric strain. In Chapter 6, a better presentation is proposed for the volumetric strains with endochronic variables.

The nonlinear stress-strain law for one-dimensional shearing where the inelastic shear strain increment (Fig. 2.7) is related with shear modulus and shear stress through the following equation:

$$d\tau = (\sigma')^{\frac{1}{2}} \times \left(c + \frac{d}{e + (\gamma_{max})}\right) \times d\gamma - \frac{\tau}{\tau_d} \frac{1}{(1 + \frac{a}{b}\xi)^b} d\xi \tag{2.7}$$

where a, b, c, d, e, τ_d are soil constants which depend on soil-type and relative density, $d\gamma$ is total shear strain, G is the shear modulus, and τ is the shear stress. By using equation (2.7) Cuellar et al. (1977) were able to describe nonlinear hysteretic behaviour of sand as shown in Fig. 2.8. However, the number of constants required for the stress-strain relationship is extremely large and it is not clear how such constants can be obtained.

The stress-strain relationship proposed for general stress conditions is extremely difficult to understand. Bazant and Krizek (1976) checked the predictive capacity of the pore pressure model for stress controlled undrained test data as shown in Fig. 2.9, and by varying the value of the correction factor arbitrarily, a good correlation between experimentally observed pore pressure and analytical results was obtained. However, it is not necessary that this convection factor will give results for samples with other cyclic stress ratios. In addition, it is not clear from the literature what values of C_b and G are used for the analytical results presented.

In conclusion, the formulation of the problem presented by

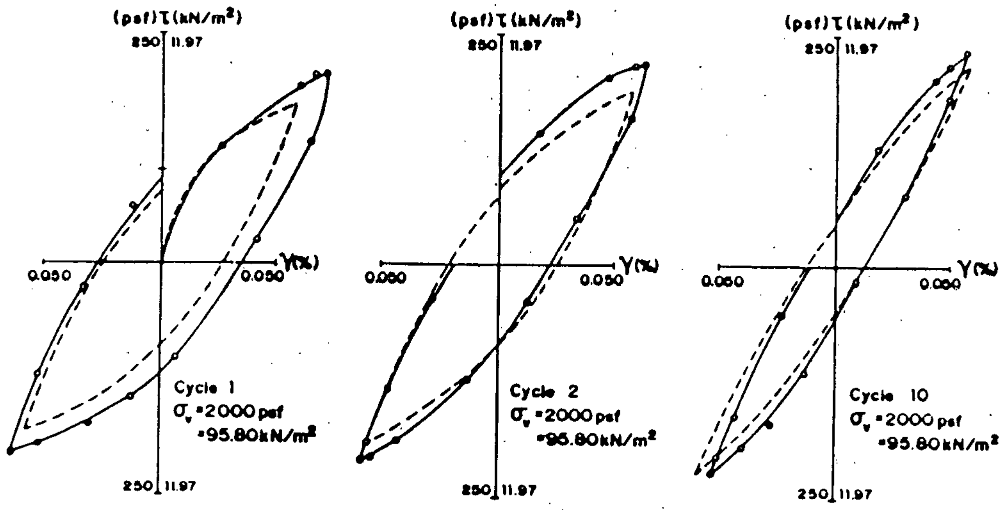

FIG. 2.8 Prediction of the Hysteretic Loops for Crystal Silica Sand (After Cuellar, 1977).

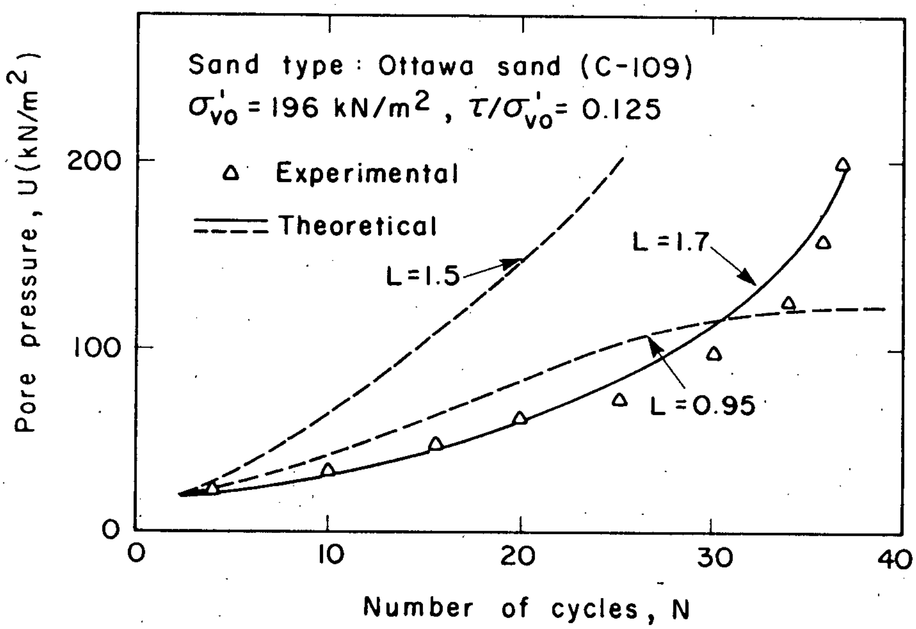

FIG. 2.9 Pore Pressure vs. Number of Cycles in Constant Stress Undrained Test (After Bazant and Krizek, 1976).

Bazant and Krizek (1976) is impressive but requires detailed verification for its pore pressure predictive capacity without which its performance is really unknown. Moreover, the constitutive relationships have not yet been verified for multi-directional loading.

In the model of Zienkiewicz et al. (1978) the volumetric strain which accounts for pore pressure rise was related to the length of the strain path, ξ (Fig. 2.10). Endochronic variables were used to relate volumetric strain (autogenous volumetric strain) with a parameter called the damage parameter. An experimental transformation was proposed to transform the length of strain path to damage parameter through the following relationship:

$$d\kappa = \exp(c \cdot \tau/\sigma'_{mo})d\xi \tag{2.8}$$

where τ/σ'_{mo} is the stress ratio and c is the constant. Data shown in Fig. 2.11 shows volumetric strain against damage parameter, where points corresponding to various stress ratios (Fig. 2.10) collapse into one curve (Fig. 2.11). To calculate pore pressure, these volumetric strains were multiplied by a constant tangent bulk modulus of sand. (Martin et al. (1975) have shown that tangential bulk modulus is a function of effective stress.)

Since volumetric strains are explicitly calculated, a non-associated theory of plasticity which combines a Mohr-Coulomb yield surface (Fig. 2.12) with a Tresca-type potential surface with zero dilatancy was used. However, as Finn (1979) points out, "to what extent a potential surface selected on the basis of dilatancy characteristics only may be capable of representing the remaining strain is yet unknown". This model is based on very limited data and its performance under idealised conditions (stress controlled undrained test) is yet to be examined.

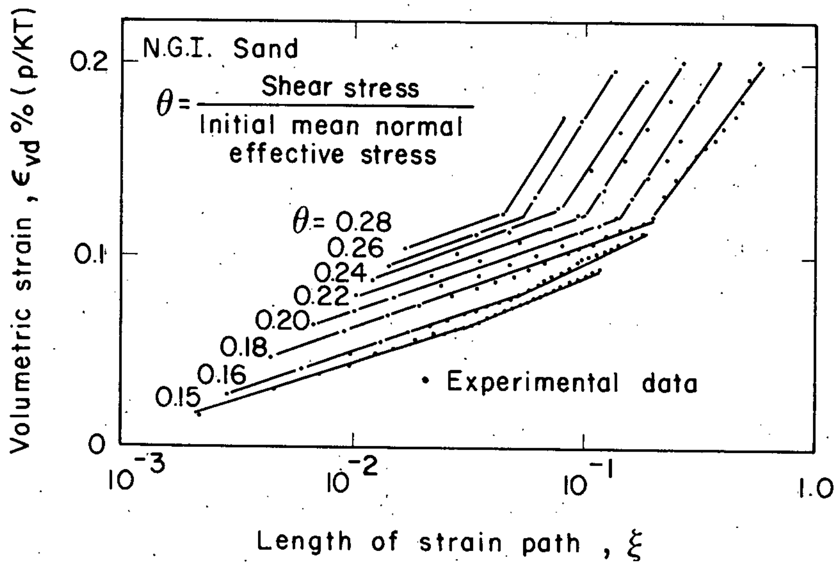

FIG. 2.10. Volumetric Strain vs. Length of Strain Path (After Zienkiewicz et al, 1978).

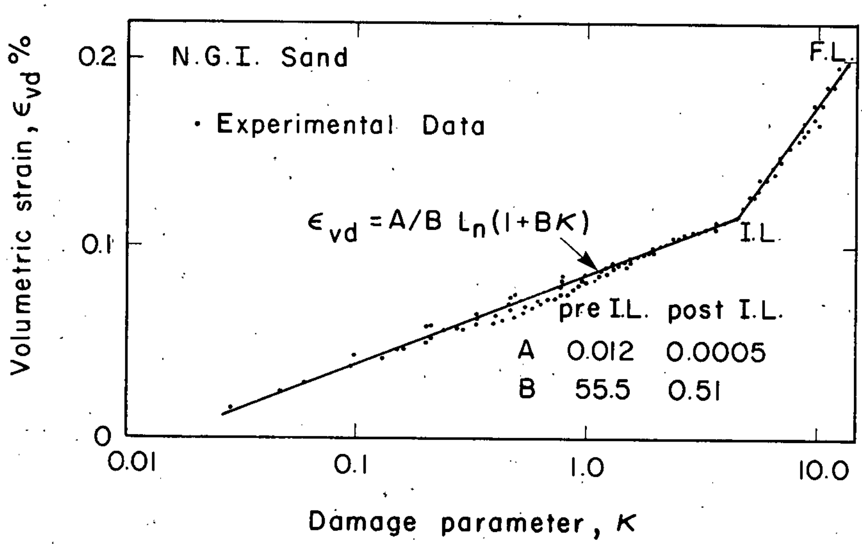

FIG. 2.11 Volumetric Strain vs. Damage Parameter (After Zienkiewicz et al, 1978).

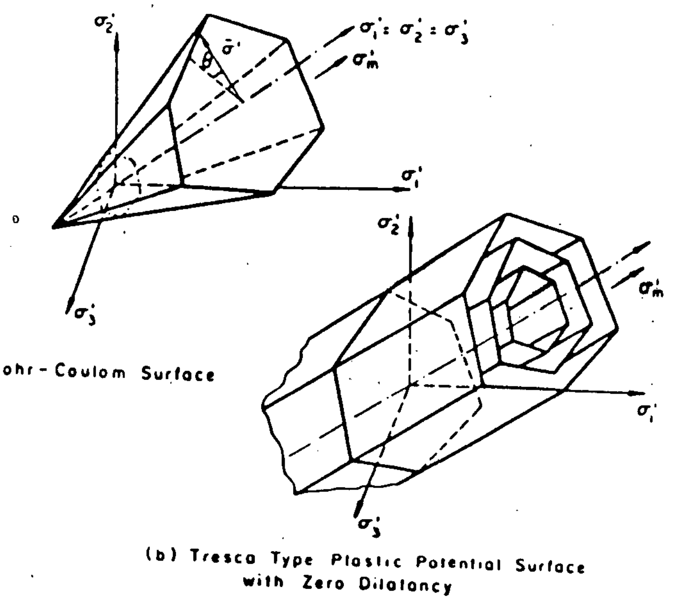

FIG. 2.12 Idealized Yield and Plastic Potential Surface (After Zienkiewicz et al, 1978).

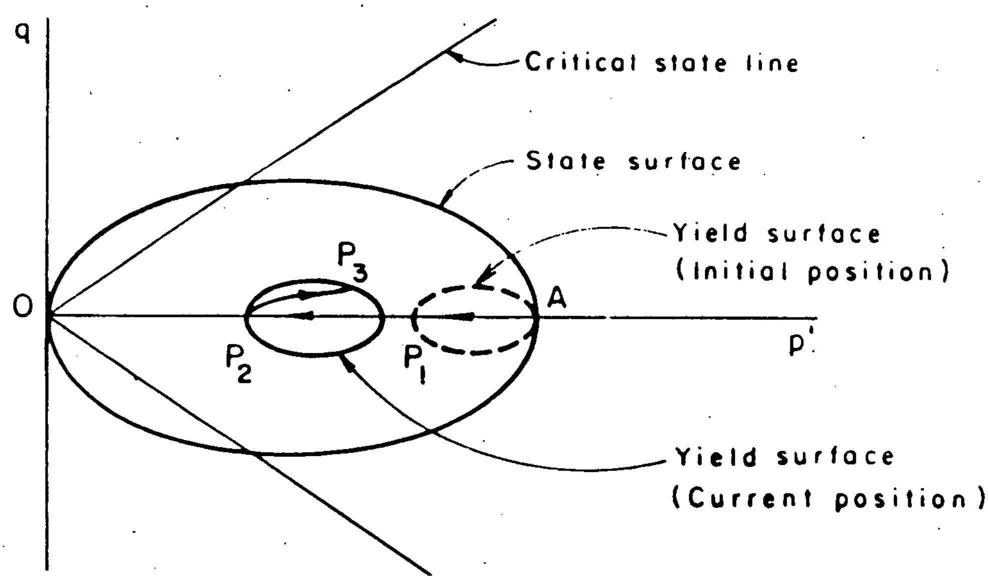

FIG. 2.13 Two-Surface Model Showing Unloading and Isotropic Consolidation (After Mroz et al, 1979).

2.1.4 Kinematic Hardening Models

Mroz et al. (1978) proposed a model for cyclic behaviour of soil based on the concept of kinematic hardening. The model, in its simplest form, assumes that a state boundary surface established by consolidation stresses, (F=0), its Roscoe-Burland surface as shown in Fig. 2.13, and the elastic domain enclosed by the yield surface, $f_o=0$, is much smaller than (F=0). [F=0 is considered as the yield surface used for the isotropic hardening model.] For inelastic material response it is assumed that the yield surface, $f_o=0$ may translate, expand or contract in the stress space but cannot intersect the existing boundary surface. An associated flow rule governing the plastic flow and hardening rule describes the variation of the yield surface and state boundary surface, together with the variation of the hardening modules along any trajectory, although with changing yield surface the flow rule retains its usual associated flow. Translation of the surface is constrained by conditions presented by Mroz (1967).

For determination of the cyclic behaviour of soil, instead of using a nest of yield surfaces with associated plastic moduli between yielding and bounding, the two-surface model uses an interpolating rule. The interpolating rule used in the model follows the work of Dafalias and Popov (1976). Recently, Finn and Martin (1980) critically reviewed the main points of the model. In Fig. 2.13, the two-surface model for the case of unloading and reloading from isotropic consolidation is shown.

Since this theory permits the occurrence of volumetric changes on unloading, it has potential for implicit determination of volumetric strain and dynamic analysis of porewater pressure. But the formulations of the theory for cyclic loading are for the pseudo-static case only. The model has not been extended to include earthquake loading which requires inertia effects.

2.1.5 Empirical Models

Since 1975, along with the development of models based on the theory of plasticity and endochronic theory, several empirical models have also been proposed, such as those of Ishibashi et al. (1977), Martin and Seed (1978), and others. These methods are, no doubt, of practical importance and represent definite progress. However, the application of such models to general conditions is always limited.

2.2 DISCUSSION

It is quite clear from the above discussion that none of the constitutive relationships considered are complete. Work in this area is still at the stage when modification and verification is required for each of the models. However, the development of all these models is so recent that any practical experience with them is very limited.

In this thesis, it is undertaken to verify the performance of one of the first models discussed, that of Martin et al. (1975). This first model, to predict pore pressure under cyclic loading, considered for the first time the fundamental mechanism of pore pressure development under cyclic loading. Lee (1975) extended this model to perform effective dynamic stress analysis. This model is very simple and realistically predicts the behaviour of soil. The method has been used in evaluation of liquefaction potential of offshore sites and in conjunction with a soil pile interaction program to predict the performance of pile foundations. Recently, it has been used in Japan to evaluate the liquefaction performance of sites in the Off-Tokachi earthquake, 1978.

It is considered essential to verify the model and check its performance under general conditions.

CHAPTER 3

CONSTITUTIVE RELATIONS FOR THE EFFECTIVE STRESS MODEL OF FINN, LEE AND MARTIN

Finn, Lee and Martin (1977) presented a complete method of dynamic effective stress response analysis for the evaluation of liquefaction potential in horizontally layered saturated sand deposits. This method is based on a set of constitutive relationships which take into account the important factors known to influence the response of a saturated sand layer in a given earthquake: the *in situ* shear modulus, the variation of shear modulus with shear strain and mean normal effective stress, the contemporaneous generation and dissipation of porewater pressure, hysteretic and viscous damping and strain hardening.

The pore pressure model adopted in this method is proposed by Martin et al. (1975). This model is the first to explain the fundamental mechanism of porewater pressure generation during cyclic loading. Lee (1975) proposes nonlinear stress-strain laws for sand under cyclic loading and presents a nonlinear effective stress model which consists of five basic elements:

1. A method for solving the nonlinear equation of motion;
2. A stress-strain law for the nonlinear behaviour of sand;
3. A procedure for calculating potential volume changes caused by cyclic shear;
4. A relationship between potential volume changes and residual porewater pressure;
5. A procedure for calculating the dissipation of excess porewater pressure.

In this chapter, only the constitutive relationships used for the effective stress model will be discussed. Broadly, the constitutive relations used in the analysis for the effective stress model can be divided into two categories:

1. Relations required for the porewater pressure generation model;
2. Relations required for the representation of the nonlinear stress-strain behaviour of sand including strain hardening and softening.

3.1 PORE PRESSURE MODEL

In the pore pressure model proposed by Martin et al (1975) the behaviour of sand under undrained cyclic loading conditions is computed from the knowledge of volume change characteristics under drained cyclic simple shear conditions and the rebound characteristics under effective stress unloading. A schematic representation of the model is shown in Fig. 3.1.

It is considered that in a saturated sand sample subjected to one cycle loading under simple shear conditions, the net volumetric strain increment occurring due to interparticle slip under drained conditions is $\Delta\varepsilon_{vd}$. If an identical saturated sample is being subjected to the same shear strain amplitude but under undrained conditions it is assumed that slip at the grain contacts resulting in volumetric strain, $\Delta\varepsilon_{vd}$, again must occur provided that the magnitude of the residual porewater pressure increase occurring during the cycle is small relative to the initial effective stress.

However, in the undrained condition slip deformation $\Delta\varepsilon_{vd}$ must transfer some of the vertical stress previously carried by intergranular

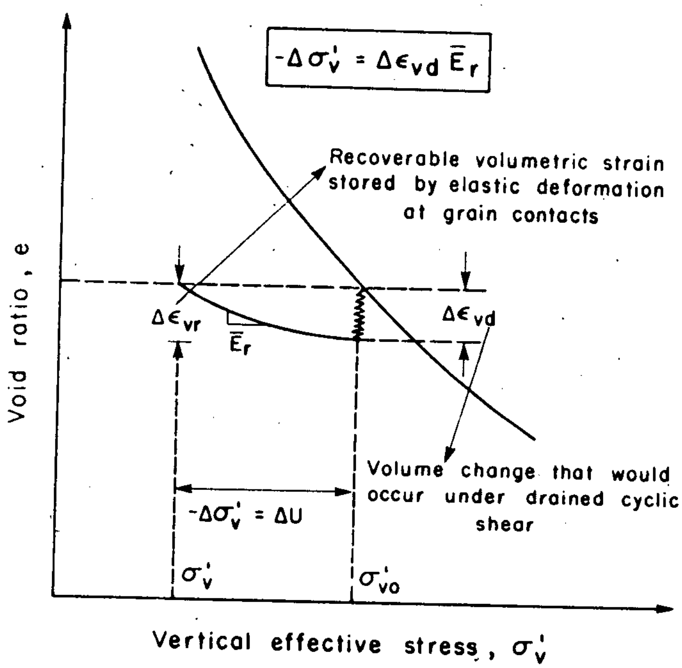

FIG. 3.1 Schematic Illustration of Mechanism of Porewater Pressure Generated During Cyclic Loading (After Seed, 1976).

forces to the less compressible water and, as porewater pressure increases, the corresponding decrease in effective stress will result in a release of recoverable strain, $\Delta\varepsilon_{vr}$, stored at grain contacts due to elastic deformation. Hence, from the volumetric compatibility at the end of the load cycle, Martin et al (1975) derived the following relationship -

$$\Delta u \cdot \left[\frac{n}{k_w} + \frac{1}{\bar{E}_r}\right] = \Delta\varepsilon_{vd} \tag{3.1a}$$

or $$\Delta u = \Delta\varepsilon_{vd} \Big/ \left(\frac{n}{k_w} + \frac{1}{\bar{E}_r}\right) \tag{3.1b}$$

in which $\Delta\varepsilon_{vd}$ is the volumetric strain due to slip deformation for the cycle, n is the porosity of the sample, k_w is the bulk modulus of water, and $\bar{E}_r$ is the tangent modulus of the one-dimensional unloading curve at a point corresponding to the initial vertical effective stress.

In saturated samples, k_w is approximately two orders of magnitude greater than $\bar{E}_r$ for the usual vertical stress interested from the liquefaction point of view, hence it can be assumed that the compressibility of the porewater pressure becomes negligible. It is usually assumed that undrained tests are constant volume tests.

The consequence of this assumption is that volumetric strain, ε_{vd}, due to interparticle slip (plastic strain) must be equal and opposite to recoverable strain, $\Delta\varepsilon_{vr}$ (elastic strain), released due to the decrease in effective stress. This, for example, is a fundamental assumption of the critical state theory as applied to undrained loading by Schofield and Wroth (1968). Hence, for the constant volume condition equation (3.1b) implies:

$$\Delta u = \bar{E}_r \, \Delta\varepsilon_{vd} \tag{3.2}$$

The key to the practical application of the theory rests in the fact that the value of $\Delta\varepsilon_{vd}$ is independent of vertical effective stress. The theory in its simplest form implies that if "saturated sand loaded to an initial vertical effective stress of σ'_{vo} has a recoverable volumetric strain of ε_{vro}, then liquefaction[1] will occur under an applied cyclic strain history that produces a volumetric strain[2], $\varepsilon_{vd} = \varepsilon_{vro}$, under drained conditions", Martin et al (1975).

The porewater pressure model of equation (3.2) gives rise immediately to the important question: how are $\Delta\varepsilon_{vd}$ and $\bar{E}_r$ to be obtained? In the model it is assumed that the plastic volumetric strain, $\Delta\varepsilon_{vd}$, which develops during one cycle of uniform shear strain, γ, in an undrained simple shear test will be the same as the volumetric strain in a drained simple shear test. A question arises - can it be proven? Therefore, a fundamental assumption of the pore pressure model is that there is a unique relationship between volumetric strain in drained tests and porewater pressure in undrained tests for samples of a given sand with corresponding strain histories.

The following sections present the volume change characteristics under drained cyclic shear conditions used to obtain $\Delta\varepsilon_{vd}$, and rebound characteristics under static unloading to calculate $\bar{E}_r$.

3.1.1 <u>Volume Change Characteristics Under Drained Cyclic Loading</u>

Consideration of volume change in drained cyclic tests is restricted to simple shear test conditions, which best simulate field deformation induced in horizontal sand deposits by earthquake excitation. The

---

[1]Liquefaction is the state where porewater pressure has become equal to initial vertical confining stress.

[2]In the later part of this thesis, volumetric strain under undrained conditions will be referred to as potential volumetric strain.

volumetric strain characteristics of sand under cyclic simple shear have been given in studies by Silver and Seed (1971), Youd (1972,1975), Pyke (1973) and Martin et al (1975). A few important observations from these studies are:

1. Due to the application of cyclic shear stress or strain in the drained condition, interparticle slip results in volumetric[3] strain (plastic) which is proportional to shear strain amplitudes (γ<0.3%) (Silver and Seed, 1971).

2. Volumetric strains are independent of vertical confining stress as shown in Fig. 3.2 (Silver and Seed, 1971).

3. Volume change characteristics are the same for both dry and saturated samples subjected to the same cyclic shear strain amplitude (Fig. 3.3) and are independent of frequency in the range 0.2 Hz to 2 Hz (Youd, 1971).

4. With increasing volumetric strains during cyclic loading in the drained condition, both shear modulus and k_o[4] increase (Pyke (1973), Youd (1975)).

Based on these observations, Martin et al (1975) suggest determining $\Delta\varepsilon_{vd}$ from experimental data on dry sand under cyclic strain conditions as shown in Fig. 3.4. For the application of data shown in Fig. 3.4 to irregular or random cyclic shear strain history, data is replotted in terms of incremental volumetric strain, $\Delta\varepsilon_{vd}$, against shear strain amplitude, γ, for constant accumulative volumetric strain, ε_{vd}. Such a representation is shown in Fig. 3.5 for Crystal Silica Sand, for which a function of the following form has been fitted:

$$\Delta\varepsilon_{vd} = C_1(\gamma - C_2\varepsilon_{vd}) + \frac{C_3\varepsilon_{vd}^{\,2}}{\gamma + C_4\varepsilon_{vd}} \qquad (3.4)$$

---

[3]Since lateral strains in the simple shear condition are zero, vertical strains are equal to volumetric strains.

[4]k_o is the ratio of lateral effective stress to vertical effective stress in a laterally confined condition.

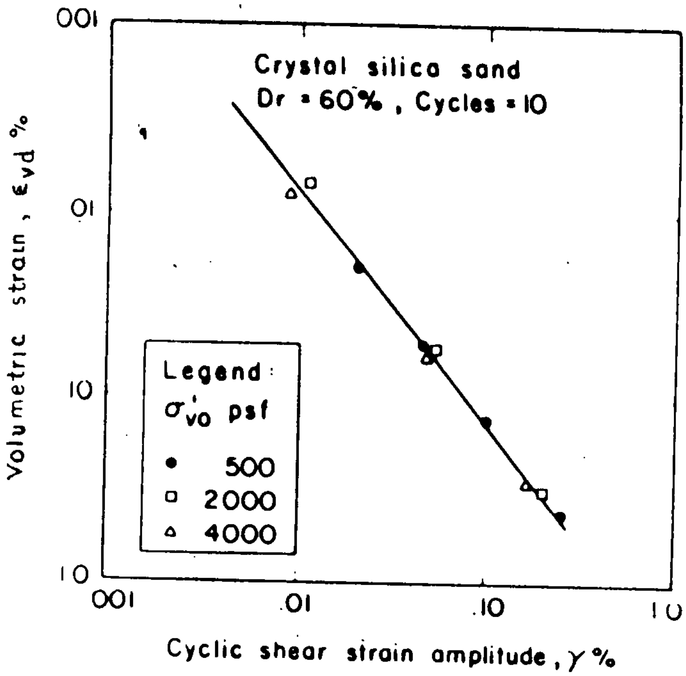

FIG. 3.2 Volumetric Strain vs. Cyclic Shear Strain Amplitude (After Seed and Silver, 1971).

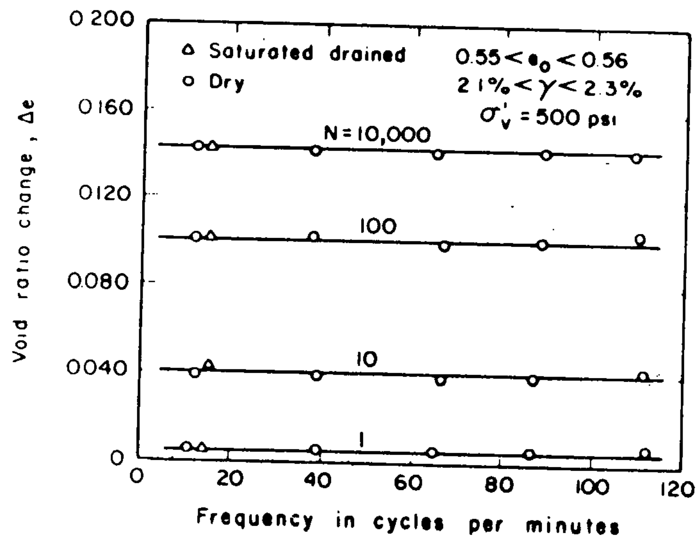

FIG. 3.3 Void Ratio Change vs. Frequency in Cyclic Strain Test on Dry and Saturated Drained Samples (After Youd, 1972).

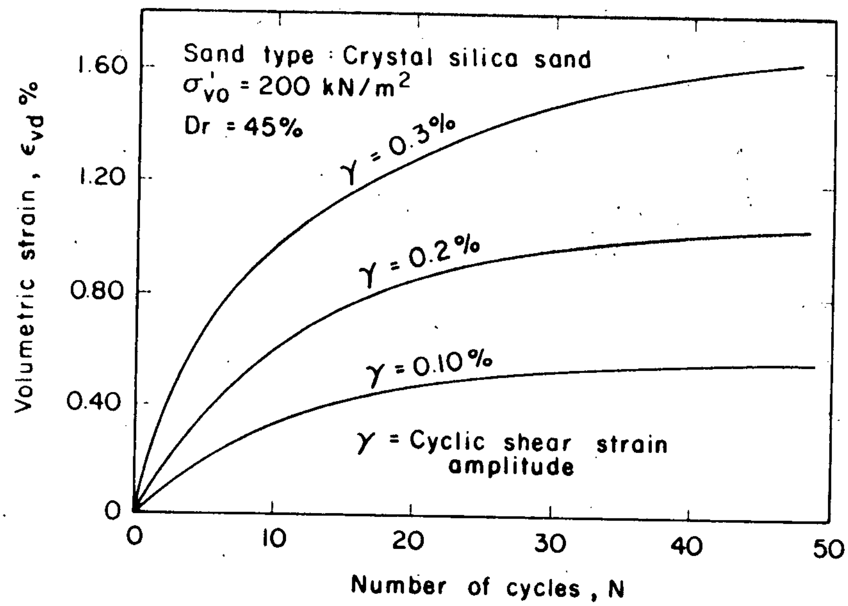

FIG. 3.4 Volumetric Strain vs. Number of Cycles of Constant Strain (After Martin et al, 1975).

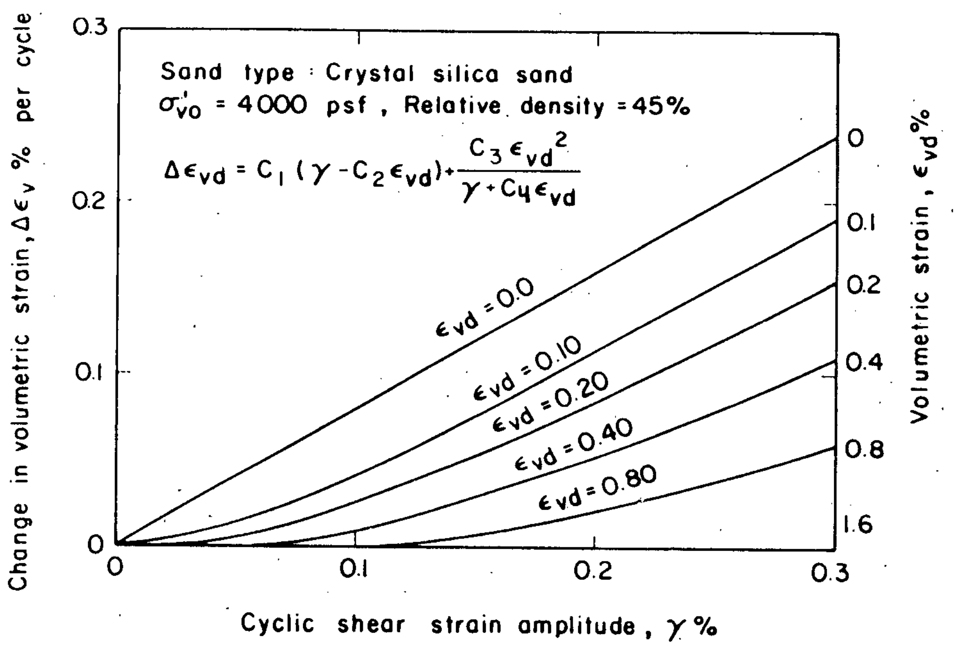

FIG. 3.5 Incremental Volumetric Strain vs. Cyclic Shear Strain for Various Volumetric Strain (After Martin et al, 1975), (1 psf = 47.9 N/m^2).

where $\Delta\varepsilon_{vd}$ is the volumetric strain[5] per cycle, ε_{vd} is the accumulated volumetric strain, γ is the shear strain[5] amplitude and C_1, C_2, C_3, C_4 are volume change constants which depend on relative density and soil type. Finn and Byrne (1976) point out that the volumetric strain increment, $\Delta\varepsilon_{vd}$, corresponding to relative density, D_{r1}, for which the volume change constants have been evaluated can be related to the volumetric strain increment at another relative density, D_{r2}, by the relation:

$$(\Delta\varepsilon_{vd})_{D_{r2}} = R(\Delta\varepsilon_{vd})_{D_{r1}} \tag{3.5}$$

in which R is a shape parameter that varies with relative density. The proposed relation (equation 3.5) interpolates volume change characteristics at relative densities other than for those which volume change constants are known.

3.1.2 One-Dimensional Volumetric Unloading Characteristics

The pore pressure model requires a knowledge of the recoverable deformation characteristics of sand during one-dimensional unloading from a given initial vertical effective stress. Martin et al (1975) explain the behaviour of sand in one-dimensional loading and unloading. The volumetric strain on loading with a vertical confining stress can be subdivided into two components:

1. Non-recoverable strain due to interparticle slip, ε_{vso}; and
2. Recoverable strain due to elastic deformation of grain contacts, ε_{vro}.

For the pore pressure model, a relationship between vertical effective stress and the recoverable component of volumetric strain is required. Martin et al. (1974) conducted a few tests on Crystal Silica

[5]Shear strain and volumetric strain are expressed in percentages.

sand in an NGI[6] type simple shear device to obtain the unloading characteristics of sand. Their experimental data shown in Fig. 3.6 indicate that:

1. The total recoverable strain, ε_{vro}, stored at grain contact points increases with increasing confining stress, σ'_{vo} (cf. Fig. 3.6) according to the following relationship:

$$\varepsilon_{vro} = k_2(\sigma'_{vo})^n \tag{3.5}$$

2. Unloading curves from different confining stresses are geometrically similar in shape (cf. Fig. 3.6) and can be related with each other by:

$$\frac{\varepsilon_{vr}}{\varepsilon_{vro}} = \left(\frac{\sigma'_v}{\sigma'_{vo}}\right)^m \tag{3.6}$$

From the above two observations Martin et al. (1975) obtained a relationship for the unloading modulus, $\bar{E}_r$, ax any stress, σ'_v, given by:

$$\bar{E}_r = (\sigma'_v)^{1-m} / mk_2(\sigma'_{vo})^{n-m} \tag{3.7}$$

where k_2, m, n are constants for a given sand and density, σ'_{vo} is the initial confining stress and σ'_v is the effective stress at a particular instant.

Seed et al. (1975) studied the recoverable characteristics of sand and determined that the total volumetric strain recovered due to unloading from a certain confining stress is increased by 20% due to cyclic shear prior to unloading. It is further observed that most of the increase in recoverable strain is in the last one-third of the unloading curve as shown in Fig. 3.7. Hence, there is a possibility that due to cyclic shearing the rebound modulus $\bar{E}_r$ might change in dry sand. Any change in $\bar{E}_r$ is crucial for pore pressure prediction, so the

---

[6]Norwegian Geotechnical Institute.

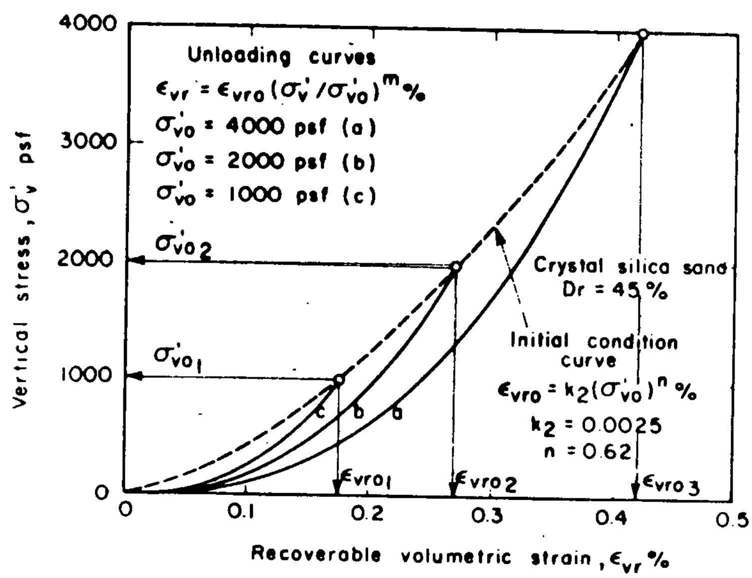

FIG. 3.6 Generalised One-dimensional Unloading Curves (After Martin et al, 1975), (1 psf = 47.9 N/m^2).

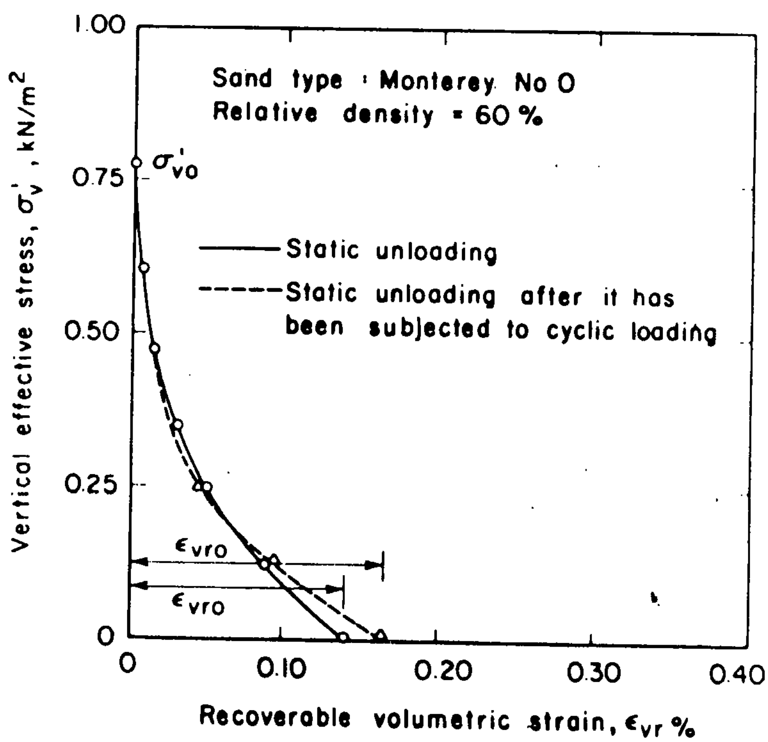

FIG. 3.7 Vertical Effective Stress vs. Recoverable Volumetric Strain for Monterey Sand (After Seed et al, 1973).

observations made by Seed et al. (1975) should be further investigated.

The most crucial point about the measurement of $\bar{E}_r$ is under which condition it should be measured. Rebound occurs during undrained conditions under cyclic loading but direct measurement of $\bar{E}_r$ under such conditions is not possible. Therefore, $\bar{E}_r$ is measured during static rebound in the simple shear apparatus. However, the basic question arises: can $\bar{E}_r$ measured in static conditions (consolidation ring) be used for the pore pressure model?

3.2 STRESS-STRAIN RELATIONSHIP

For the range of strains expected during earthquake loading, sand manifests a hysteretic stress-strain relationship which indicates both a nonlinear behaviour and the capacity of dissipating a considerable amount of energy especially at high levels of shear strain. The extent to which this behaviour is manifested depends on shear strain amplitude and the relative density of the soil. Also, as a consequence of continuous application of cyclic shear stress or strain, it is observed that shear modulus increases with increasing number of cycles for a constant shear strain amplitude. This behaviour is reported by Pyke (1975) for simple shear as shown in Fig. 3.8 for Monterey Sand.

In addition, Hardin and Drnevich (1972) are the first to observe that shear modulus is a function of mean effective stress. Under undrained conditions it gradually decreases with increasing pore pressure. Hence, in any generalised stress-strain relationship to describe the nonlinear hysteretic behaviour of sand for irregular loading under drained and undrained conditions, the shear modulus has to be continuously modified for the hardening and softening behaviour of sand. Constitutive laws used

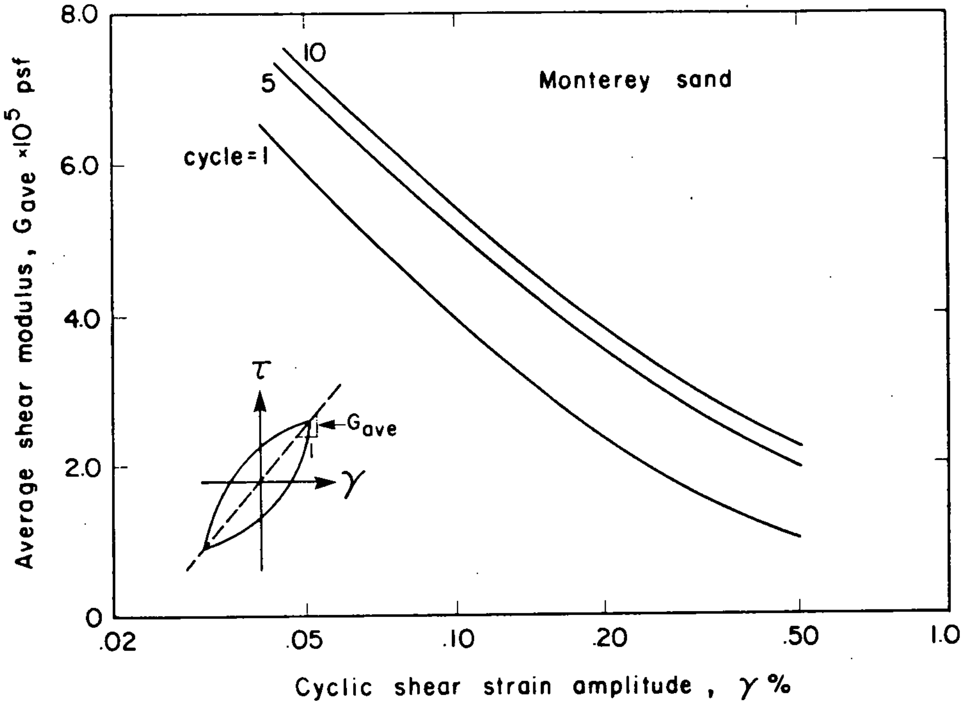

FIG. 3.8 Increase in Av. Shear Modulus with Various Number of Cycles of Constant Shear Strain (After Lee, 1975).

for the effective stress analysis by Finn et al. (1977) are those proposed by Lee (1975) which include strain hardening and softening behaviour. The difference in behaviour of sand under initial loading, unloading and reloading is recognised by Lee (1975) and behaviour in each phase is treated separately.

3.2.1 Initial Loading

Up to the first reversal in loading, it is assumed that the response of the sand is defined by the hyperbolic stress-strain relationship formulated by Konder and Zelasko (1963) and illustrated in Fig. 3.9:

$$\tau = G_{mo}\gamma \,/\, (1 + \frac{G_{mo}\gamma}{\tau_{mo}}) \tag{3.8}$$

in which τ is the shear stress corresponding to a shear strain amplitude γ, G_{mo} is initial shear modulus, and τ_{mo} is the maximum shear stress which can be applied to sand in the initial state without failure.

Finn et al. (1977) suggest evaluating the values of G_o and τ_{mo} from the equations proposed by Hardin and Drnevich (1972):

$$G_{mo} = 14760 \frac{(2.973-e)^2}{1+e} (\frac{1+2k_o}{3})^{\frac{1}{2}} \sqrt{\sigma'_v} \tag{3.9}$$

$$\tau_{mo} = (\frac{1+k_o}{2} \sin\phi')^2 - (\frac{1-k_o}{2})^{\frac{1}{2}} \quad \sigma'_v \tag{3.10}$$

where e is the void ratio with a maximum value of 2.0, σ'_v is vertical effective stress in psf., k_o is the coefficient of earth pressure at rest, and ϕ' is effective angle of shearing resistance.

3.2.2 Unloading and Reloading

While a hyperbolic stress-strain relationship is considered suitable to describe the initial loading curve, the hysteresis loop that

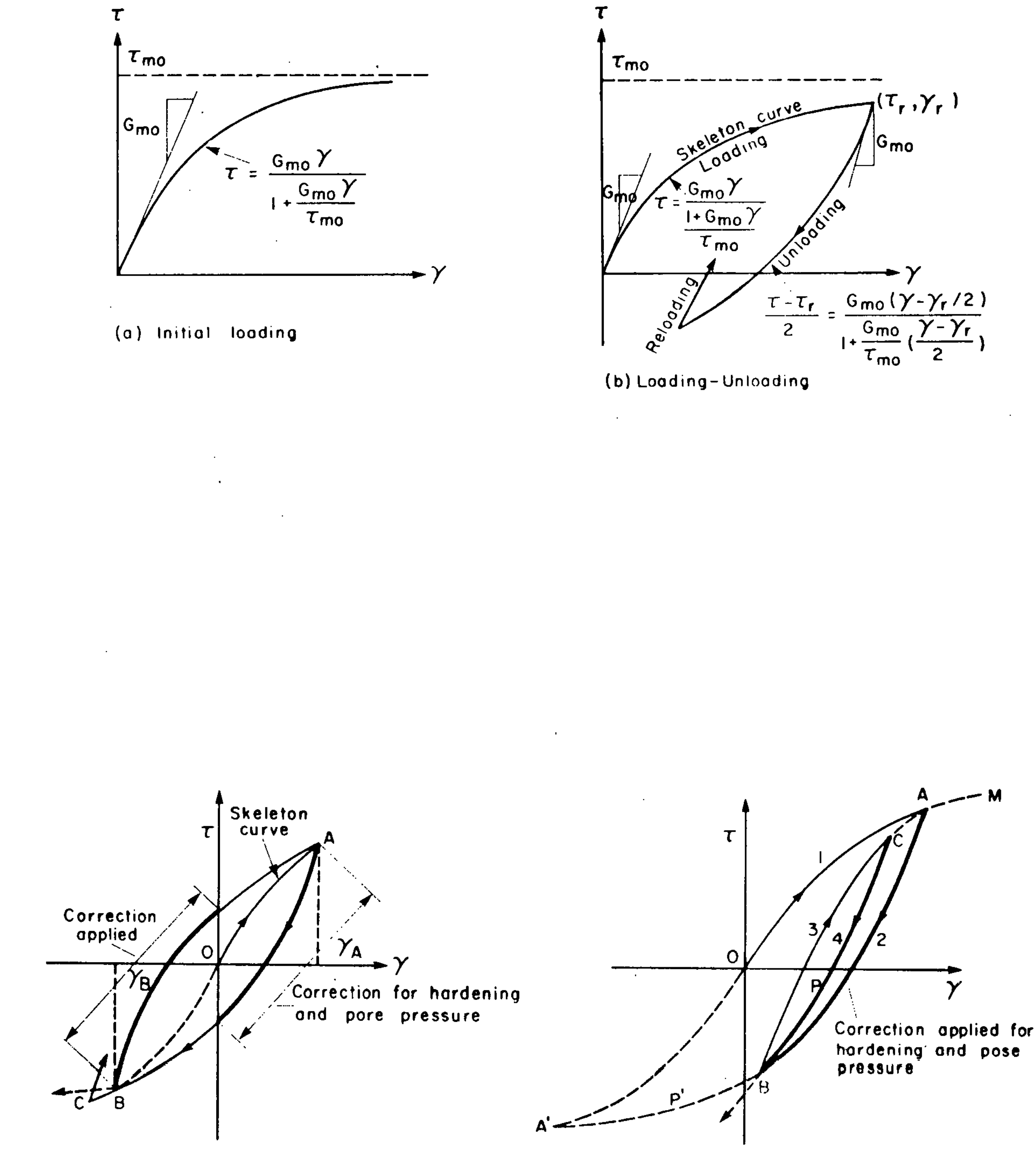

(c) For first loading cycle

(d) Generalised loading pattern

FIG. 3.9 Stress-Strain Relationship by Finn, Lee and Martin (1977).

appears to simulate the actual behaviour of sand during cyclic loading can be constructured by the rule suggested by Masing (1936). The rule is generally stated as: the shape of the unloading and reloading curve is the same as that of the initial loading curve except that the scale is enlarged by a factor of two. If the initial loading curve is described by a function, $\tau = f(\gamma)$, and loading reversal occurs at (γ_r, τ_r), then the stress-strain curve for subsequent unloading and reloading from a reversal point is

$$\frac{\tau - \tau_r}{2} = f\left(\frac{\gamma - \gamma_r}{2}\right) \tag{3.11}$$

Such behaviour is shown in Fig. 3.9(b).

Lee (1976) proposes the following rules for general stress-strain conditions:

1. The unloading and reloading curves should follow the initial loading curve if the previous maximum shear strain is exceeded. In Fig. 3.9(c) the unloading path beyond point B will lie on the extended skeleton curve.

2. If the current loading or unloading curve intersects the curve described by the previous loading or unloading curve, the stress-strain relation will follow the previous curve. Newmark and Rosenblueth (1971) suggest the same behaviour. (In Fig. 3.9(d) at point B, after path 4 the curve will follow path BA'.)

The above two rules require that the model refer to the coordinates of the greatest excursion in either direction. The coordinates are also required for descending sequences of strains.

3.2.3 Influence of Hardening and Porewater Pressure

During the process of cyclic shear stress or strain on dry sand or saturated sand under drained conditions, interparticle slip results in volumetric strain and shear modulus gradually increases with increasing volumetric strain as shown in Fig. 3.10. Martin et al. (1974) suggest incorporating the effect of hardening in the stress-strain relationship. It is proposed that the stress-strain relationship be a function of cummulative volumetric strain. For a given volumetric strain, ε_{vd}, the smoothed shear stress and strain curve can be approximated by hyperbola, and

$$\tau_{hv} = \frac{\gamma\sqrt{\sigma_v'}}{a+b\gamma} \quad \text{where} \quad a = A_1 - \frac{\varepsilon_{vd}}{A_2+A_3\varepsilon_{vd}} \tag{3.12}$$

$$b = B_1 - \frac{\varepsilon_{vd}}{B_2+B_3\varepsilon_{vd}}$$

and A_1, A_2, A_3, B_1, B_2 and B_3 are constant for a given sand at a given relative density, σ_v' is effective vertical stress and τ and γ are the shear stress and shear strain.

Lee (1975) suggests a simpler and more efficient way to relate shear modulus, shear stress and cummulative volumetric strain as follows:

$$G_{mn} = G_{mo}\left[1 + \frac{\varepsilon_{vd}}{H_1+H_2\varepsilon_{vd}}\right] \tag{3.13}$$

and

$$\tau_{mn} = \tau_{mo}\left[1 + \frac{\varepsilon_{vd}}{H_3+H_4\varepsilon_{vd}}\right] \tag{3.14}$$

where G_{mn} is maximum shear modulus in the n^{th} cycle,

τ_{mn} is maximum shear stress in the n^{th} cycle,

ε_{vd} is volumetric strain up to the n^{th} cycle, and

H_1, H_2, H_3, H_4 are hardening constants.

The stress-strain behaviour is now completely defined by equations (3.10),(3.11),(3.13) and (3.14) for the cyclic drained condition.

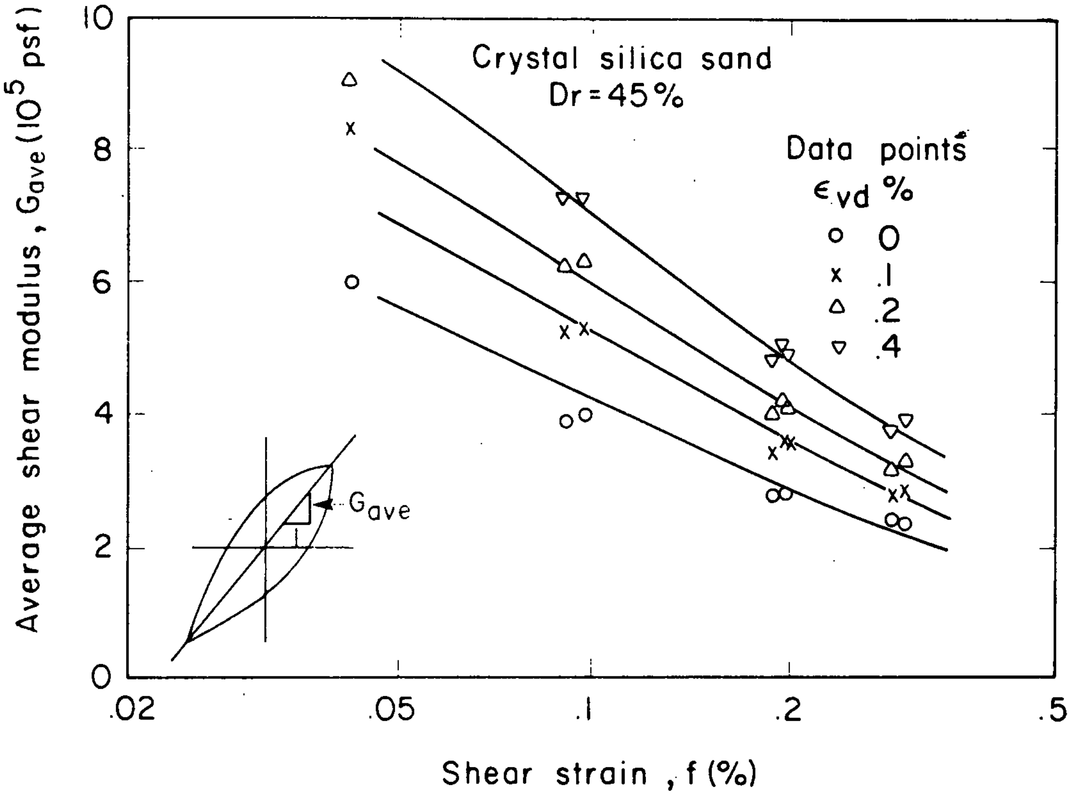

FIG. 3.10 Av. Shear Modulus vs. Shear Strain for Various Volumetric Strains.

Using the proposed stress-strain law, Finn et al. (1977) calculate the stress-strain behaviour of Crystal Silica Sand in a strain controlled drained condition and compare it with experimental data. This comparison is shown in Fig. 3.11 for the 2nd and 4th cycles of loading where the theoretical stress-strain loops appear to be a good approximation of the measured stress-strain loops. This suggests that the assumptions that the skeleton curve is hyperbolic, unloading and reloading curves are Masing, and shear modulus, shear stress are functions of cummulative volumetric strain are realistic.

To incorporate the effect of porewater pressure, it is suggested that equations (3.17) and (3.18) be modified to read:

$$G_{mn} = G_{mo} \left(1 + \frac{\varepsilon_{vd}}{H_1 + H_2 \varepsilon_{vd}}\right) \left(\frac{\sigma'_v}{\sigma'_{vo}}\right)^{\frac{1}{2}} \tag{3.15}$$

$$\tau_{mn} = \tau_{mo} \left(1 + \frac{\varepsilon_{vd}}{H_3 + H_4 \varepsilon_{vd}}\right) \frac{\sigma'_v}{\sigma'_{vo}} \tag{3.16}$$

where σ'_{vo} is the initial vertical stress and σ'_v is the vertical effective stress at the beginning of the n^{th} cycle.

The generalised stress-strain relationships which account for hardening and porewater pressure increase are given by equations (3.10), (3.11), (3.15) and (3.16). These stress-strain relations are incorporated in the dynamic effective stress method of Finn et al. (1977).

Can the strain hardening effect occur during undrained conditions in which the potential volumetric strains (plastic) are absorbed by rebound, or is it postponed until the volumetric strains develop after drainage? In the critical state theory of Schofield and Wroth (1967) the strain hardening is considered to occur in clays in undrained shear and, therefore, the area enclosed by the yield surface increases. Finn

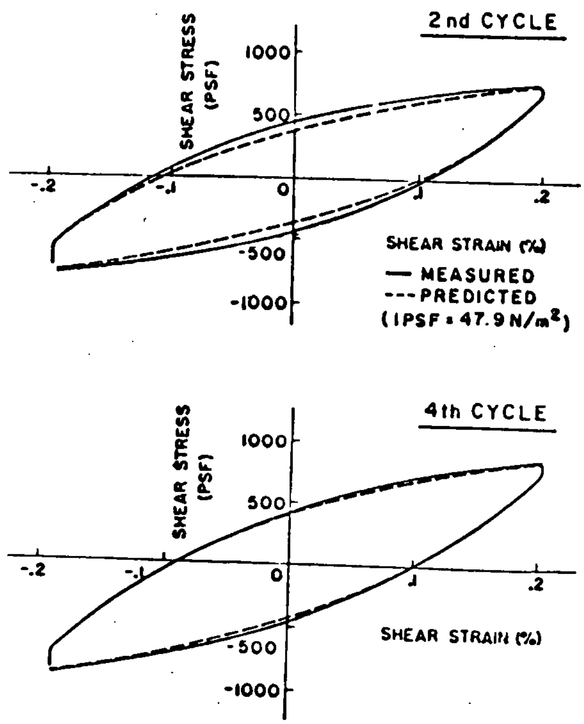

FIG. 3.11 Comparison Between Predicted and Measured Stress-Strain Curve.

et al. (1977) suggest that, since the major contribution to strain hardening comes from the generation of a stable structure due to inter-particle slip, rather than from increased density, hardening should occur under undrained conditions. It is further assumed that strain hardening under drained and undrained cyclic shear should be the same, although in applying their method in engineering practice they were not including strain hardening effects for undrained conditions. It is felt that it is still not settled whether strain hardening should be included in the undrained condition.

Correction for hardening and porewater pressure are made only during the unloading phases as shown in Fig. 3.9(c). This is based on the observation in laboratory cyclic simple shear tests, that most of the volumetric strain in dry sand and porewater pressure in undrained saturated sand occurs during the unloading portion of the load cycle. However, recently Finn et al. (1980) have showed that in cyclic drained tests, volumetric strane takes place during loading and unloading phase for the first few cycles, and later on most of the volumetric strain takes place during the unloading phase as shown in Fig. 3.12. Correction of the stress-strain curve should be made continuously over the loading and unloading phases.

3.3 VERIFICATION OF CONSTITUTIVE RELATIONSHIPS

The porewater pressure model and stress-strain relations are verified by Finn et al. (1977) for the cyclic undrained stress controlled test. For porewater pressure computation, both strain hardening and softening behaviour is considered and computed results agree well with the experimental data (Finn et al., 1977). However, the performance of the model is only verified by a liquefaction strength curve. Moreover,

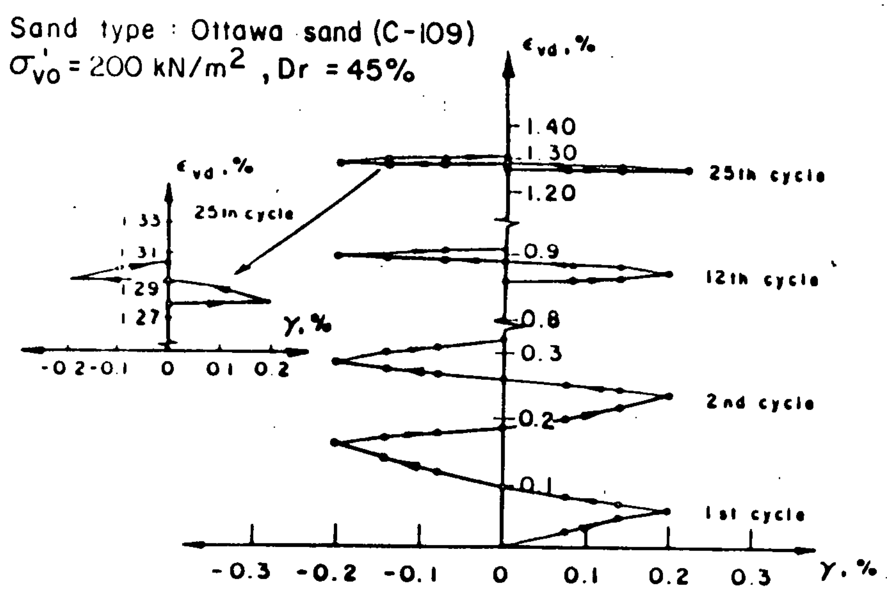

FIG. 3.12 Volumetric Strain Variation with Cyclic Shear Strain in Drained Tests (After Finn et al, 1980).

the simple shear equipment employed to perform the undrained test had a considerable shear equipment employed to perform the undrained test had a considerable amount of compliance and as Finn and Vaid (1977) show, the presence of compliance considerably affects the pore pressure[7] response. Hence, it is important to verify the pore pressure predictive capacity against experimental data obtained under constant volume conditions. With the modification of cyclic simple apparatus at the University of British Columbia by Finn and Vaid (1977) to perform drained constant volume cyclic simple shear, it is possible to carry out a constant volume test and make this comparison. It is further important to check whether this model can accurately predict the history of development of porewater pressure in undrained stress controlled tests and not just the liquefaction strength curve. From a practical point of view, it is very important to check whether this model can make any useful predictions for overconsolidated sand.

3.4 DISCUSSION

The constitutive relationships used for effective stress analysis by Finn et al. (1977) require the verification of the basic assumptions of the model. This would consist of providing adequate and experimentally based answers to the following questions:

1. Are volumetric strains in undrained tests the same as that of drained tests when both samples are identical and subjected to the same shear strain history?
2. In constant strain cyclic loading tests, is there a unique relationship between volume changes in drained tests and porewater pressure in undrained tests?
3. Can $\bar{E}_r$ be measured statically?

---

[7]Refer to Appendix I for details.

4. Can the model accurately predict the history of development of porewater pressures in constant stress tests and not just the liquefaction strength curve?

5. Does strain hardening occur during undrained tests?

6. Can the model predict the effect of strain history under previous loading?

7. Can the model make useful predictions for over-consolidated sand under stress control conditions?

8. Finally, can the model make useful predictions of porewater pressures under general loading and drainage condition in simple shear?

CHAPTER 4

VERIFICATION OF CONSTITUTIVE RELATIONSHIPS FOR EFFECTIVE STRESS MODEL

This chapter undertakes the verification of the fundamental assumptions of the model by Martin et al. (1975). First, that the plastic volumetric strains which develop during an undrained simple shear test are the same on the volumetric strains which would develop in a drained simple shear test and, second, that there is a unique relationship between volumetric strains in drained tests and porewater pressures in undrained tests when tests are performed on a given sand and use the same shear strain histories.

In 1976, Finn and Vaid showed that in a constant volume cyclic simple shear test, the reduction in effective pressure is equivalent to the increase in porewater pressure in the corresponding undrained test. They also observed that the constant volume test is almost free of compliance and has an extraordinarily high degree of reproducibility and consistency. In this study, Martin's model is verified using the effective stress data from constant volume test instead of porewater pressure data from undrained test. For these constant volume (undrained) tests, the change in effective stress is referred to as an increase in porewater pressure.

To verify the performance of the pore pressure model, required sand characteristics such as volume change behaviour during cyclic shearing in the drained condition and rebound characteristics are measured. Rebound characteristics of sand are measured under both static unloading conditions, as suggested by Martin et al. (1975), and dynamic conditions. A comparison of dynamic and static rebound characteristics is made and a correction factor proposed by which the static rebound modulus can be modified so that it is suitable for pore pressure effective stress prediction in the undrained constant volume cyclic loading condition. The effective stress predictive capacity of the model is evaluated for stress controlled undrained tests and for tests with irregular cyclic loading histories representative of earthquake loading.

The constitutive relationships for the nonlinear, hysteretic stress-strain behaviour of sand as proposed by Lee (1975), when coupled with the porewater pressure model, are used to predict pore pressure response in stress controlled undrained tests. Moreover, the performance of the pore pressure model and stress-strain relationship is evaluated for samples with previous strain histories.

4.1 VERIFICATION OF FUNDAMENTAL ASSUMPTIONS

To verify that the plastic volumetric strains are the same under undrained and drained cyclic loading conditions, a series of experiments has been performed where plastic volumetric strains occurring in undrained and drained samples were measured. One typical set of these experiments is shown in Fig. 4.1(a) and (b). Two samples prepared in exactly the same manner are consolidated to a vertical confining stress, $\sigma'_{vo} \simeq 210.0$ kN/m^2. The resulting volumetric strains during initial consolidation are shown in Fig. 4.1(a) and (b) by curve A.

The first sample, tested under undrained (constant volume) conditions, is subjected to 21 cycles of $\gamma = 0.198\%$. Due to cyclic shearing the vertical effective stress decreases from 209.0 kN/m^2 to 15 kN/m^2, shown in Fig. 4.1(b) as curve B. The second sample is also subjected to 21 cycles of $\gamma = 0.198\%$ but under drained conditions, which results in a plastic volumetric strain of the order of 0.975%. Since both drained and undrained samples are subjected to exactly the same cyclic shear strain history, it is

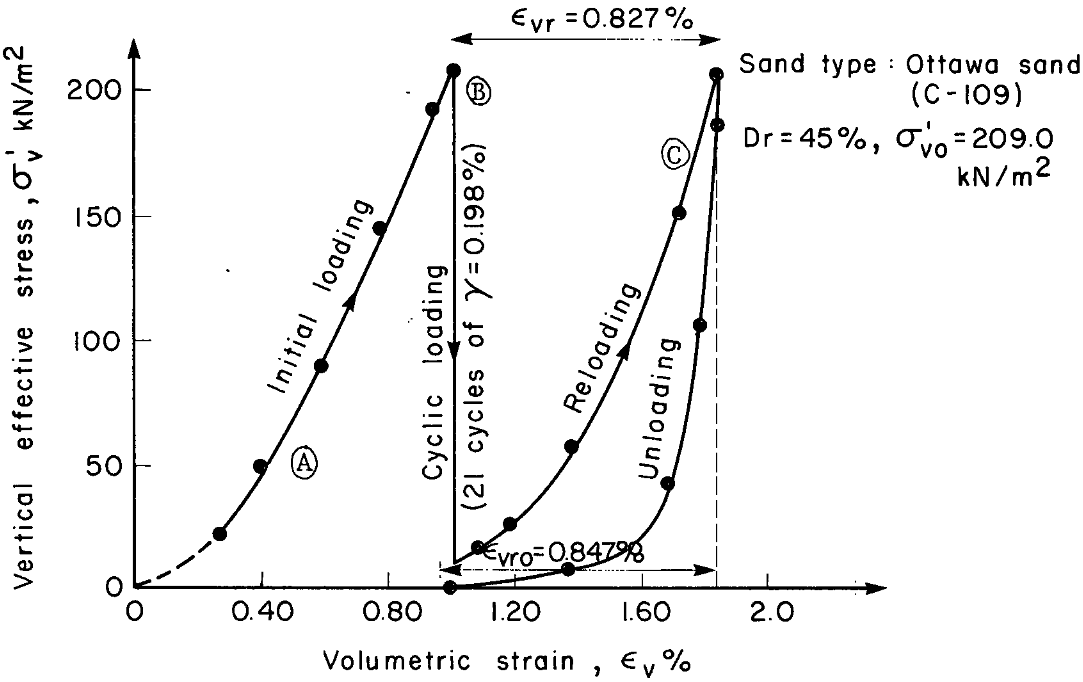

FIG. 4.1(a) Vertical Effective Stress vs. Volumetric Strain for Strain Controlled Undrained Tests.

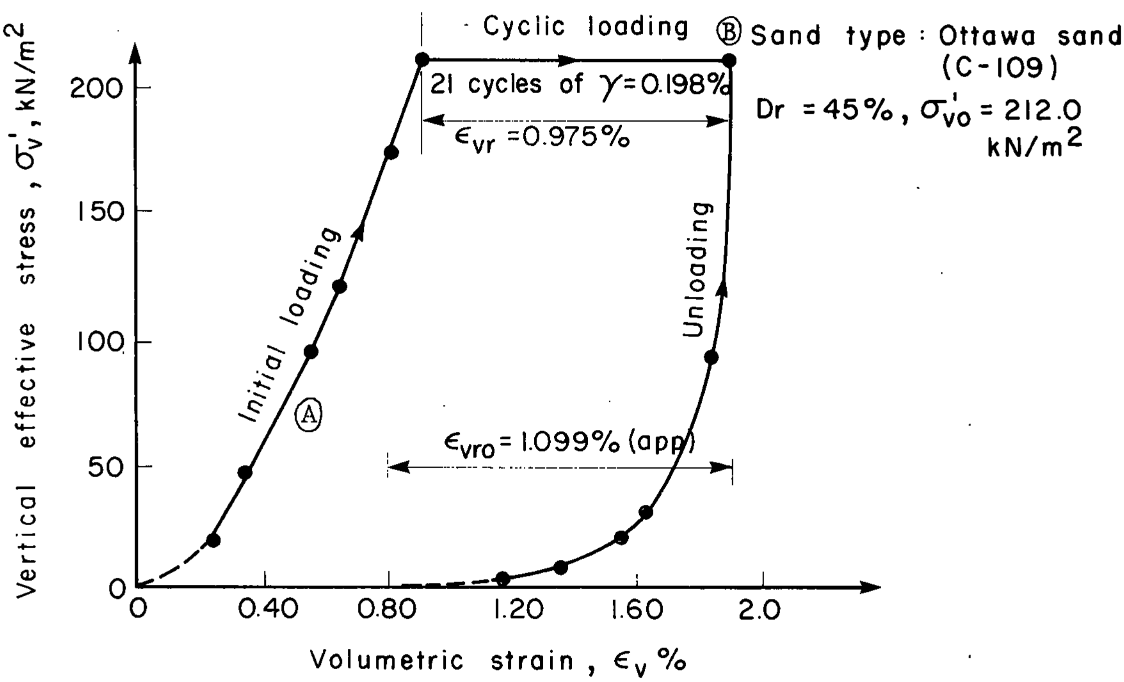

FIG. 4.1(b) Vertical Effective Stress vs. Volumetric Strain for Strain Controlled Drained Tests.

conceivable that the porewater pressure developed in the undrained test is a consequence of a plastic volumetric strain of 0.975% (as occurs in the drained condition). In order to measure the plastic volumetric strain occurring in the undrained test, the sample is allowed to drain after cyclic shearing and the resulting volumetric strains measured (see curve C in Fig. 4.1(b)). The plastic volumetric strain measured in the undrained test is 0.847% which is 85% of that measured in the drained test. This lack of complete correspondance may be due to one or more of the following factors:

1. The process during which the plastic volumetric strains are recorded is different in the drained and undrained tests. During the drained test, volumetric strains are measured when sand particles are undergoing cyclic shearing, whereas in the undrained condition the plastic volumetric strains are measured after cyclic shearing has ceased.
2. Frictional forces acting at the sides of the simple shear equipment may resist the recovery of plastic volumetric strains in the undrained test.
3. The sample used for the undrained test is not exactly similar to that used for the drained test. It can be noted from Fig. 4.1(a) and (b) that the volumetric strains due to initial consolidation are different.

However, the experimental data obtained in the drained and undrained conditions when both samples are subjected to 1,3,5 and 10 cycles of $\gamma = 0.198\%$ show that the plastic volumetric strains in the undrained condition are generally 80 to 85% of those observed in the drained condition. It is felt that the 20 to 15% difference in volumetric strains in drained and undrained conditions may be due to the three reasons mentioned above and it is justified to conclude that plastic volumetric strains in undrained conditions are the same as those in the drained conditions when both the drained and undrained samples are subjected to the same shear histories.

To verify the existence of a unique relationship between volumetric change under drained conditions and porewater pressures under undrained

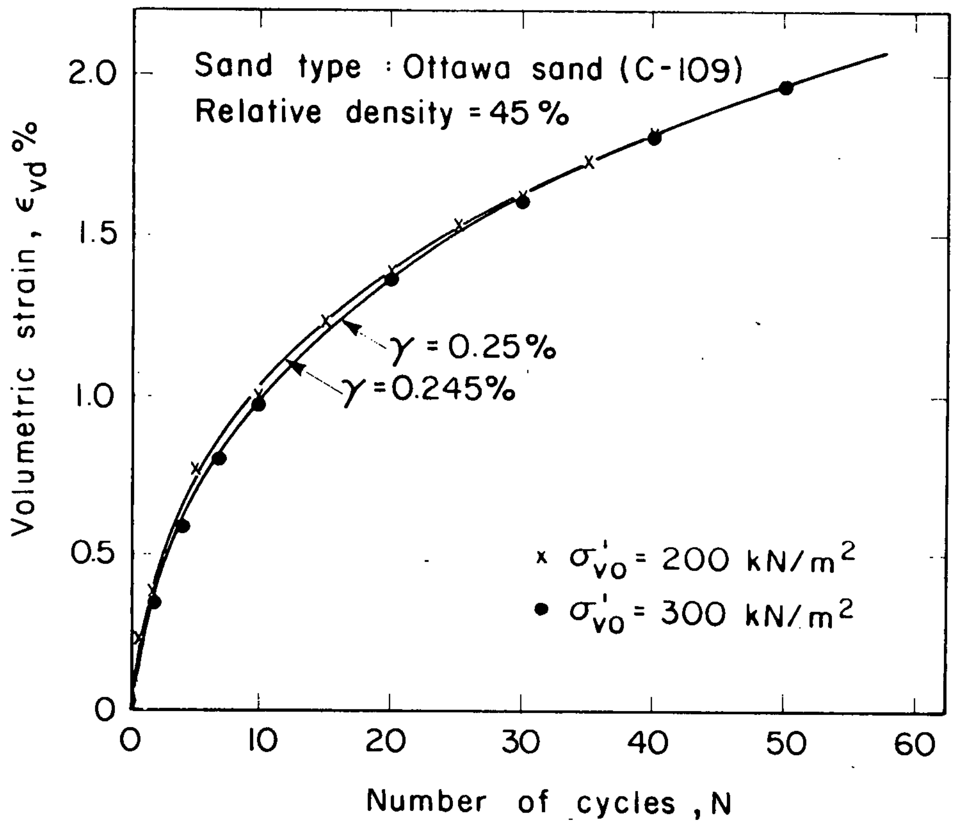

FIG. 4.2 Plot Between Volumetric Strain vs. Number of Cycle for Constant Cyclic Shear Strain Test on Loose Ottawa Sand (C-109).

conditions for samples with the same strain history, strain controlled tests in both drained and undrained conditions have been performed. In drained tests on Ottawa sand, volumetric strain are measured while sample consolidated to 200 kN/m^2 and 300 kN/m^2. The results presented in Fig. 4.2, show that the resulting volumetric strains are independent of confining stress.

Experiments for the undrained strain controlled condition have been performed on sand specimens identical to those used in the drained condition. Volumetric strains, ε_{vd}% are plotted against the porewater pressure ratio, u/σ'_{vo}, in Figs. 4.3 and 4.4 for Ottawa sand at D_r = 45% and 60%, respectively, where each point represents the corresponding value of these variables for a given number of cycles of constant strain amplitude. For example, in Fig. 4.2 point A represents the state of the volumetric strain, ε_{vd}%, due to 2 cycles of shear strain amplitude of γ = 0.10%, and the porewater pressure ratio, u/σ'_{vo}, developed due to 2 cycles of shear strain γ = 0.10%. From Fig. 4.3, it can also be seen that there is a slight deviation in shear strain level amplitudes used for drained and undrained tests, the difference ranging from 0% to 5% but this is not considered significant. This scatter is due to the slight difference in relative densities for the drained and undrained tests.

Experimental data shown in Figs. 4.3 and 4.4 clearly indicate the existence of a unique relationship between volumetric strain in the drained condition and porewater pressure in the undrained condition. In addition, this assumption is tested for samples consolidated to a vertical confining stress, σ'_{vo} = 300 kN/m^2 as shown in Fig. 4.5.

4.2 EVALUATION OF THE PREDICTIVE CAPACITY OF THE PORE PRESSURE MODEL

To verify the predictive capacity of the porewater pressure

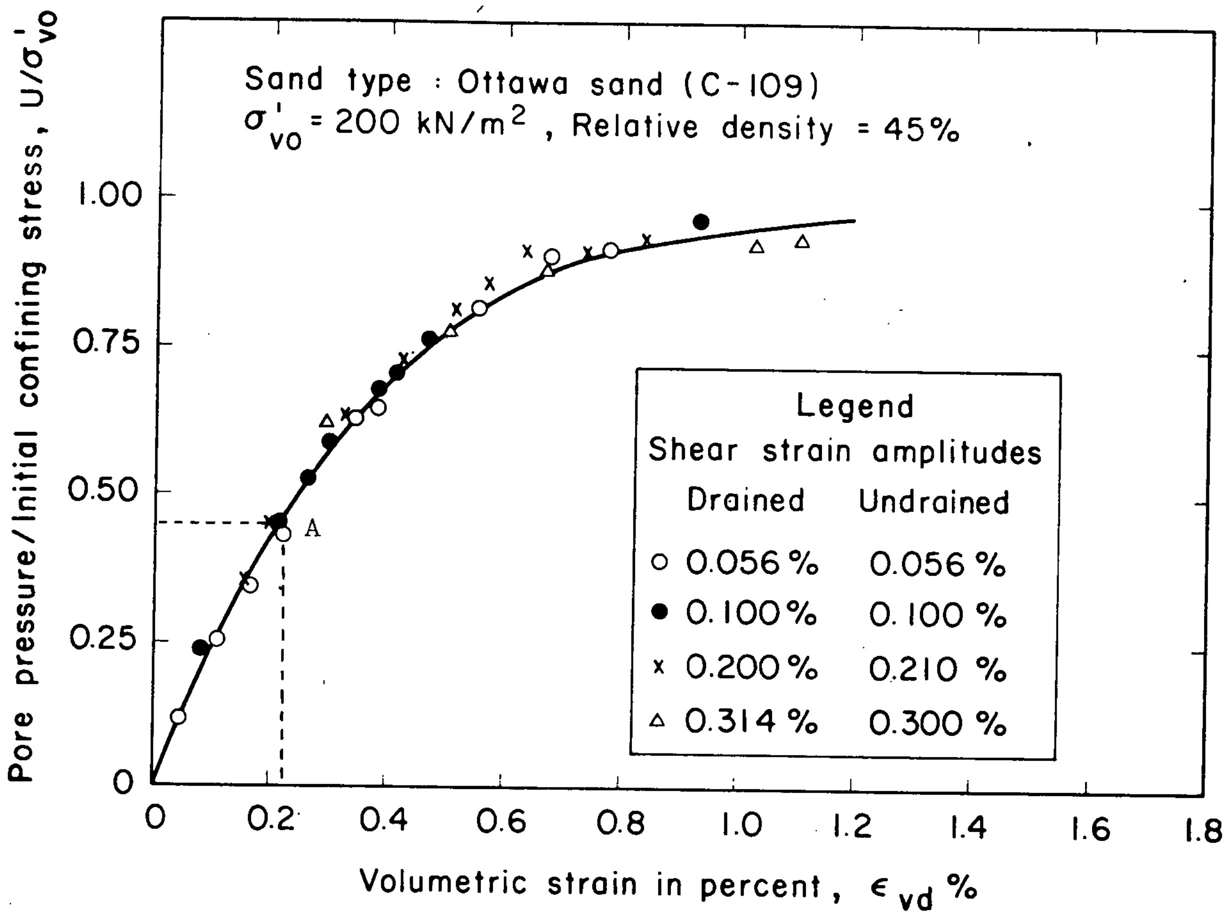

FIG. 4.3 Relationship Between Volumetric Strains and Porewater Pressures in Constant Strain Cyclic Simple Shear Tests, D_r = 45%.

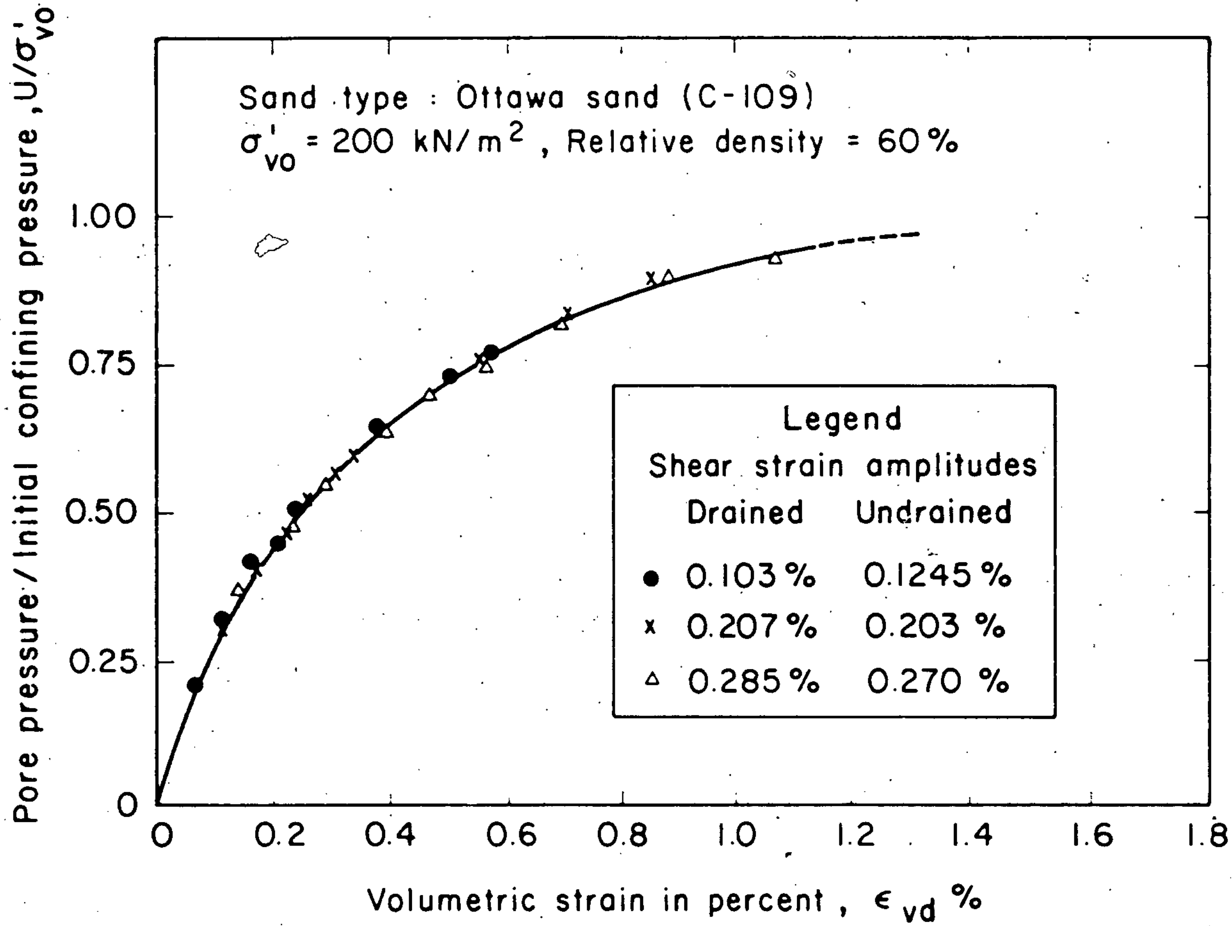

FIG. 4.4 Relationship Between Volumetric Strains and Porewater Pressures in Constant Strain Cyclic Simple Shear Tests.

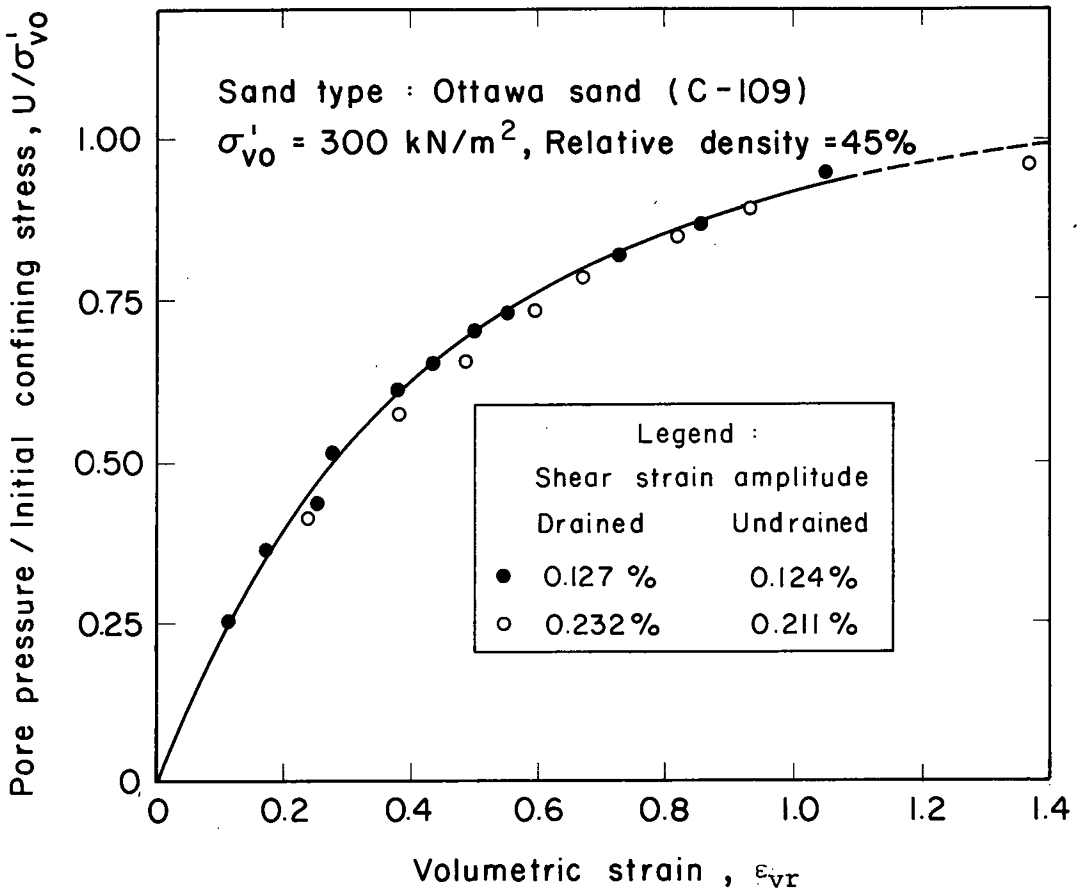

FIG. 4.5 Relationship Between Volumetric Strains and Porewater Pressures in Constant Strain Cyclic Simple Shear Tests.

model, we need the following two physical properties of the soil skeleton:

(a) volumetric change characteristics during a cyclic loading test; and

(b) rebound characteristics of sand.

4.2.1 Rebound Characteristics of Sand

The porewater pressure model in its simplest form implies that under undrained (constant volume) conditions the plastic volumetric strain, $\Delta\varepsilon_{vd}$, is equal and opposite to the elastic or recoverable volumetric strain, $\Delta\varepsilon_{vr}$.

The plastic volumetric strain increment in the undrained condition is the same as that in the drained condition as shown in section 4.1, hence, the plastic volumetric strain in the undrained condition is a known quantity. From the undrained strain controlled test, the decrease in effective vertical stress, $\Delta\sigma_v'$, caused by plastic volumetric strain, $\Delta\varepsilon_{vd}$, is also known. Therefore, the rebound modulus, E_r, corresponding to the increment of effective stress, $\Delta\sigma_v'$, is

$$\bar{E}_r = \frac{\Delta\sigma_v'}{\Delta\varepsilon_{vr}} = \frac{\Delta\sigma_v'}{\Delta\varepsilon_{vd}} = \frac{\Delta_u}{\Delta\varepsilon_{vd}} \tag{4.1}$$

Hence, to measure the rebound modulus, the increase in porewater pressure measured during a strain controlled undrained test and volumetric strains during a strain controlled drained test are required. A typical set of such data is plotted in Fig. 4.6, for samples subjected to a cyclic shear strain amplitude, $\gamma = 0.10\%$, in both drained and undrained strain controlled tests. The curve shown is called the dynamic unloading curve.

Since there is a unique relationship between pore pressure increase in the undrained condition and volumetric strain in the drained for all levels of shear strain amplitude (as shown in Figs. 4.3 and 4.4),

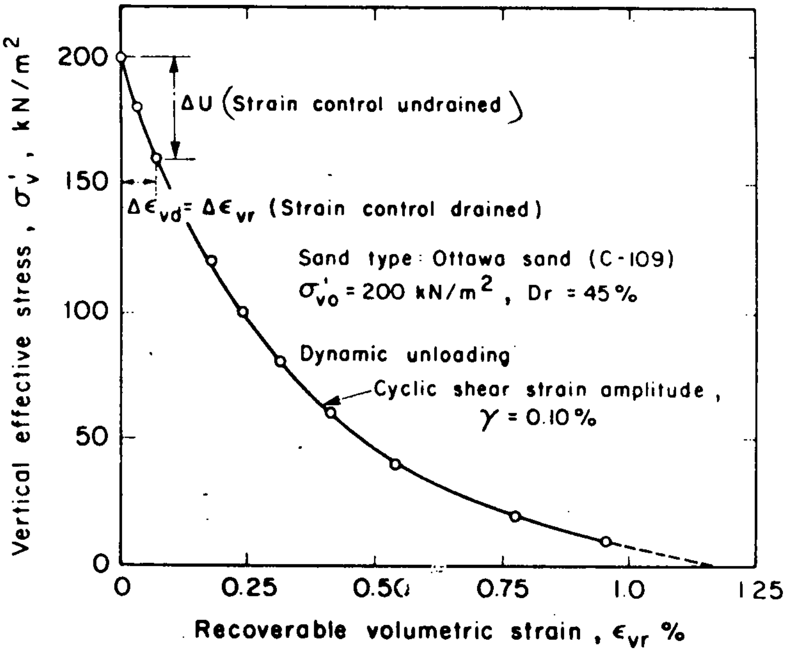

FIG. 4.6 Vertical Effective Stress vs. Volumetric Strain During Dynamic Unloading.

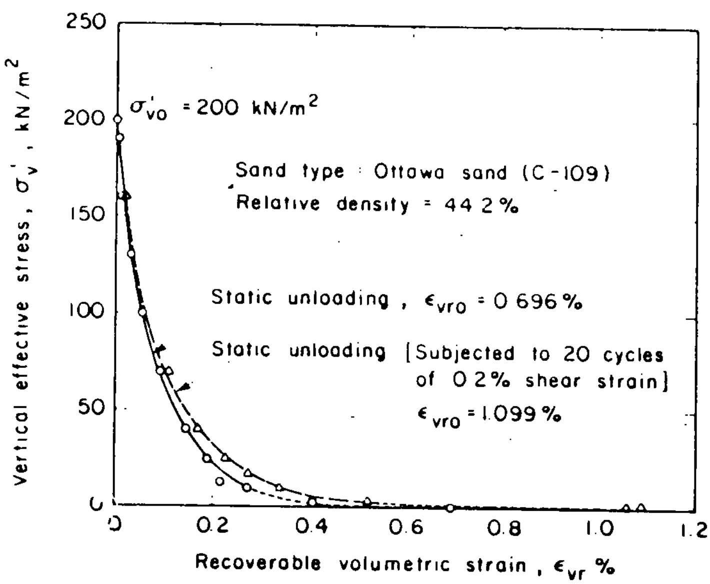

FIG. 4.7 Vertical Effective Stress σ'_v vs. Recoverable Volumetric Strain During Static Unloading Conditions.

the dynamic unloading curve is also a unique curve for all levels of shear strain amplitude. The rebound modulus, E_r, is the incremental slope of the curve shown in Fig. 4.6. Since this modulus is determined from data produced under cyclic loading conditions, it will be called the dynamic rebound modulus ($(E_r)_{dynamic}$).

Martin et al. (1975) suggest that the rebound modulus of sand under one-dimensional, laterally confined conditions should be determined from static unloading curves. In Fig. 4.7, the static unloading curve for Ottawa sand at D_r = 44.2% consolidated to a vertical effective stress of 200 kN/m^2 is shown as a solid line. From this curve, it is observed that about 80% of the total recoverable strain is measured in the last 15% of unloading. To evaluate the increase in recoverable volumetric strain due to cyclic shear prior to unloading, as discussed in section 3.1.2, a cyclic shear of 20 cycles at γ = 0.20% is applied to another sand sample before unloading. Results of this test are also plotted in Fig. 4.7 as a dotted curve.

In Fig. 4.7 results from samples with no shear strain history show a rebound modulus about 5% to 20% higher than that for the strained samples, with a difference for the last 20% unloading becoming quite marked. However, it should be noted that by measuring rebound characteristics of sand in this manner, the sand particles are not under cyclic shearing conditions.

4.2.1.1 <u>Comparison between static and dynamic rebound modulus</u>

A comparison has been made between static and dynamic unloading curves from initial vertical effective stress 200 kN/m^2 for Ottawa sand at D_r = 45%. One dynamic and two static unloading curves are plotted in Fig. 4.8. This figure clearly shows that in most of the range of vertical

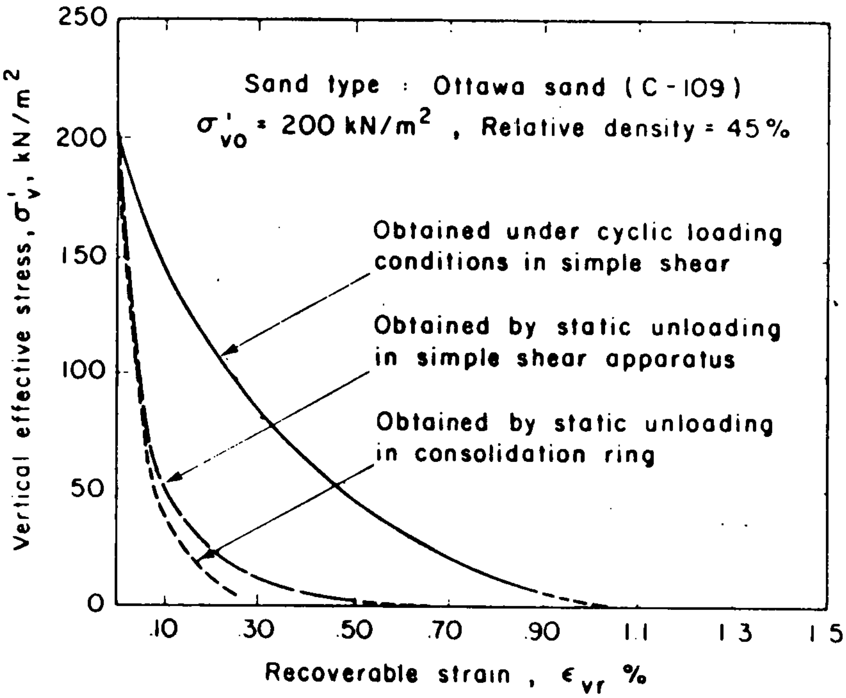

FIG. 4.8 Rebound of Ottawa Sand Under Various Loading Conditions.

effective stress, recoverable strains obtained by static unloading even with the strain history effect, are considerably lower than dynamic recoverable strain. Figure 4.9 contains a comparison between static recoverable strain without shear strain history and dynamic recoverable strain at various levels of vertical effective stress. It can be noted that, in most of the range of vertical effective stress, static recoverable strains are about 3 to 5 times smaller than dynamic strains. In other words, the static rebound modulus is about 3 to 5 times higher than dynamic rebound modulus.

The static rebound modulus is also measured by the consolidation equipment where the error due to lateral flexibility of the equipment does not influence the measurement of recoverable strains. These tests performed on loose Ottawa sand resulted in rebound modulus values 10% to 15% higher than those for identical samples in the simple shear equipment. In this case, the static rebound modulus is 5 to 5.5 times higher than the dynamic rebound modulus.

To use the pore pressure model to predict porewater pressures in stress controlled undrained tests, it is necessary to use the rebound modulus and volumetric strain for the sand under consideration. In the latter part of this chapter it is shown that pore pressure response predicted using the dynamic rebound modulus is close to experimentally determined pore pressures. From the remarks above it will be obvious that predictions using the static rebound modulus cannot be realistic.

In order to use the pore pressure model, it is necessary to evaluate the dynamic rebound modulus at various levels of vertical effective stress. For that purpose dynamic unloading curves from various levels of initial vertical effective stress are obtained. In Fig. 4.10, dynamic unloading curves from three different initial vertical effective stresses are shown. Although the curves look geometrically similar, they are not quite algebraically similar. However, by assuming one algebraic equation for all these curves, the error involved is not significant. Hence, the generalised form of the equation for dynamic rebound modulus can be of the same form as given in equation (3.7).

Experimental data similar to that shown in Fig. 4.10 can be used to calculate dynamic rebound constants m,n and k_2[1]. It should be noted that for porewater pressure verification, rather than using a generalised form similar to equation (3.7), the dynamic rebound modulus at a particular effective stress σ' is obtained by the slope of the dynamic unloading curve for a given initial vertical confining stress, σ'_{vo}.

Since the porewater pressure model requires verification of its predictive capacity for sand under various relative densities, it is necessary to obtain dynamic unloading characteristics of Ottawa sand for various relative densities. Experimental data plotted for relative densities of 45,54,60 and 68%, shown in Fig. 4.11, indicate that dynamic rebound characteristics of Ottawa sand are independent of relative density. This finding is significant since this obviates the need for measuring dynamic unloading characteristics at different relative densities.

4.2.2 Volume Change Characteristics of Sand under Cyclic Loading Conditions

In order to verify the porewater pressure model, apart from the dynamic rebound characteristics, volume change characteristics under cyclic loading in the drained condition are also required. For this purpose,

---

[1]Values of these constants will be different for static rebound modulus.

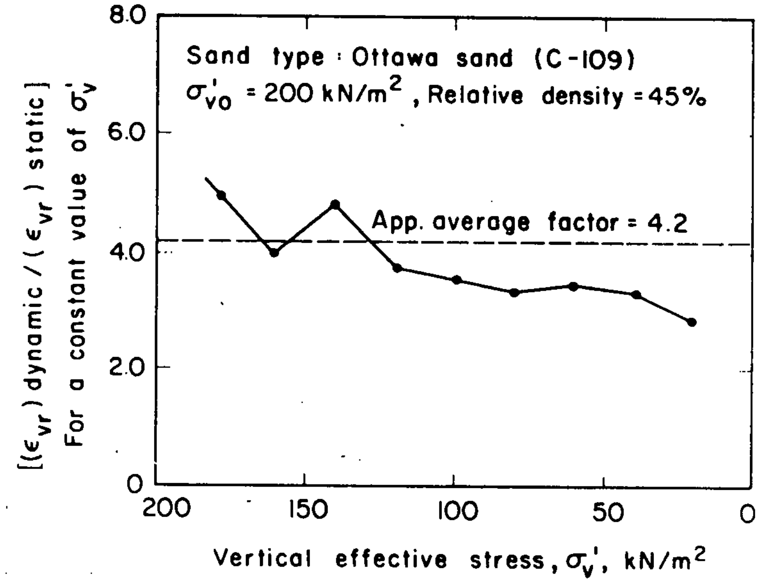

FIG. 4.9 Ratio of Dynamic Recoverable Strain to Static Recoverable Strain for Various Values of Effective Vertical Stress.

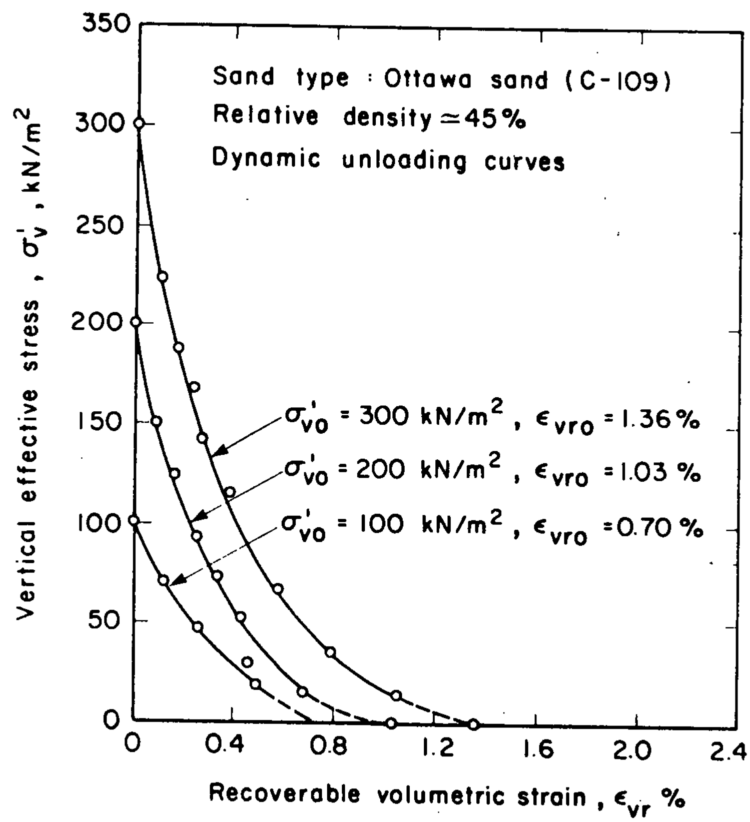

FIG. 4.10 Dynamic Unloading Curves from Three Initial Vertical Effective Stress for Ottawa Sand.

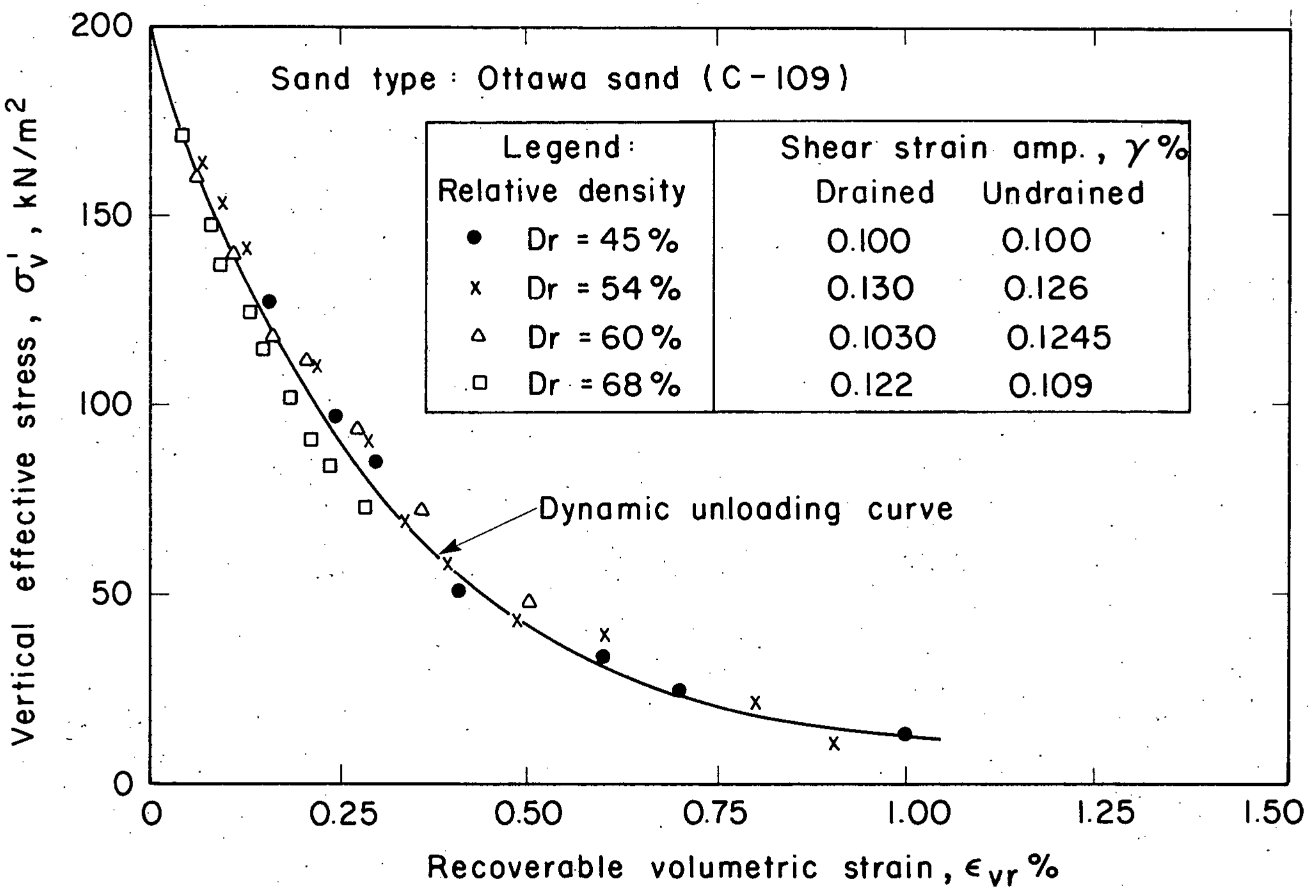

FIG. 4.11 Vertical Effective Stress vs. Dynamic Recoverable Strain for Various Relative Densities.

cyclic strain controlled tests have been performed on Ottawa sand at $D_r = 45\%$.

Experimental data from cyclic drained tests on Ottawa sand ($D_r = 45\%$) are replotted in terms of incremental volumetric strain, $\Delta\varepsilon_{vd}$, vs. cyclic shear strain amplitude, γ, for a given value of cumulative volumetric strain, $\varepsilon_{vd}\%$, as shown in Fig. 4.12. The analytical function as given in equation (3.4) is fitted with a family of curves and four volume change constants obtained which are: $C_1 = 0.913$, $C_2 = 0.462$, $C_3 = 0.161$ and $C_4 = 0.376$. The set of constants obtained give an almost exact fit with the experimental data. However, cyclic drained tests also performed at three other relative densities 54%, 60% and 68% yielded the volume change constants given in Table 4.1. During experiments on dense sand it was observed that some dilation was present within a cycle, however, the net effect of cyclic shear is a reduction in volumetric strain.

4.3 PORE PRESSURE PREDICTION

At this stage it seems best to first check the porewater pressure model before evaluating the validity of the stress-strain law. Hence, the porewater pressure response is calculated in stress controlled undrained tests by the following two procedures:

1. The shear strains measured during a stress controlled undrained test are used to calculate the incremental plastic volumetric strain, $\Delta\varepsilon_{vd}$, and hence pore pressure. Thus, the validity of the pore pressure model is checked without involving the stress-strain relationship.

2. The generated strain under stress controlled undrained conditions is calculated using the proposed constitutive relationship for stress-strain, and from that the porewater pressure is predicted.

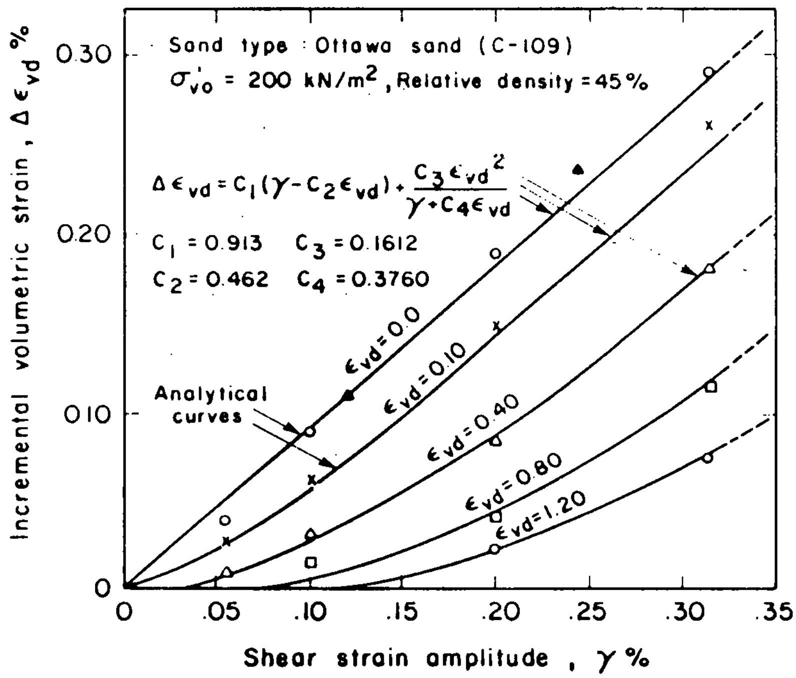

FIG. 4.12 Incremental Volumetric Strain vs. Shear Strain Amplitude for Various Levels of Cummulative Volumetric Strain.

TABLE 4.1

VOLUME CHANGE CONSTANTS FOR OTTAWA SAND (C-109)

D_r%	C_1	C_2	C_3	C_4
45	0.913	0.462	0.1612	0.376
54	0.626	0.525	0.100	0.258
60	0.467	0.658	0.100	0.235
68	0.357	1.060	0.1100	0.05

The pore pressure response is calculated for stress controlled undrained (constant volume) tests performed on Ottawa sand at D_r = 45%. During these tests, in addition to the measurement of porewater pressures, shear strains were also monitored down to a level of 0.02%. These measured shear strains are used to calculate volumetric strain from equation (3.4) with the constants given in Table 4.1 for D_r = 45%, and the dynamic rebound modulus is calculated from the slope of the dynamic unloading curve as shown in Fig. 4.3.

A comparison between predicted and measured porewater pressures is shown in Fig. 4.13 for D_r = 45%. The predictive capability of the pore pressure model appears to be very good. Hence, it can be safely concluded that the pore pressure model can predict accurate pore pressure response provided the dynamic rebound modulus is used in conjunction with incremental volumetric strains. Porewater pressures have also been calculated for two tests from strains calculated by the following equation:

$$\frac{\tau-\tau_r}{2} = \frac{G_{mn}(\gamma-\gamma_r)}{2} \Big/ \left[1 + \frac{G_{mn}(\gamma-\gamma_r)}{2\tau_{mn}}\right] \tag{4.2}$$

where G_{mn} and τ_{mn} are given by equations (3.15) and (3.16) and the definition of τ_r and γ_r is the same as that given in equation (3.11). Since G_{mo} could not be measured, both it and τ_{mo} are computed for void ratios e = 0.676 (D_r = 45%) and e = 0.628 (D_r = 60%) using the well-known Hardin-Drnevich equations (3.9).

The magnitude of G_{mn} and τ_{mn} in equation (4.2) are modified during the strain calculations for the effect of increasing porewater pressure by the equations:

$$G_{mn}/G_{mo} = (\sigma'_v/\sigma'_{vo})^{\frac{1}{2}} \tag{4.3}$$

and

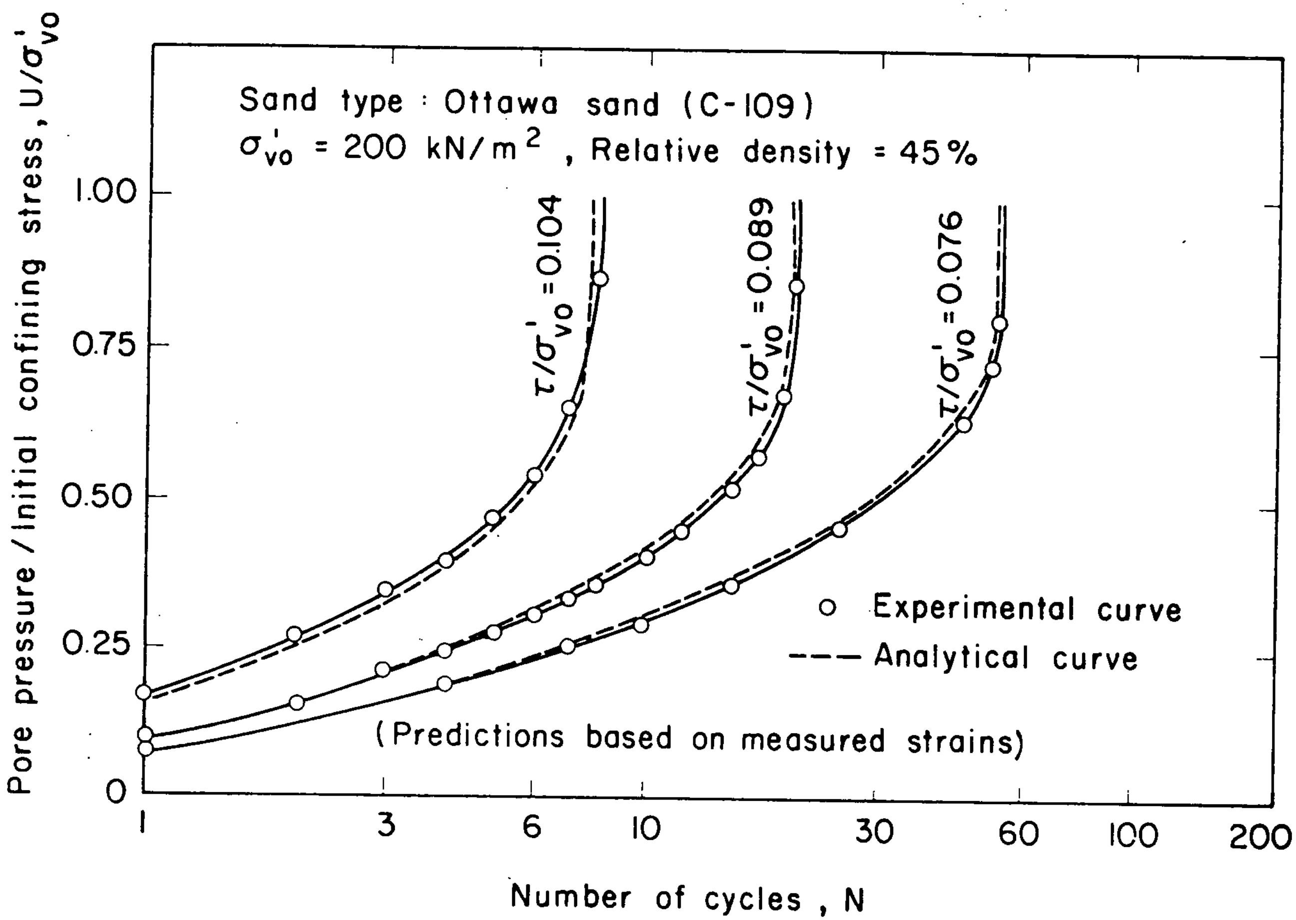

FIG. 4.13 Predicted and Measured Porewater Pressure in Constant Stress Cyclic Simple Shear Tests, D_r = 45%.

$$\tau_{mn}/\tau_{mo} = \sigma'_v/\sigma'_{vo} \tag{4.4}$$

These expressions neglect the strain hardening functions in equations (3.15) and (3.16). Neglecting strain hardening (strain history) effects for undrained tests appears justified on the evidence of Finn et al. (1970) and Seed et al. (1977) that increased resistance to pore pressure development as a result of previous loading or strain history is achieved only if dissipation of the porewater pressures caused by the previous loading is allowed. Later on, in section 4.4, the correctness of this approach will be demonstrated by comparisons between predicted and measured porewater pressures as shown in Fig. 4.14 for D_r = 45% and in Fig. 4.15 for D_r = 60%. The comparisons are quite good, although not as good as when measured shear strains have been used in the porewater pressure model. This is not unexpected since the actual initial in-situ moduli were not measured but calculated by the Hardin-Drnevich equations. It can be concluded that the constitutive relationships for the nonlinear stress-strain behaviour of sand calculate realistic shear strain history for the undrained condition, provided hardening is not included. Moreover, the constitutive relationships for the pore pressure model predict accurate pore pressures in the stress controlled undrained conditions provided instead of static, dynamic rebound modulus is used.

4.3.1 Pore Pressure Prediction for Irregular Strain History

A more severe test of the predictive capability of the pore pressure model is provided by the irregular strain history shown in Fig. 4.15(a). The computed porewater pressure response to this strain pattern is shown in Fig. 4.15(b) and is quite satisfactory. Some of the difference between experimental and analytical pore pressure curves is probably due to the fact that the irregular strain pattern has been imposed by manual

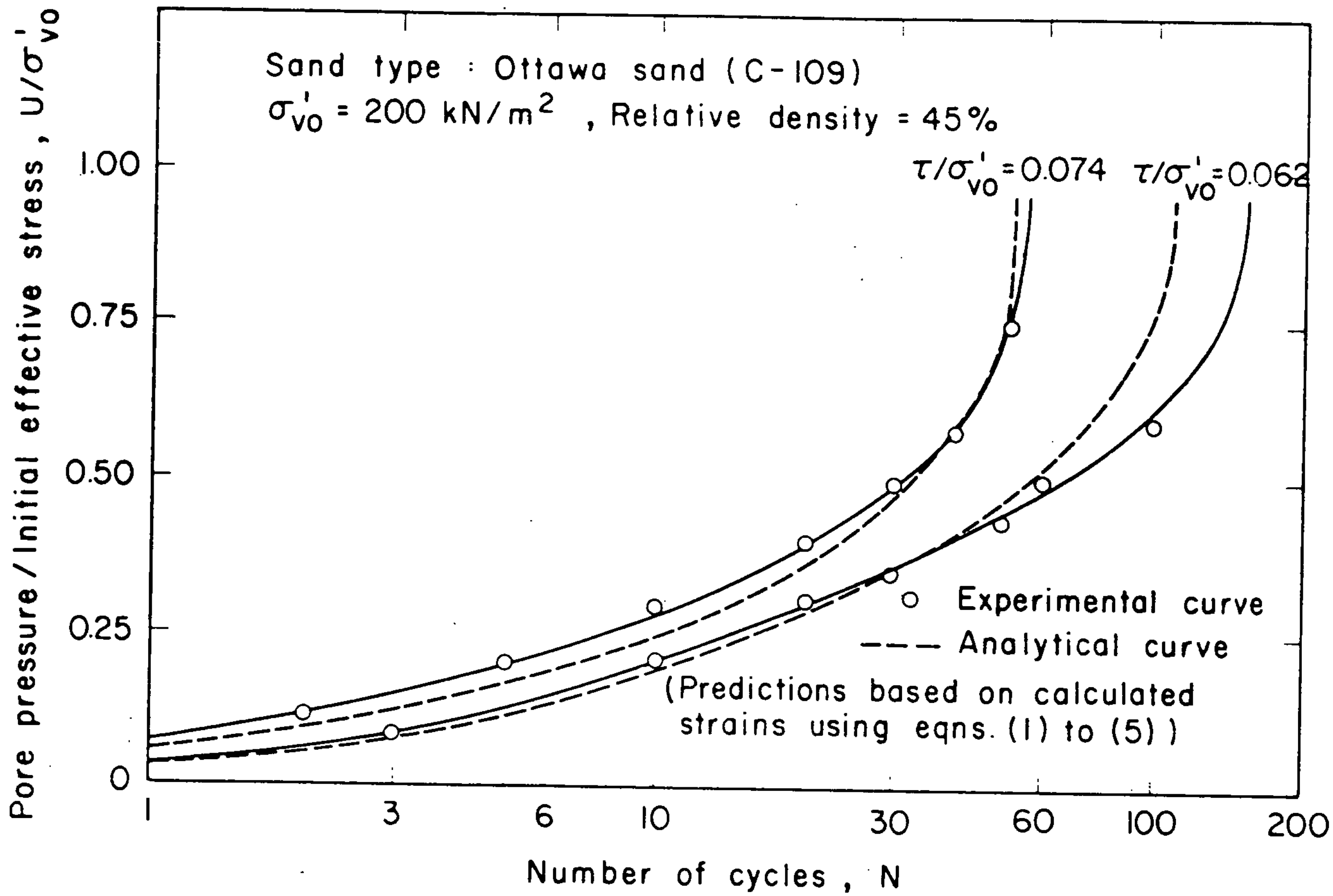

FIG. 4.14 Predicted and Measured Porewater Pressures in Constant Stress Cyclic Simple Shear Tests, D_r = 45%.

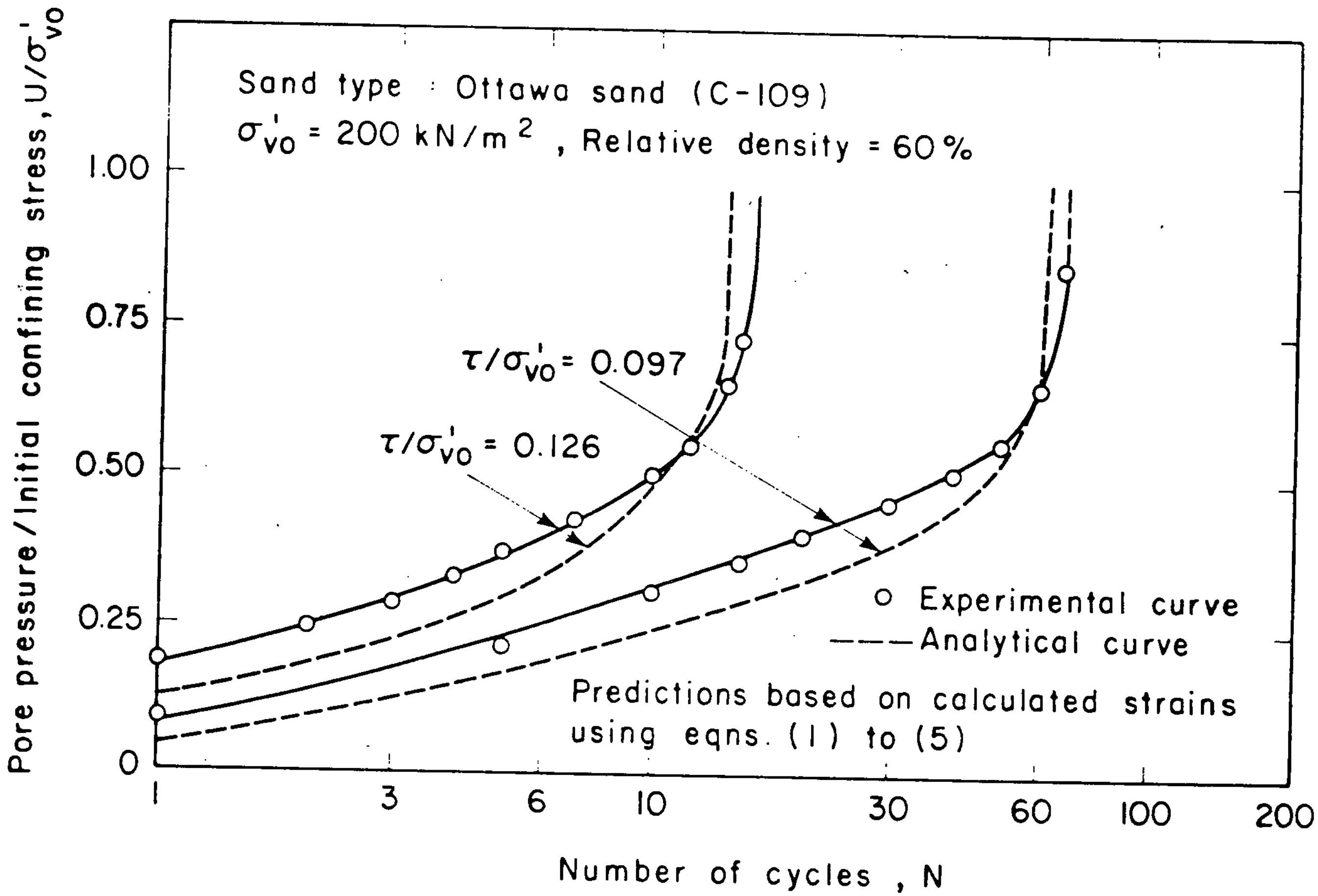

FIG. 4.15 Predicted and Measured Porewater Pressures in Constant Stress Cyclic Simple Shear Tests, D_r = 60%.

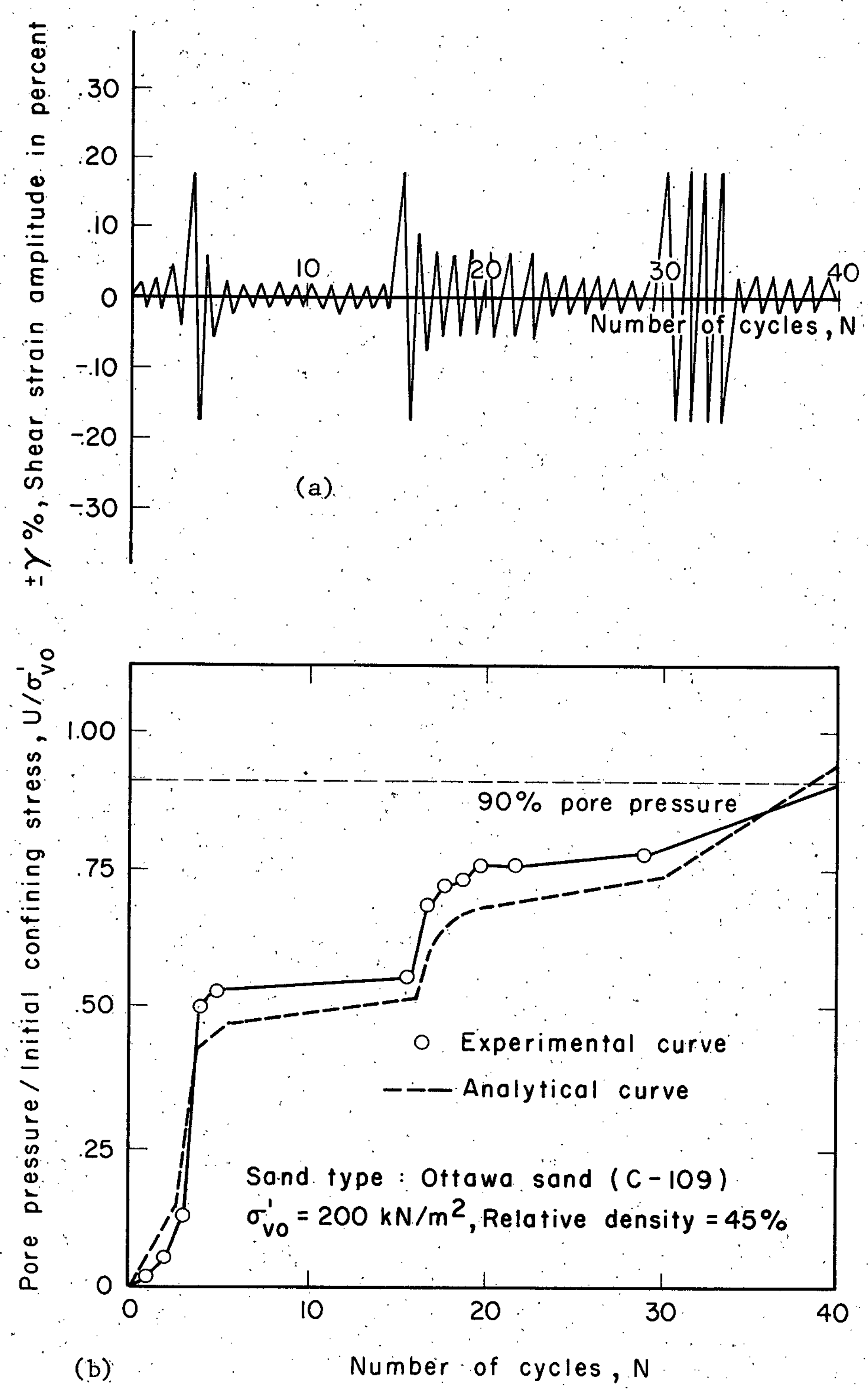

FIG. 4.16 Comparison of Calculated and Analytical Pore Pressure Ratios for Irregular Strain History.

control and not by a programmed automatic control. Thus, the measured shear strain history may not be accurate enough.

Hence, the pore pressure predictive capacity of the model is quite good for irregular strain history as generated during earthquakes.

4.4 PORE PRESSURE PREDICTION FOR SAMPLES WITH PREVIOUS STRAIN HISTORY

The primary aim of this section is to check whether the model can predict pore pressure response for samples with previous strain histories. In addition, the underlying mechanism of increase of resistive capacity against liquefaction due to prior strain history is studied.

Three series of tests are performed where samples consolidated to σ'_{vo} = 200 kN/m^2 are subjected to cyclic shear (τ/σ'_{vo} 0.04 to 0.068) until the porewater pressure ratio becomes equal to 0.30, 0.5 and 0.65, respectively. Once the desired porewater pressures are achieved, the experiment is stopped and the pore pressures allowed to drain. The net change in volumetric strain due to drainage is recorded. Next, the samples which have been subjected to previous strain histories are subjected to cyclic shear stress until complete liquefaction is reached. In Fig. 4.17 cyclic shear stress ratios used for samples with strain history are plotted against the number of cycles to liquefaction for various levels of strain histories. Figure 4.16 shows that the resistance to liquefaction increases with previous strain history and the increase is proportional to pore pressure level developed during shear strain history.

However, it should be noted that the maximum cyclic shear strain generated during strain history in these tests is always lower than 0.4%. Finn et al. (1970) suggest a threshhold value of cyclic shear strain of beyond which the resistance to liquefaction decreases due to

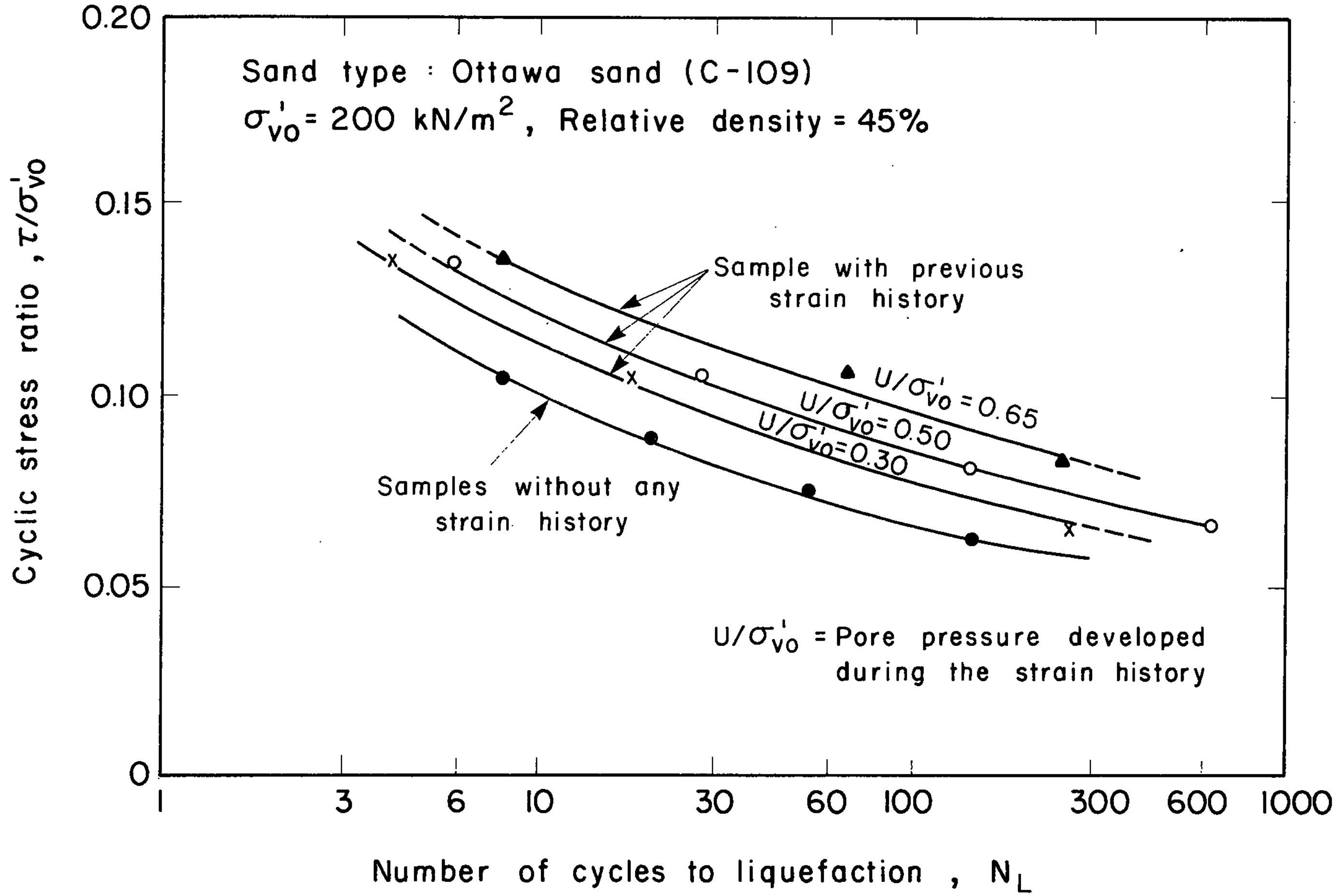

FIG. 4.17 Cyclic Stress Ratio vs. Number of Cycles to Liquefaction for Samples with Previous Strain History.

strain history. Nonetheless, it is possible that larger cyclic shear strains ($\gamma > 0.05\%$) developed during shear strain history create a structure in the sand which is more sensitive to liquefaction than the structure created by initial consolidation. However, the experimental data confirms the shared conclusion from Finn et al. (1970) and Seed et al. (1977) that resistance to liquefaction increases due to previous strain history. Such an increase in resistance is often considered due to change in particle structure, increase in lateral stress and small change in density. Although no attempt is being made in this research to measure the change in particle structure, its contribution to increase resistance is evaluated by measuring increase in lateral stress and change in density.

In Fig. 4.18 the variation of vertical effective stress against horizontal effective stress is plotted for a test in which an initially consolidated sample is subjected to 70 cycles of $\tau/\sigma'_{vo} = 0.066$ producing a pore pressure ratio of about 0.50. The sample is drained and allowed to reconsolidate to initial vertical effective stress. It can be noted from the figure that the difference, k_o, in an initially consolidated stage and after the application of the strain history is negligible. In addition, the change in relative density due to preshearing is very small (0.30%). Thus, it can be postulated that since the contribution of increase in relative density and increase in lateral stresses due to cyclic preshearing is very small for the observed increase resistance due to strain history, the primary underlying cause is the change in the particle structure of the sand.

To incorporate the influence of strain history in the constitutive relation, it is important to associate a physical variable with the underlying factors involved in increasing the resistance to pore pressure

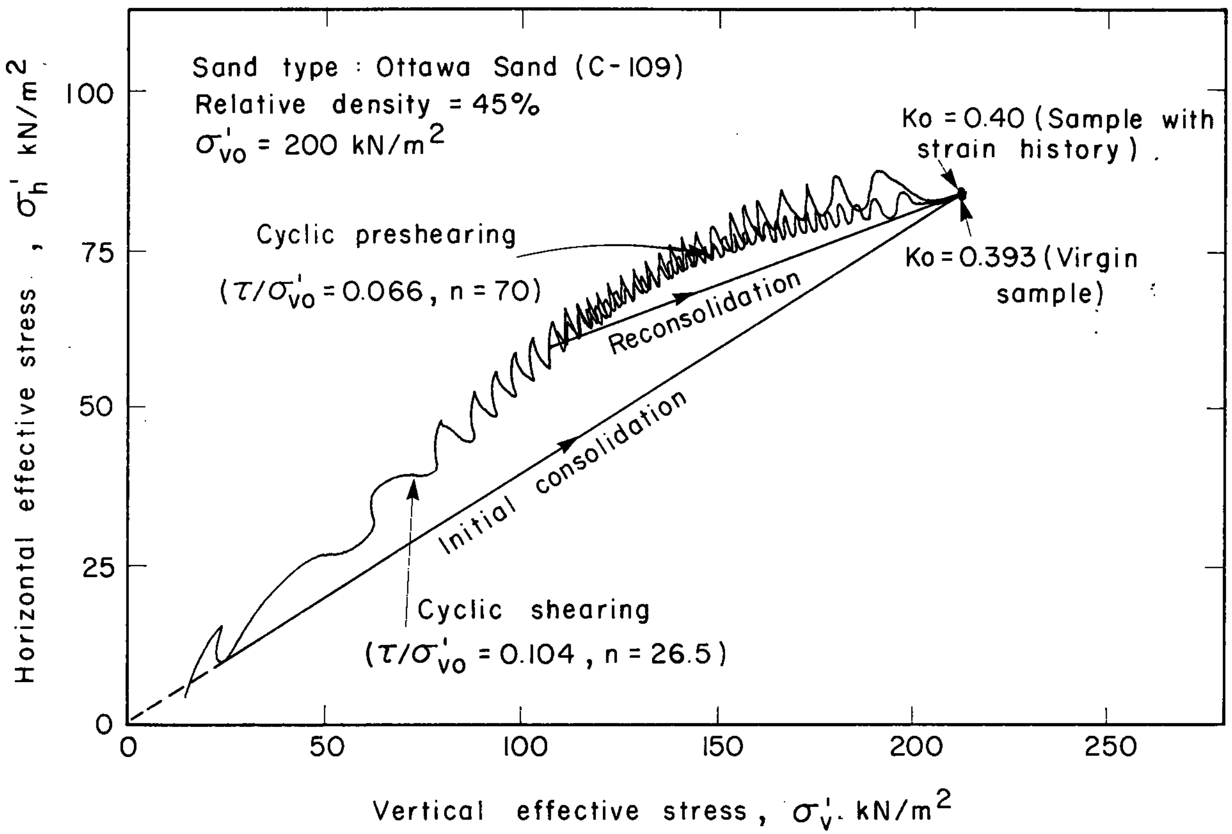

FIG. 4.18 Horizontal Effective Stress vs. Vertical Effective Stress for Cyclic Stress Controlled Undrained Test on Samples with Previous Shear Strain History.

development due to strain history. Such a variable as suggested by Martin et al. (1975) is a cumulative volumetric strain.

The cumulative volumetric strain is used as an index to account for strain hardening effects in the constitutive relationships for stress-strain behaviour of sand by Lee (1975). These relationships are used for dynamic effective stress analysis by Finn et al. (1977). It is considered that during the shear strain history no hardening occurs, but once the sample is allowed to drain a small increase in volumetric strain, ε_{vd}, can take into account a part of increase in stiffness by increasing shear moduli G_{mn} and τ_{mn} with hardening constants. In addition, the resulted volumetric strain after the strain hardening decreases the volumetric potential for the sample for further cyclic loading. The evidence of increase in stiffness of sand due to strain history is provided by Toki and Kitago (1974), who observed an increase in the static modulus of a loose dry sand which has undergone several hundred cycles of small-amplitude cyclic stress.

The evaluation of the pore pressure predictive capacity of the constitutive relations for the pore pressure model and stress-strain relationship is performed by subjecting a sample to a loading-drainage-loading sequence. Sample A at D_r = 45% is first subjected to 70 cycles of a stress ratio τ/σ'_{vo} = 0.066 and then allowed to drain. The rate of development of porewater pressure under this loading is shown in Fig. 4.19(a) by curve A. After drainage the resulting volumetric strain and change in relative density are recorded (see Table 4.2, Sample 2). The recovered potential plastic strains are used in conjunction with hardening constants to calculate modified G_{mn} and τ_{mn} (equation 3.13 and 3.14).

When Sample A is next subjected to a cyclic stress ratio

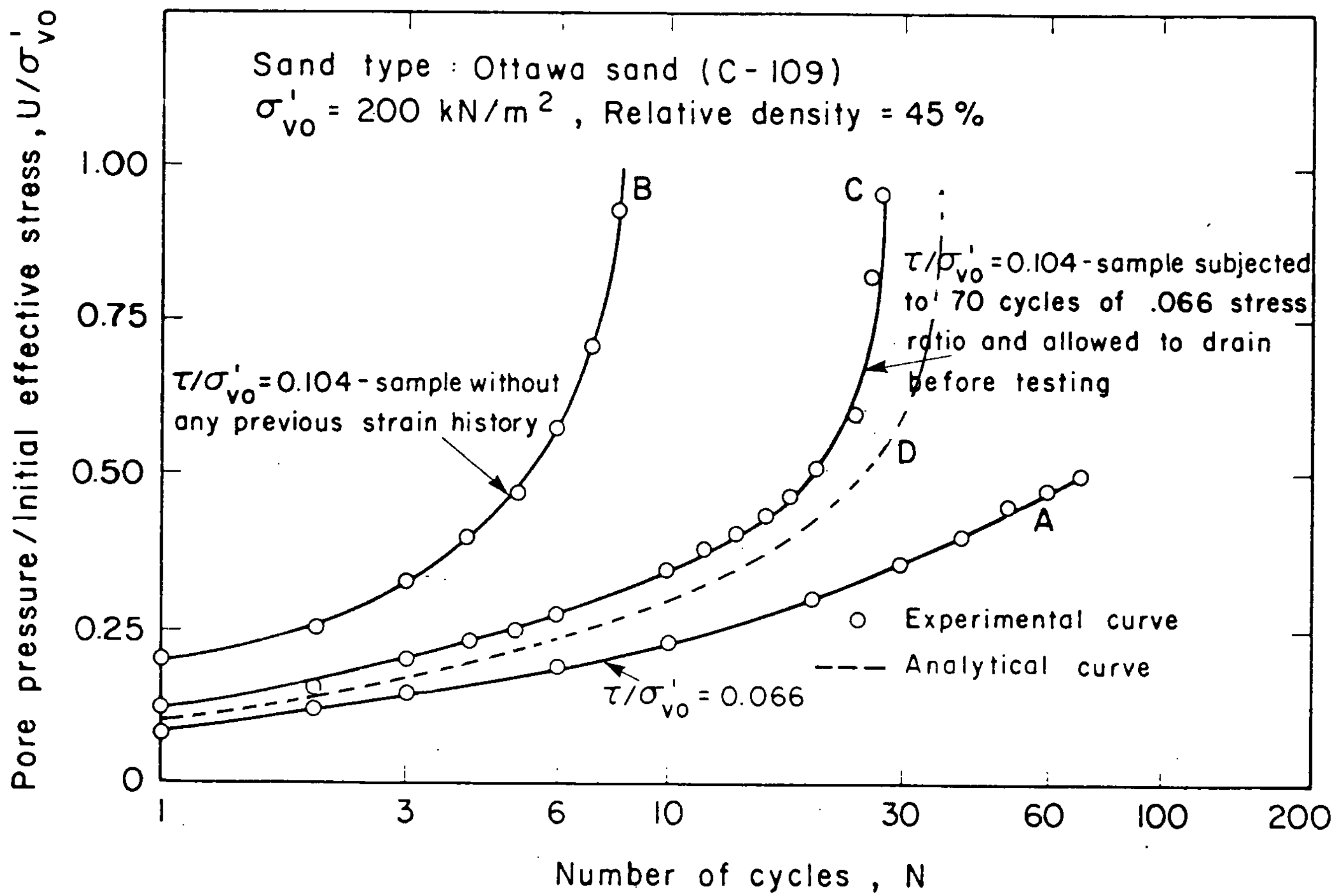

FIG. 4.19(a) Predicted and Measured Porewater Pressures in a Sand with Previous Loading History.

TABLE 4-2

INCREASE IN SHEAR MODULUS AND SHEAR STRENGTH DUE TO STRAIN HISTORY

SAMPLE NO.	Pore Pressure Ratio due to Strain History	VOID RATIOS		Change in Relative Density	Change in Volumetric Strain	$\frac{G_{mn}}{G_{mo}}$	$\frac{\tau_{mn}}{\tau_{mo}}$
		Before Strain History	After Strain History				
1	0.30	0.676	0.674	0.62%	0.108%	1.211	1.0488
2	0.50	0.678	0.675	0.94%	0.295%	1.277	1.1333
3	0.65	0.674	0.664	2.80%	0.4669%	1.445	1.2110

$$G_{mn} = G_{mo}\left[1 + \frac{\varepsilon_{vd}}{H_1 + H_2\varepsilon_{vd}}\right], \qquad \tau_{mn} = \tau_{mo}\left[1 + \frac{\varepsilon_{vd}}{H_3 + H_4\varepsilon_{vd}}\right]$$

where $H_1 = 0.947$, $H_2 = 0.394$, $H_3 = 2.212$, $H_4 = 0.0001$ for $D_r = 45\%$, Ottawa sand.

τ/σ'_{vo} = 0.104 porewater pressure develops, as shown by curve C in Fig. 4.19(a). In the same figure, curve B shows the rate of pore pressure development for a sample which has not been subjected to any shear strain history. It can be observed that the rate of development of pore pressure in Sample C is considerably less than that generated in Sample B.

To calculate the pore pressure response for Sample C, the modified values of G_{mn} and τ_{mn} for strain hardening effects are used as G_{mo} and τ_{mo} for the second application of cyclic loading and volumetric strain constants were adjusted to account for the recovered plastic potential strains which occurred during strain hardening. The softening effect of the increasing porewater pressure is also included. The predicted porewater pressure is given by curve D in Fig. 4.19(a). In Fig. 4.19(b), similar results are shown for a sample which was subjected to stress ratio, τ/σ'_{vo} = 0.068 for 16 cycles and then allowed to drain. The increase in G_{mn} and τ_{mn} due to resulting volumetric strain are shown in Table 4.2 (Sample 1). The predicted and experimental curve for this sample are shown in Fig. 4.19(b) by curves C and D.

The comparison between predicted and measured porewater pressures, shown in Fig. 4.19(a) and (b), is good and may reasonably be viewed as indicating that strain hardening due to plastic volumetric strains in sands occurs only after drainage.

4.5 DISCUSSION

The porewater pressure model developed by Martin, Finn and Seed (1975) has been tested under a variety of drained and undrained loading conditions. The basic assumptions of the model appear to be well-founded. There is a strong verification of a unique relationship

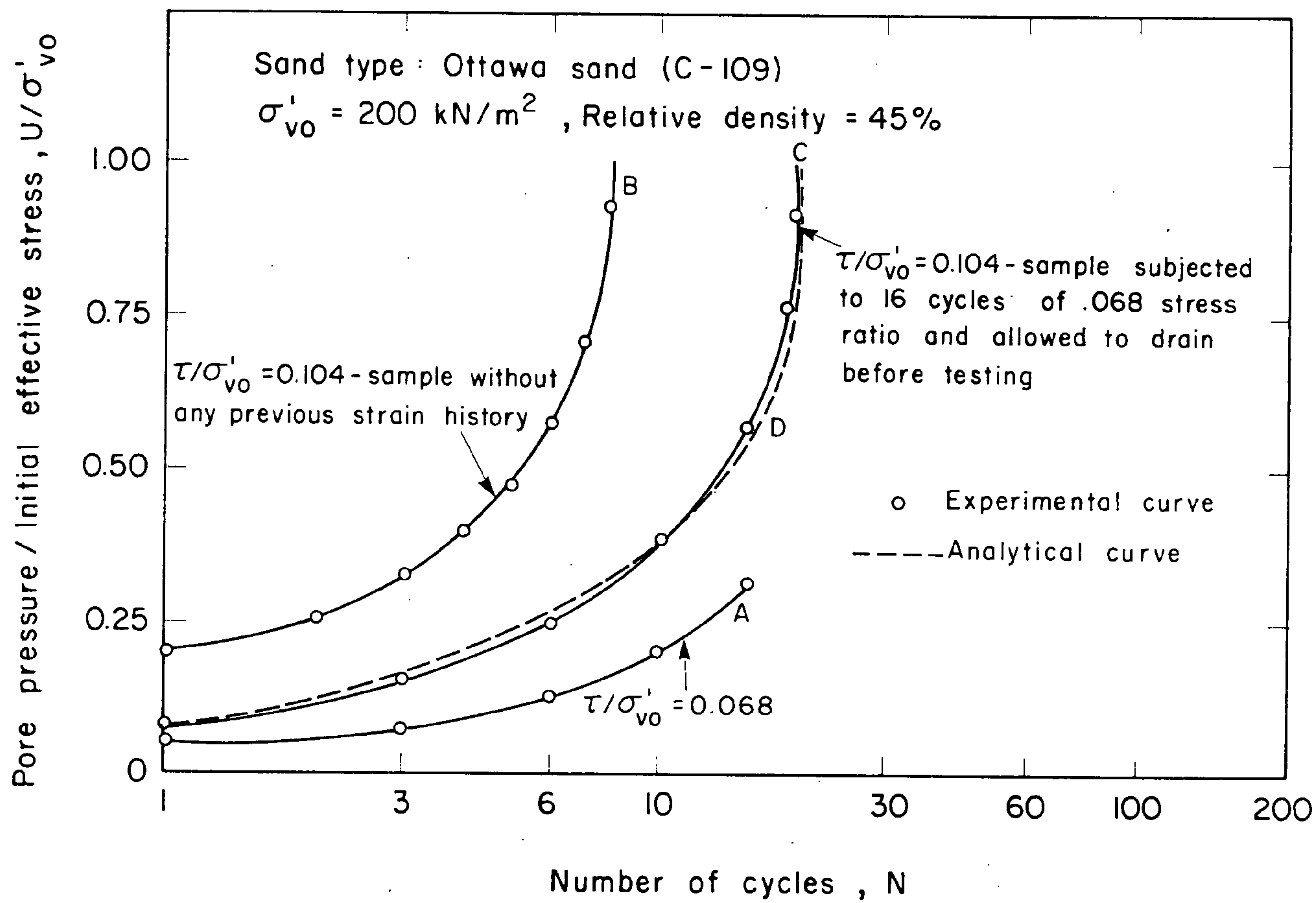

FIG. 4.19(b) Predicted and Measured Porewater Pressures in a Sand with Previous Loading History.

between volumetric strains in drained tests and porewater changes in undrained tests for samples of given sand with similar strain histories. An important point to emerge from the study is that the rebound modulus used to convert volumetric strains to porewater pressures must be measured under cyclic loading conditions. Moduli measured under static rebound conditions are too stiff and for a given volumetric strain generate too much porewater pressure.

The model predicts successfully the porewater pressure response under drained conditions for uniform loading and for irregular cyclic loading histories representative of earthquake loading. When combines with the constitutive stress-strain relations used by Finn et al. (1977) in their dynamic effective stress analysis, it predicts successfully the effect of previous cyclic loading history on porewater pressure response. It appears from the test data that in undrained tests strain-hardening or strain history effects do not occur. However, at the conclusion of such tests if drainage is allowed to take place plastic strains are recovered and the sands strain-harden.

If proper values for the rebound modulus are used and the effects of strain-hardening are included whenever drainage occurs, it appears that the constitutive relationship used for nonlinear effective stress analysis by Finn et al. (1977), can make good predictions of the development of porewater pressure under fairly general loading patterns and drainage conditions in simple shear.

CHAPTER 5

VERIFICATION OF CONSTITUTIVE RELATIONSHIPS FOR OVERCONSOLIDATED SAND

The original porewater pressure model developed by Martin et al. (1975) is based entirely on tests with normally consolidated sands. In this chapter, performance of the model for overconsolidated sands will be evaluated. It is well known that overconsolidated sands have a greater resistance to liquefaction, the resistance increasing with overconsolidation ratio, OCR (Seed and Peacock, 1971). The process of overconsolidation increases the coefficient of lateral earth pressure, k_o, of sand hence mean effective stress. It is generally considered (Seed and Peacock, 1971; Ishibashi and Sherif, 1974) that the increase in liquefaction potential is caused by higher mean effective stress. The higher mean effective stress results in increased shear modulus and lower shear strainthe tests are generally performed in stress controlled conditions. Lower shear strain procedures smaller potential volumetric strain, hence lower porewater pressure.

Ishibashi and Sherif (1974) observed that there is a unique relationship between τ/σ'_{mo}[1] and the number of cycles to initial liquefaction, irrespective of the initial k_o values and confining pressures (Fig. 5.1).

If it is considered that the process of overconsolidation yields only increased k_o then there should be a unique liquefaction strength curve, plotted in terms of τ/σ'_{mo} and number of cycles to liquefaction, for normally and overconsolidated sand samples.

---

[1] τ/σ'_{mo} is the ratio of cyclic shear stress to initial mean effective stress.

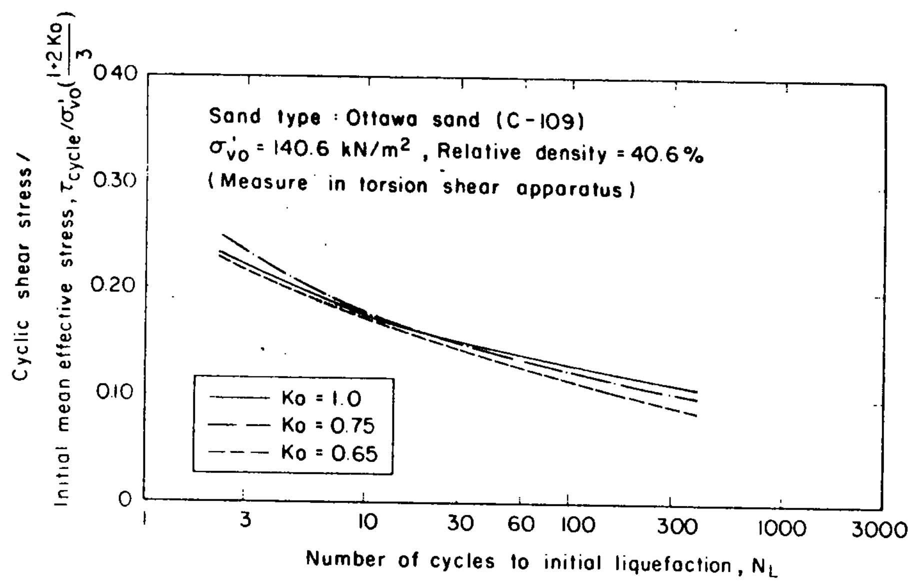

FIG. 5.1 Cyclic Shear/Initial Mean Effective Stress vs. Number of Cycles to Initial Liquefaction for Various k_o values (After Ishibashi and Sherif, 1974).

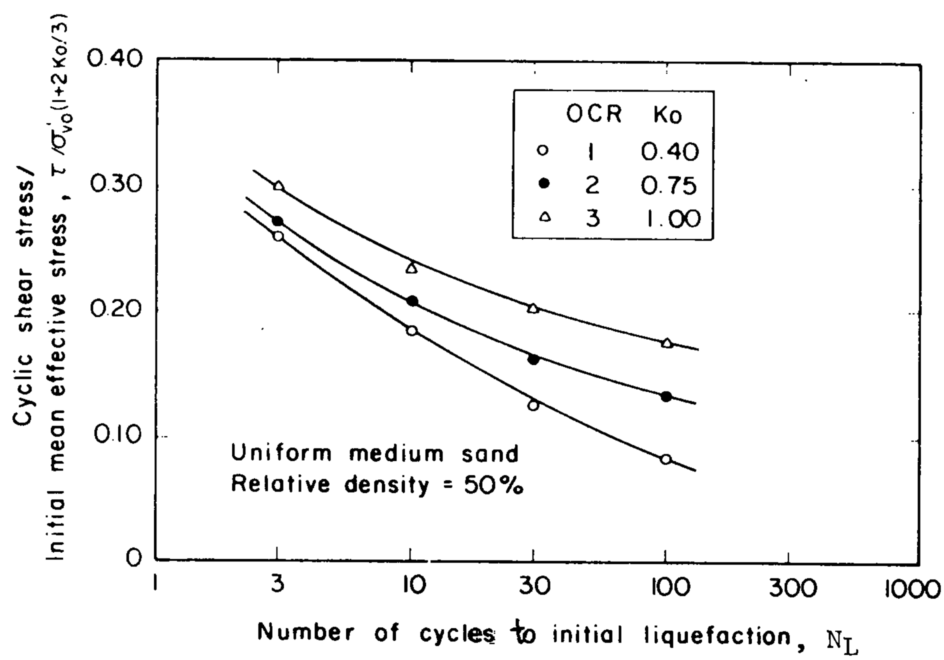

FIG. 5.2 Cyclic Shear Stress/Initial Mean Effective Stress vs. Number of Cycles to Initial Liquefaction for Various OCR (After Seed and Peacock, 1971).

However, when the experimental data from Seed and Peacock (1971) are plotted in terms of τ/σ'_{mo} vs. number of cycles for liquefaction for various overconsolidation ratio, as shown in Fig. 5.2, it shows that the increase in resistance due to overconsolidation can not be assigned to an increased k_o value. In the comprehensive study by Ishihara and Takatsu (1979) the effect of increase in k_o value and OCR value on liquefaction potential are discussed. The authors observe that for a constant k_o value, the resistance to liquefaction increases with increasing OCR and present an empirical formula to relate the cyclic stress ratio required for liquefaction for both normally and overconsolidated samples. For this study a torsional shear apparatus was used. For their study overconsolidated samples in torsional shear apparatus were prepared where, during overconsolidation, the ratio of horizontal to vertical effective stresses (k_o) were kept constant. However, the overconsolidated samples should be prepared in laterally confined conditions where k_o increases during the overconsolidation process.

The contribution of increases in k_o value to the increased resistance to liquefaction could not be obtained from simple shear data as has been done by Seed and Peacock (1971) and Finn et al. (1978) as the k_o value could not be measured after overconsolidation. Since it is now possible to monitor lateral stress in the cyclic simple shear apparatus, results of a study of the contribution of k_o on increased resistance due to OCR can be presented.

5.1 COMPARISON BETWEEN NORMALLY AND OVERCONSOLIDATED SAND BEHAVIOUR

Constant volume tests on normally and overconsolidated samples are performed in the stress controlled conditions. The samples were consolidated to vertical effective stress of 400, 600 and 800 kN/m^2

and, by reducing vertical effective stress to 200 kN/m^2, samples of OCR = 2,3 and 4 were obtained. During the process of initial consolidation and unloading, the lateral stresses were monitored. Figure 5.3 shows the variation of effective lateral stress with respect to vertical effective stress for specimens with OCR = 1,2,3 and 4. It is clear from the figure that, inspite of approximately the same initial k_o value for all tests the overconsolidation process results in significantly higher k_o which increases with increasing OCR value. The variation of lateral and vertical effective stresses during cyclic shearing for OCR = 1,2,3 and 4 are shown by the dotted curves in Fig. 5.3. The cyclic loading curves are quite similar for normally and overconsolidated samples. In Fig. 5.4 cyclic shear stress ratio, τ/σ'_{vo}, is plotted against the number of cycles for initial liquefaction for various OCR values. This figure reveals a significant increase in liquefaction resistance due to overconsolidation. Average values of k_o from several overconsolidated samples are given in Table 5.1 corresponding to different OCR. In Table 5.2 an empirical relationship between k_o' of overconsolidated sample and normally consolidated sample, given by Ishihara and Takatsu (1979), is given where the constant m obtained from experimental data lies within the observed range by several investigators. Hence, it can be assumed that measured k_o values are fairly reliable. Using these average values of k_o (Table 5.1), experimental data from Fig. 5.4 could be plotted in terms of τ/σ'_{mo} versus the number of cycles to liquefaction where σ'_{mo} is

$$\sigma'_{mo} = \sigma'_{vo} / \left(\frac{1+2k_o}{3}\right) \tag{5.1}$$

Figure 5.5 clearly shows that though the increase in resistance to liquefaction due to OCR is partially due to an increase in k_o value, the remaining increase in strength can only be attributed to changed particle

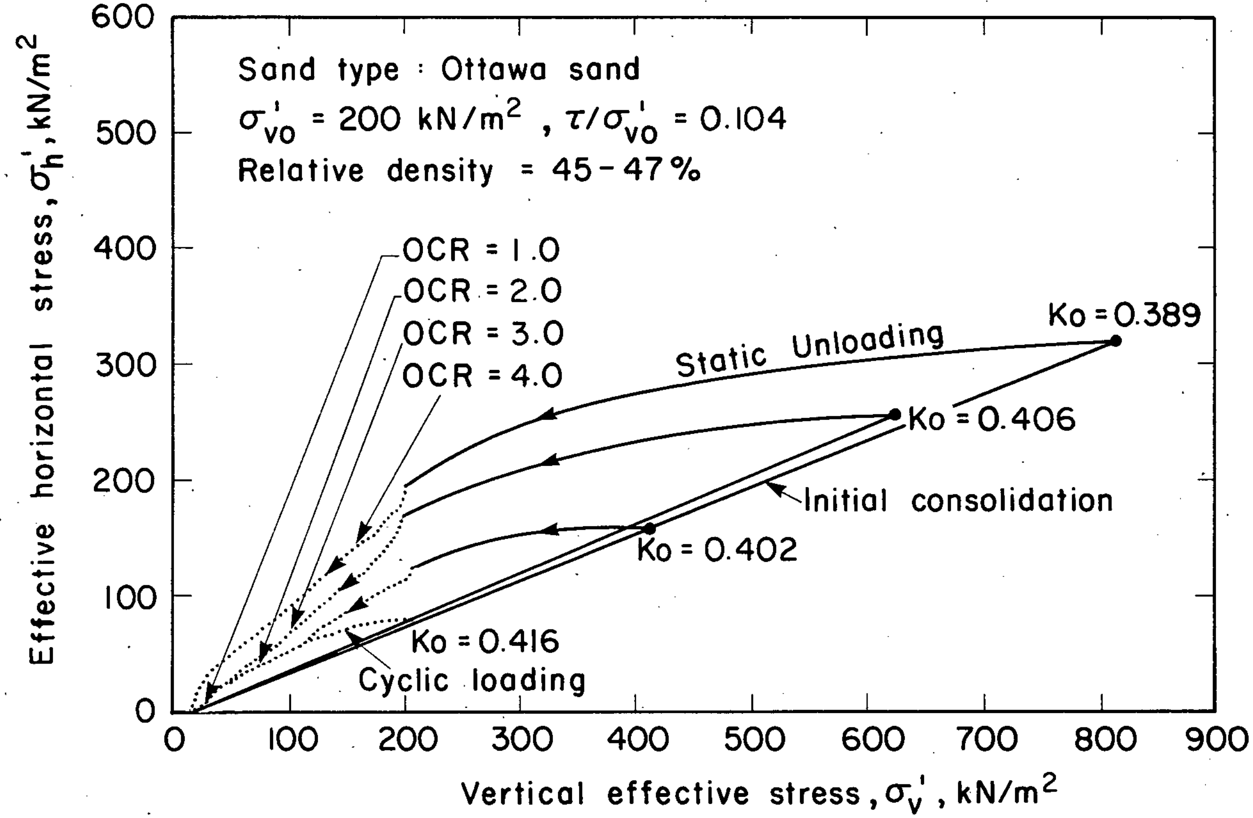

FIG. 5.3 Variation of Effective Horizontal and Vertical Stresses During Initial Consolidation, Static Unloading and Cyclic Loading for Samples with OCR = 1,2,3 and 4.

TABLE 5.1

EXPERIMENTAL k_o VALUES FOR VARIOUS OCR

Overconsolidation Ratio	k_o^*
1	0.39
2	0.67
3	0.83
4	0.93

NOTE: k_o^* - these values are the average k_o value obtained from several test data.

TABLE 5.2

RELATIONSHIP BETWEEN k_o' FOR OVERCONSOLIDATED SAMPLES TO NORMALLY CONSOLIDATED SAMPLES

$k_o' = k_o \ (OCR)^m$ (Ishihara and Takatsu, 1979)

Experimental Data	$m \simeq 0.68$
Ishihara and Takatsu (1979)	$m \simeq 0.71$ to 0.84
Sherif et al. (1979)	$m \simeq 0.68$

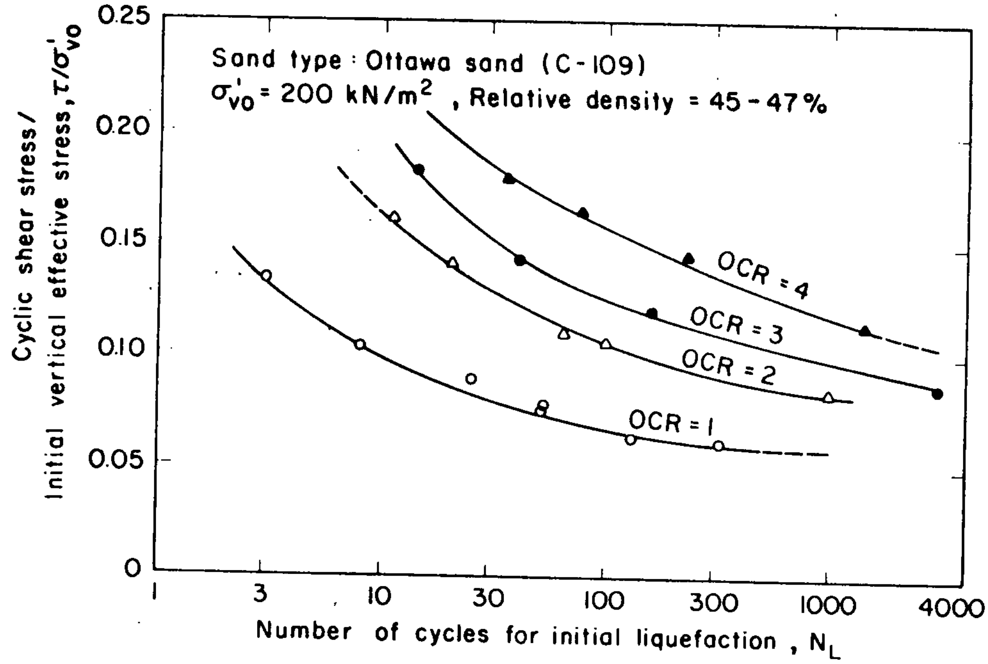

FIG. 5.4 Cyclic Shear Stress/Initial Vertical Confining Stress vs. Number of Cycles to Initial Liquefaction for Various Values of OCR.

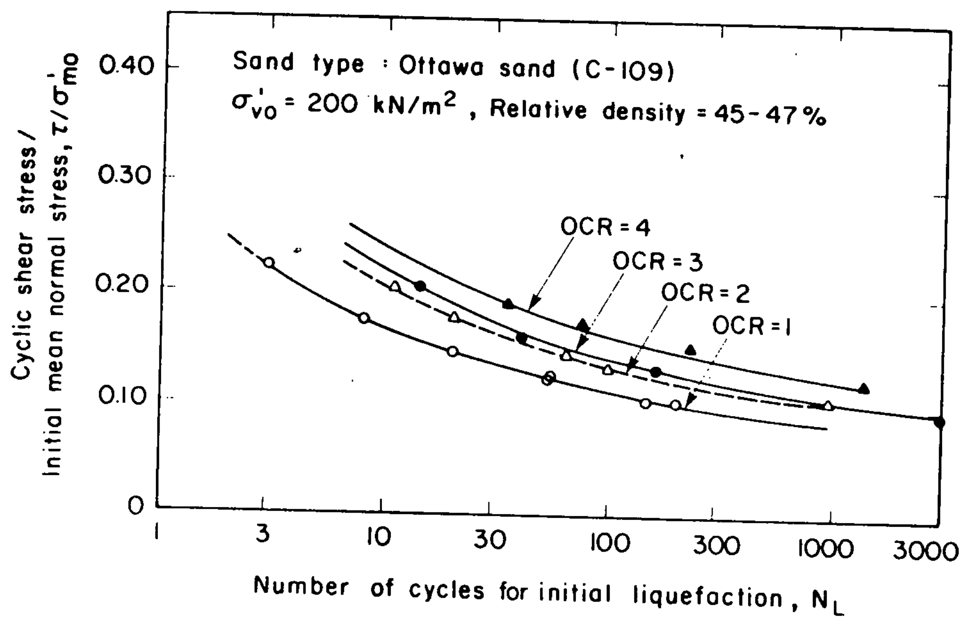

FIG. 5.5 Cyclic Shear Stress/Initial Mean Normal Stress vs. Number of Cycles to Initial Liquefaction for Various Values of OCR.

structure during the process of overconsolidation. Hence, it can be stated that it is not possible to relate the behaviour of normally and overconsolidated samples on the basis of mean normal effective stress. It seems that during the process of overconsolidation specimens acquire a particle arrangement which is more resistant to cyclic loading.

However, in the following section, when predictive capacity of Martin et al. (1975) will be checked for overconsolidated samples, a detailed study of volumetric strain in cyclic loading and dynamic rebound modulus will further distinguish the behaviour of normally and overconsolidated samples.

5.2 VERIFICATION OF THE CONSTITUTIVE RELATIOUSHIPS

The pore pressure model proposed by Martin et al. (1975) is not restricted to normally consolidated sand samples but can also be used for overconsolidated sand specimens as long as volume change characteristics, rebound modulus characteristics, shear modulus and shear strength used in the model are for the overconsolidation state. In this section an attempt is made to predict porewater pressure for sand specimens with OCR of 2,3 and 4, under stress controlled undrained conditions. The calculated porewater pressure is then compared with measured porewater pressure.

In order to use the model for predicting porewater pressures the volumetric strain characteristics under drained, strain controlled conditions and the dynamic rebound modulus are required for various levels of OCR. In this study the maximum overconsolidation ratio used is 4, thus conclusions derived here are limited to this maximum value.

In addition to volume change and dynamic rebound modulus, G_o and τ_o are also required for the constitutive stress-strain law used for the pore pressure model.

5.2.1 Volume Change Characteristics

To evaluate the volume change characteristics of overconsolidated sand specimens, a special series of tests has been performed. Loose specimens of Ottawa sand (C-109) were prepared by the method described in Appendix I and consolidated to vertical effective stresses of 400, 600 and 800 kN/m^2. During consolidation, lateral stress σ_h' and volumetric strain were monitored. To achieve a specimen with OCR = 2,3 and 4, respectively, vertical effective stress was decreased in increments to σ_v = 200 kN/m^2 and, with monitored σ_v' and σ_h', it was possible to plot loading and unloading curves in σ_v'-σ_h' space and k_o^*[2] value achieved after consolidation was calculated.

There were two main observations which can be made from the data obtained during cyclic shear in undrained conditions:

1. As shown in Fig. 5.6, during the process of cyclic shearing, lateral stresses in the sand specimens gradually decreased in contrast to the increase in lateral stress in normally consolidated samples. For specimens with OCR = 3 or 4 and higher initial k_o (before cyclic shearing), there was a larger decrease in lateral stress compared to specimens with OCR = 2.0. The drop in lateral stress was generally observed within the first 15 cycles with the most pronounced drop observed in the first 5 cycles. With specimens subjected to a higher shear strain amplitude, lateral stresses decreased and stabilized much faster compared to specimens with the same OCR but smaller cyclic shear strain amplitude (cf. Fig. 5.6).

2. For specimens with an overconsolidation ratio of 4,

---

[2] $k_o^* = \left(\frac{\sigma_h'}{\sigma_v'}\right)_{\epsilon_h = 0}$ is the ratio of horizontal stress to vertical effective stress under the conditions of complete lateral confinement in the horizontal direction.

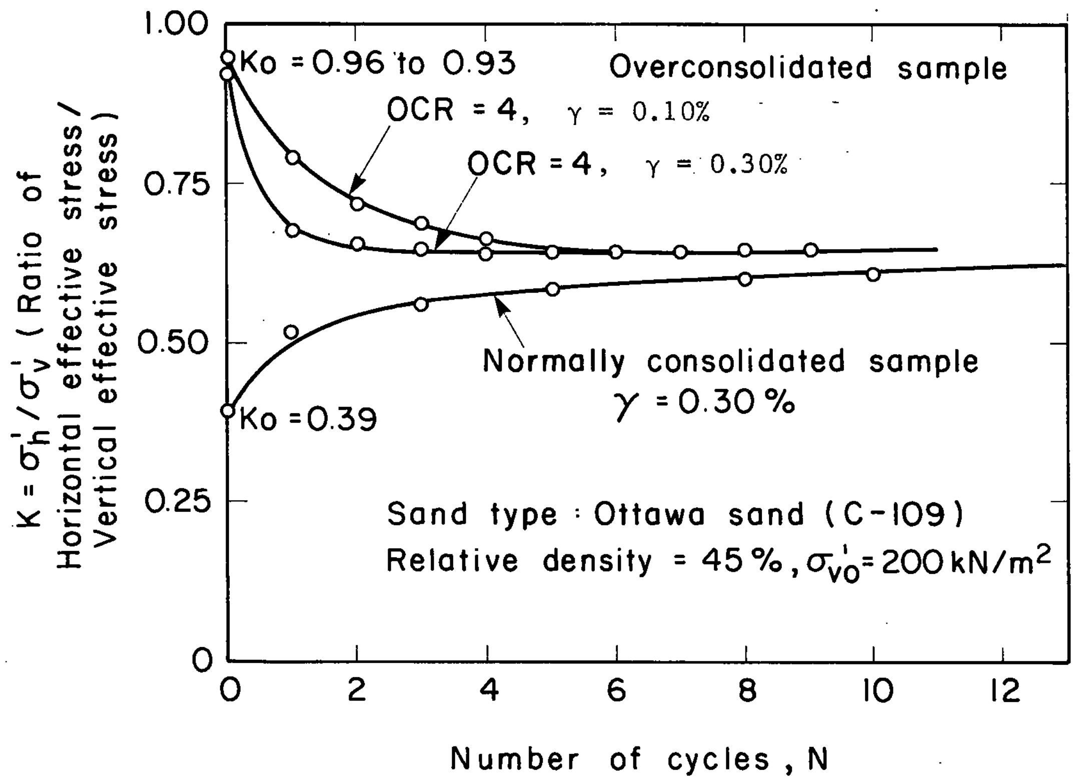

FIG. 5.6 Decrease in the Ratio of Horizontal to Vertical Effective Stress vs. Number of Cycles for Various Cyclic Shear Strain Amplitude for Overconsolidated Sample.

the application of a cyclic shear strain amplitude γ = 0.30%, caused dilation for the first half cycle, although the net effect of the first cycle was a decrease in volume (Fig. 5.7). This typical behaviour was only observed for speciments with OCR = 4. It was observed that for specimens with OCR = 4, the volumetric strain increment in the first cycle was always less than in the second cycle of shear strain. It is anticipated that the presence of very high lateral stresses on sand grains restricts the relative movemovement of particles. Since volumetric strains are generated due to interparticle slip, presence of higher k_o value may reduce it. This influence is more pronounced for the first 10 cycles of cyclic shearing during which the lateral stress reduces and stabilizes to a particular value.

In Fig. 5.8, where the total volumetric strains are plotted against cycles of shear strain amplitude, $\gamma \simeq$ 0.10% for sand specimens with various overconsolidated ratios, it can be seen that for the first 10 cycles of shearing the shape of the curves for OCR = 2,3 and 4 are distinctly different from that for OCR = 1. The most important observation which can be made from Fig. 5.8 is that volumetric strain behaviour considerably reduces with increasing overconsolidation ratio inspite of the fact that all sand specimens were at the same D_r of 45% to 47%. Pyke (1973) also reports that volumetric strains occurring in cyclic tests on overconsolidated samples are less than those occurring in similar normally consolidated samples. Figure 5.9 illustrates this remarkable decrease in volume change behaviour where incremental volumetric strain for the first cycle of cyclic shear is plotted against shear strain amplitude for normally and overconsolidated samples. For example, at a cyclic shear strain amplitude, γ, of 0.10% the incremental volumetric strain for a

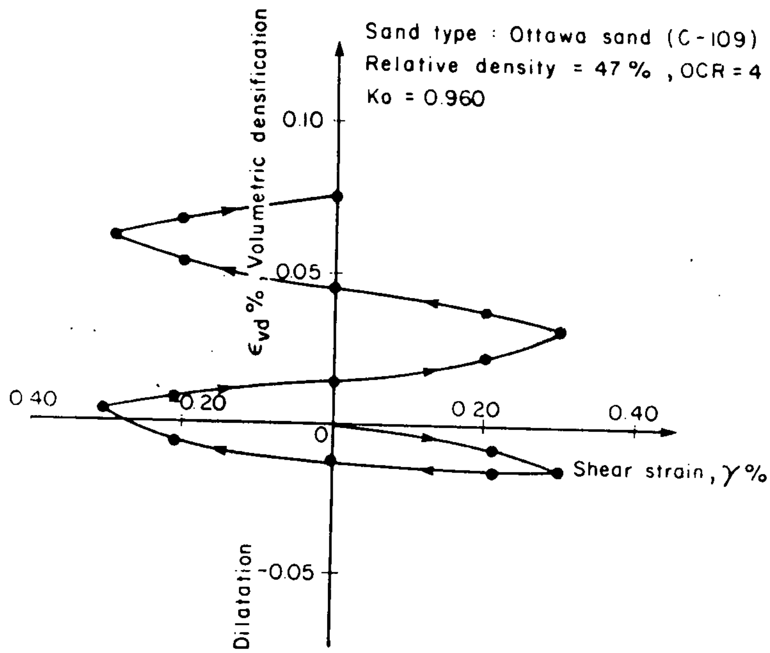

FIG. 5.7 Volumetric Strain Behaviour for First Two Cycles of Shearing for an Overconsolidated Sample.

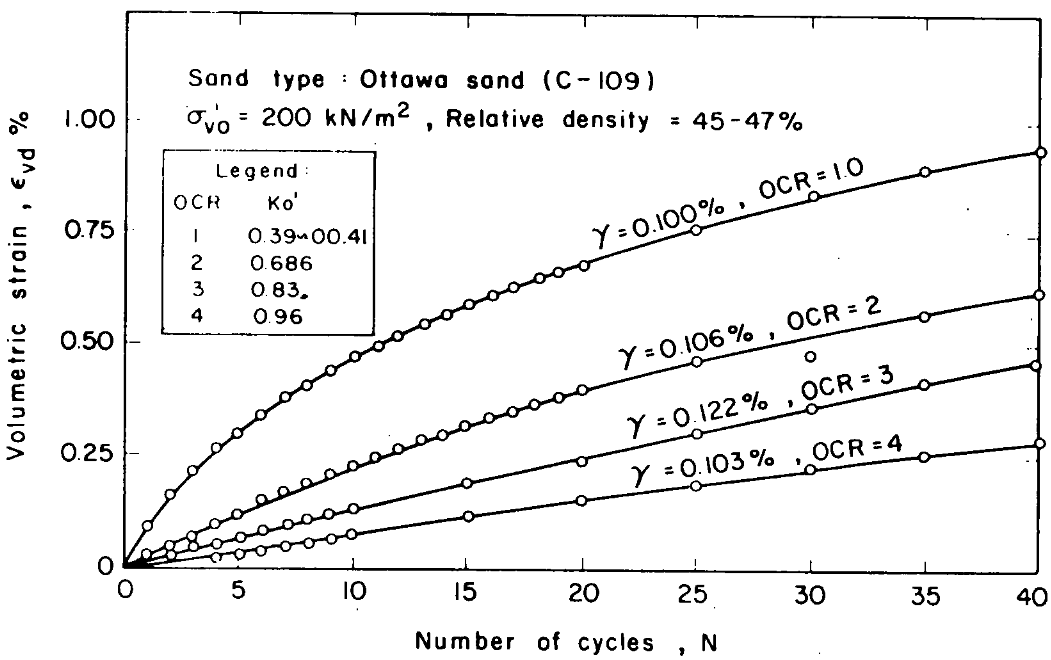

FIG. 5.8 Volumetric Strain vs. Cycles of Constant Shear Strain Amplitude $\gamma \simeq 0.10\%$ for Various OCR.

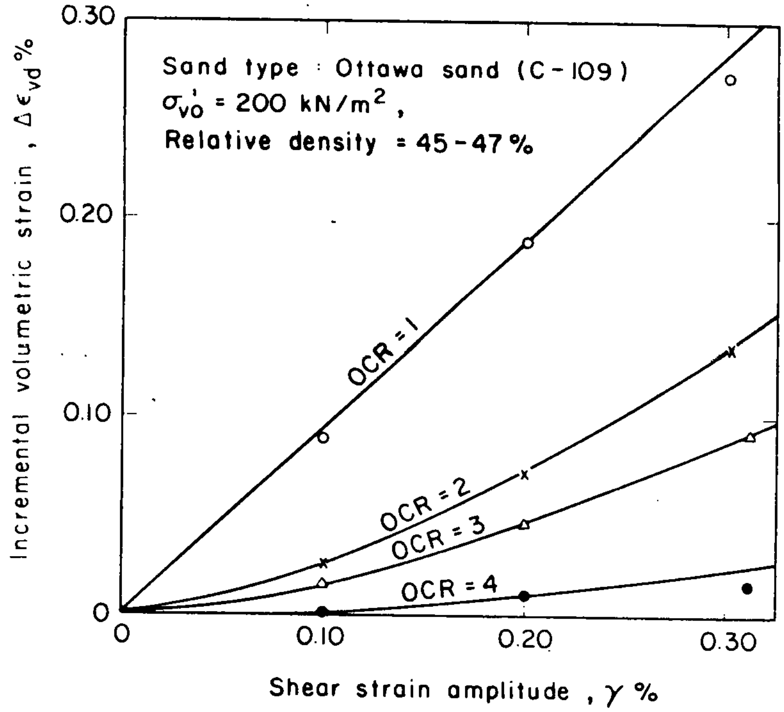

FIG. 5.9 Incremental Volumetric Strain in First Cycle for Ottawa Sand for Various OCR Values.

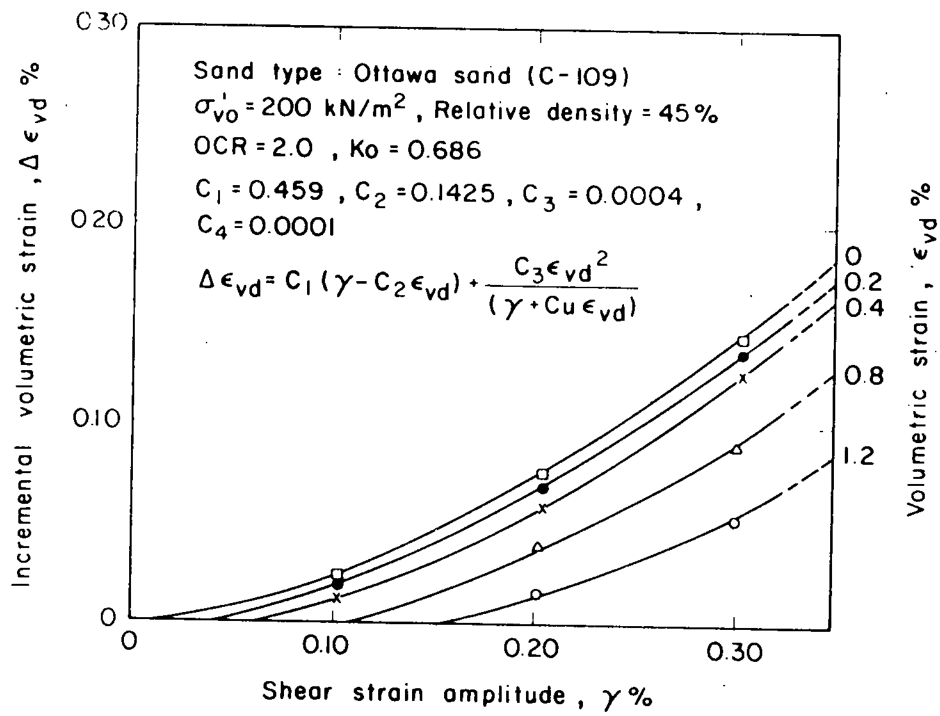

FIG. 5.10(a) Incremental Volumetric Strain vs. Shear Strain Amplitude for Various Levels of Volumetric Strains.

sample with OCR = 2 is 28% of that for a normally consolidated sample.

Measurement of incremental volumetric strain per cycle vs. shear strain amplitude are plotted in Figs. 5.10(a),(b) and (c) for various OCR. From these data, volume change constants needed for the prediction of porewater pressure from the model are calculated. Figure 5.10(c) shows plainly that the curve corresponding to ε_{vd} = 0.0 or the first cycle is much lower than curves for ε_{vd} = 0.10, 0.20%, etc. In order to fit analytical relations given in equation (3.4) to experimental curves for various volumetric strains, data corresponding to ε_{vd} = 0.0 is ignored. Equation (3.4) was also fitted to the data shown in Fig. 5.10(a) and (b) and respective volume change constants were obtained. Values of these constants for each OCR are given in their respective figures (Fig. 5.10(a),(b) and (c)).

5.2.2 Dynamic Rebound Modulus

As described in Chapter 4, to measure the dynamic rebound modulus it is necessary to perform strain coutrolled undrained and drained tests, hence, for overconsolidated sand specimens in addition to strain controlled drained tests used to calculate volume change constants, strain controlled constant volume undrained tests for specimens with OCR = 2,3 and 4 were performed. When porewater pressure ratios were plotted against recoverable volumetric strains for various levels of cyclic shear strain amplitudes for specimens with OCR = 2, as shown in Fig. 5.11(a), the following points become evident:

1. Apart from experimental discrepancy, there is a unique relationship between porewater pressure developed in the undrained condition and volumetric strains in the drained condition for all levels of shear strain amplitude.

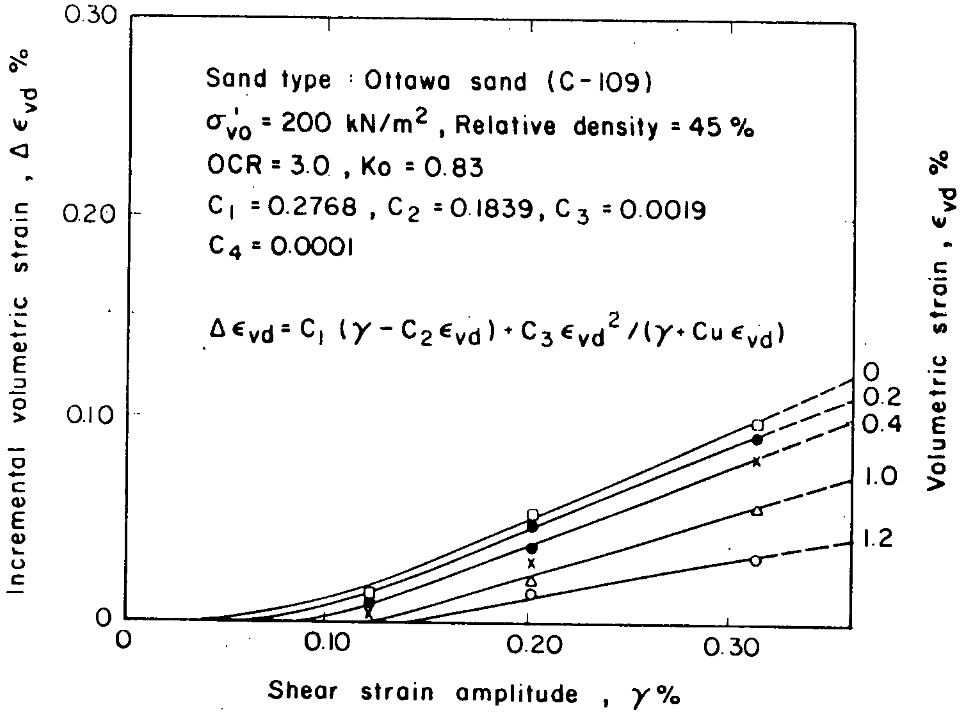

FIG. 5.10(b)

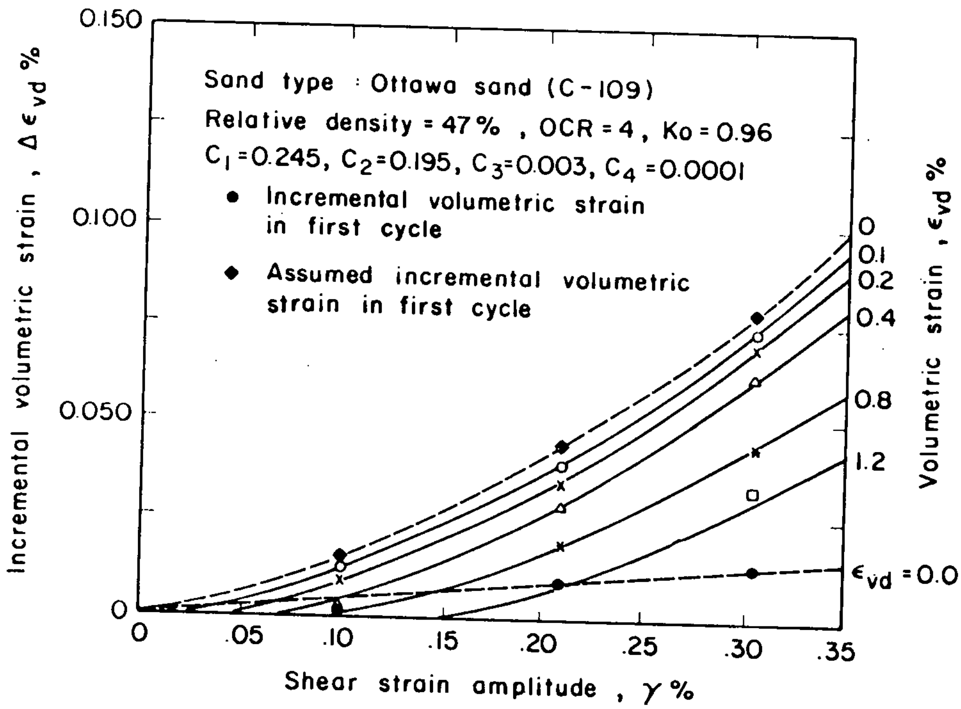

FIG. 5.10(c) Incremental Volumetric Strain vs. Shear Strain Amplitudes for Various Values of Volumetric Strains.

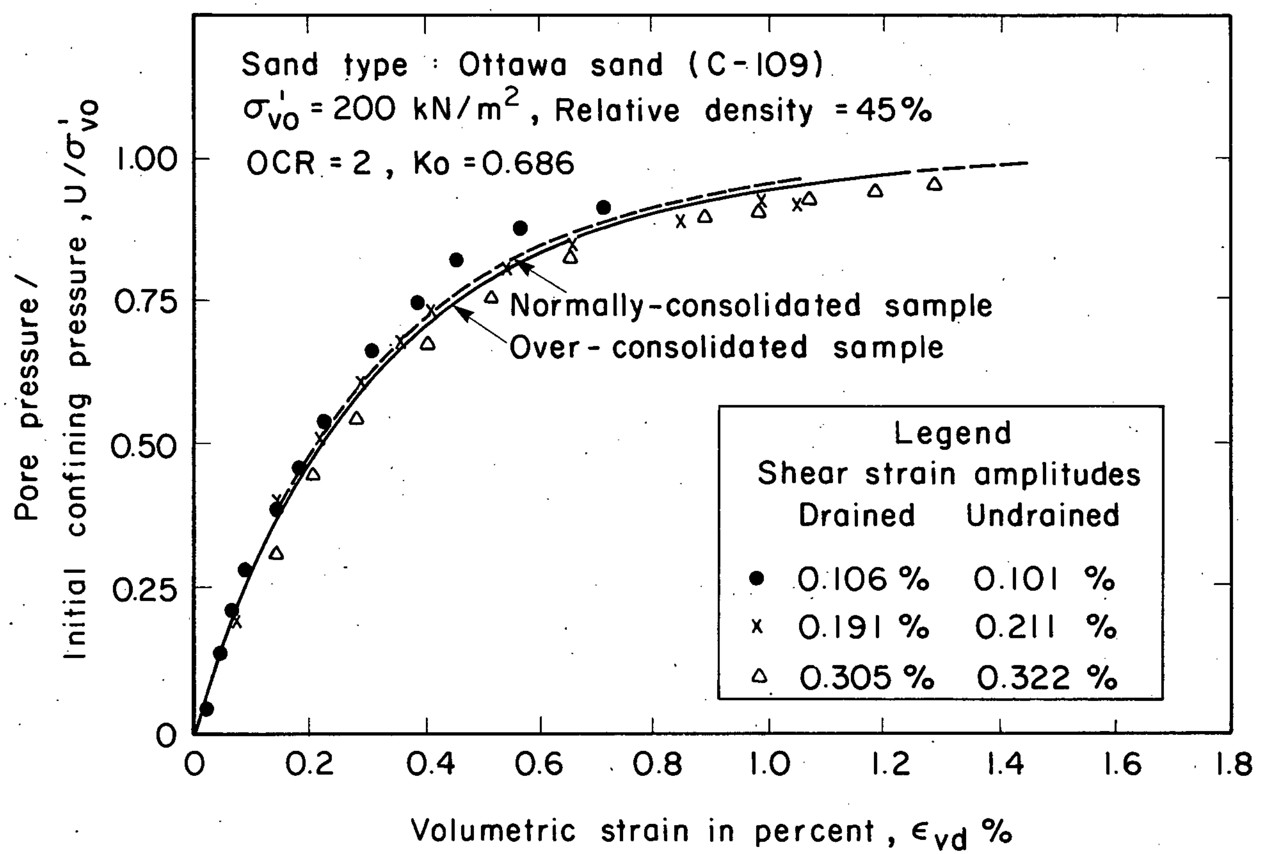

FIG. 5.11(a) Relationship Between Volumetric Strains and Porewater Pressures in Constant Strain Cyclic Simple Shear Tests.

2. Curves shown in Fig. 5.11(a) for normally and overconsolidated sand samples lie very close to each other. The dynamic rebound modulus which is the slope of these curves, normalized with respect to initial confining pressure, is the same for normally and overconsolidated samples. This observation is further strengthened by the data shown in Fig. 5.11(b) for OCR = 3.

The above information again confirms the basic assumption made in the model of Martin et al. (1975) about the relationship between porewater pressure and volume change. This assumption has now been verified for normally consolidated samples with different relative densities and for overconsolidated samples with various overconsolidation ratios.

However, before it can be stated that there is a unique value for dynamic rebound modulus for normally and overconsolidated state, it was considered appropriate to check the validity of OCR = 4. The experimental data obtained for a sample with overconsolidation ratio 4 are shown in Fig. 5.11(c). The data lie on the curve for normally consolidated sand until the pore pressure ratio has reached a value of 0.50. Beyond that the experimental data for OCR = 4 lie on a different curve. Aside from the possibility of experimental error, the reason for this divergence may be that the dynamic rebound moduli for normally consolidated and heavily overconsolidated sands are different.

It can be concluded that the dynamic rebound modulus value for normally consolidated samples at various relative densities and overconsolidated samples (OCR = 2,3,4) is the same for Ottawa sand when samples are being dynamically unloaded from σ'_{vo} = 200 kN/m^2.

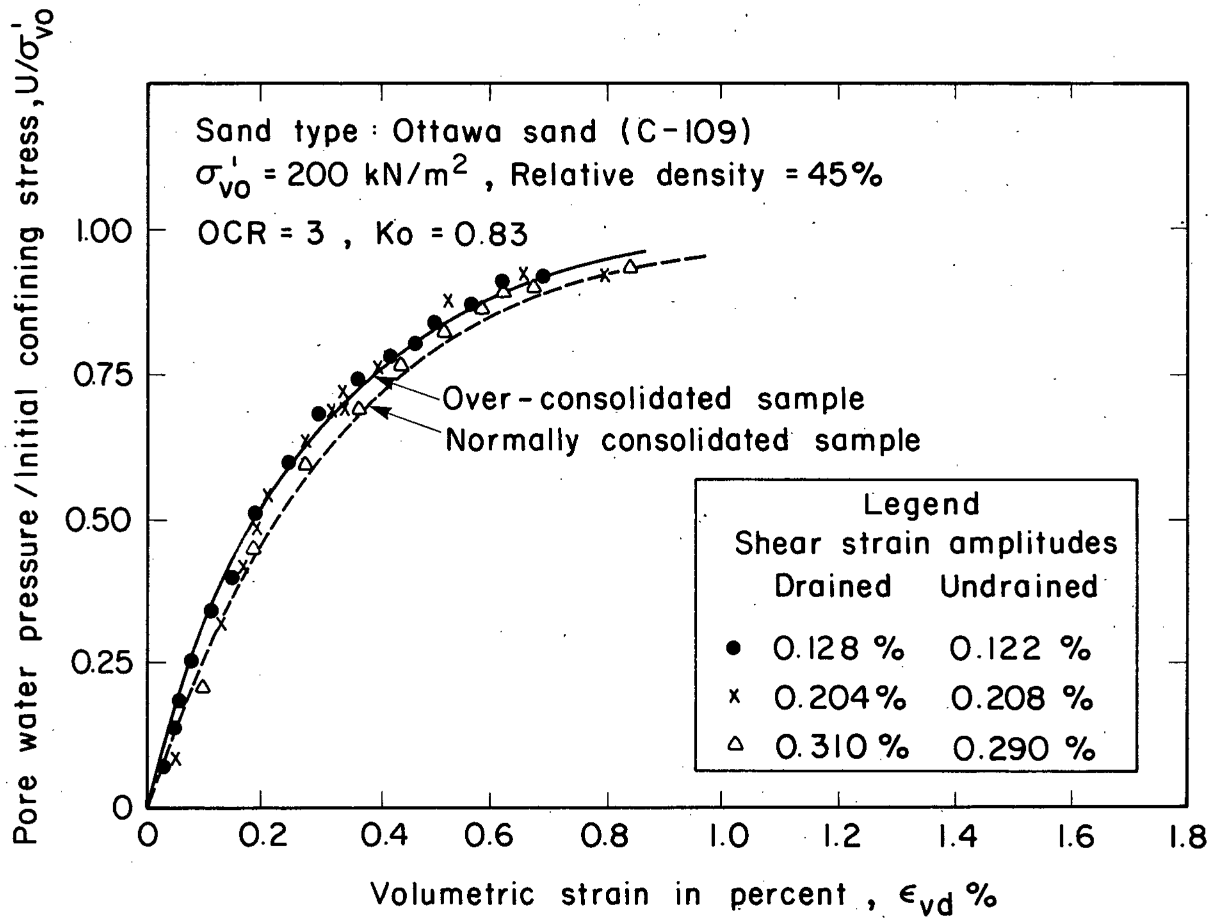

FIG. 5.11(b) Relationship Between Volumetric Strains and Porewater Pressures in Constant Strain Cyclic Simple Shear Tests.

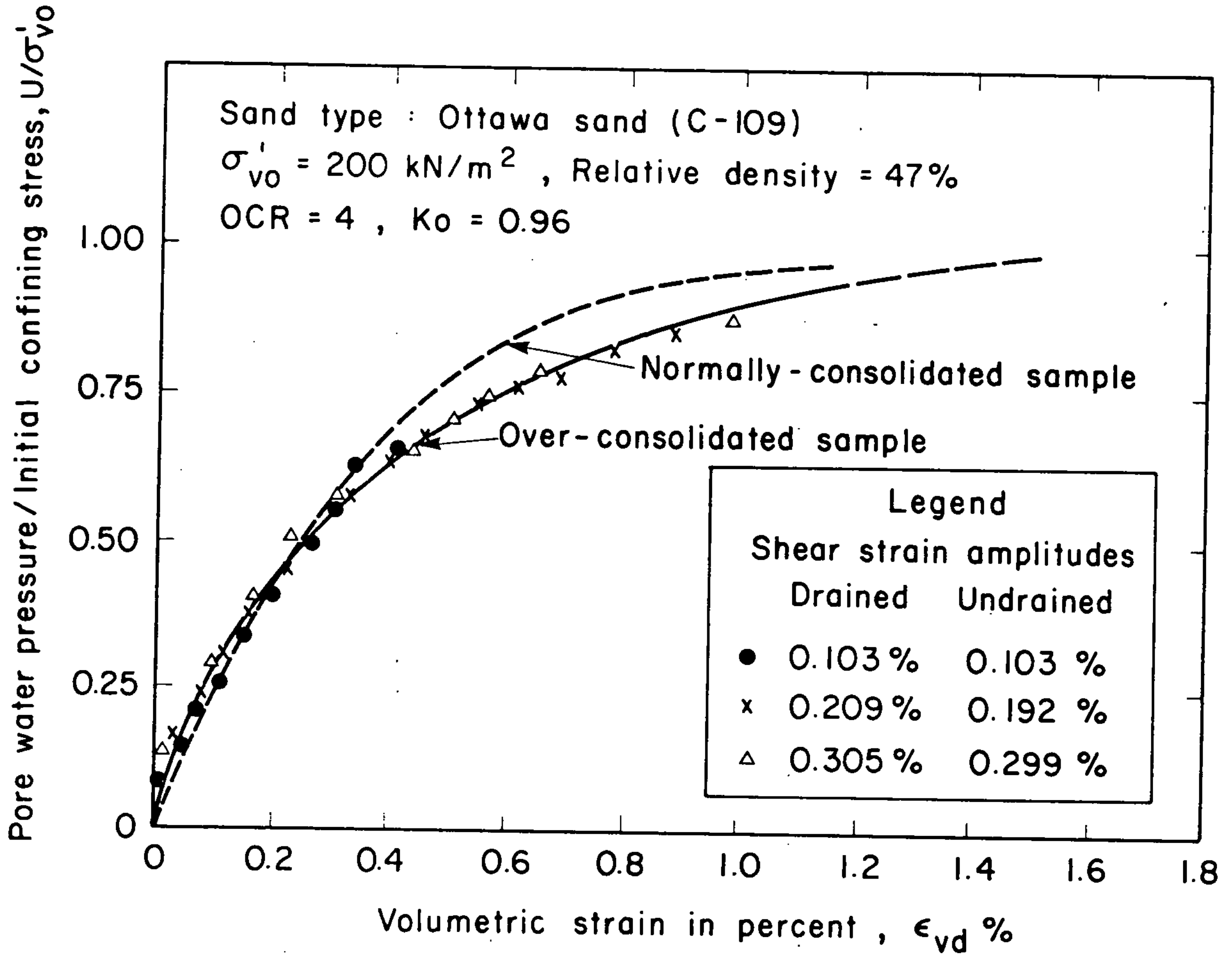

FIG. 5.11(c) Relationship Between Volumetric Strains and Porewater Pressures in Constant Strain Cyclic Simple Shear Tests.

5.2.3 Initial Shear Modulus and Shear Strength

Apart from the porewater pressure model, constitutive stress-strain relations are also required to calculate pore pressure analytically and for those G_{mo} and τ_{mo} are needed. As mentioned in the previous chapter, initial shear modulus can be calculated by the equation suggested by Hardin and Drnevich (1972). They showed that the overconsolidation ratio is a relatively unimportant parameter for the shear modulus of clean sand. The effect of overconsolidation is to increase G_{mo} depending on the plasticity index, PI, and for soil with no plasticity there are almost no effects from overconsolidation.

In addition, Afifi and Richart (1973) show that the increase in shear modulus of clean sand for $\gamma = 2.5 \times 10^{-5}$ due to overconsolidation history is quite small. In Fig. 5.12 results obtained by Afifi and Richart are shown for sand with a varying percentage of fines. For sands similar to Ottawa sand, the increase in shear modulus due to OCR 1.32 shown as 0.08% which is an insignificant amount. However, it should be noted that these results were obtained by Afifi and Richart in a resonant column apparatus in which overconsolidation was achieved by increasing and decreasing the all round pressure of the sand specimen. It is anticipated that by this method the overconsolidation did not result in any increase in k_o. The influence of overconsolidation of initial shear modulus, where overconsolidation is achieved under laterally confined conditions, has never been studied. The Roscoe-type simple shear apparatus available at the University of British Columbia is not suitable for measurement of shear modulus at low strain (γ<0.05%), the influence of overconsolidation on initial shear modulus cannot be checked.

However, from the experimental data obtained for shear strain

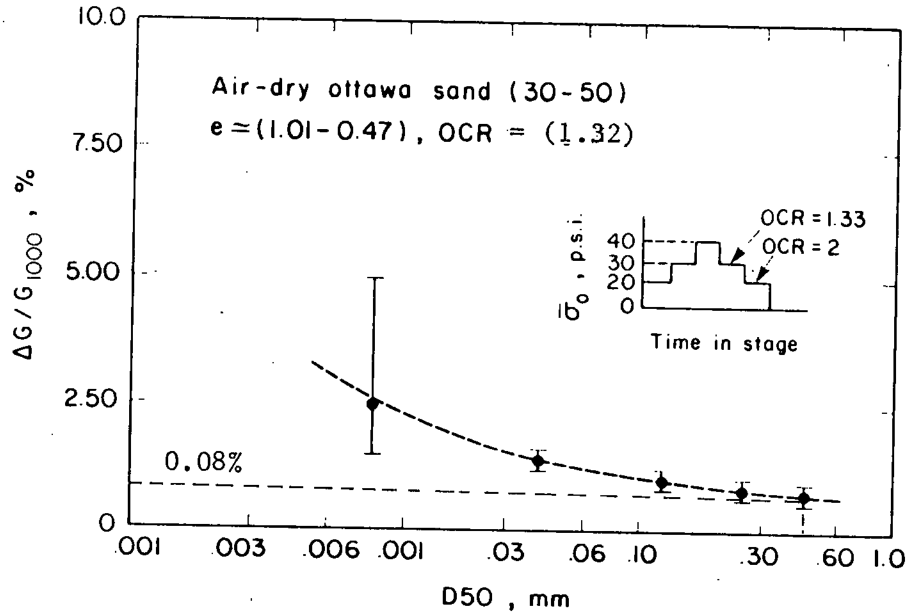

FIG. 5.12 Average Value of Shear Modulus vs. Mean Particle Size for Soils with OCR = 1.33 to 2 (After Afifi and Richart, 1973).

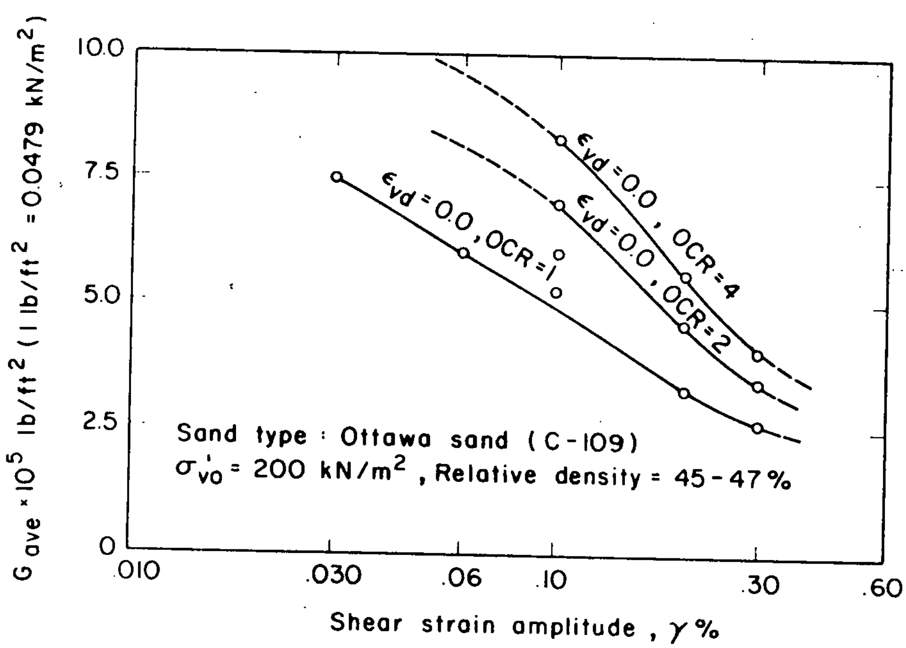

FIG. 5.13 Av. Shear Modulus vs. Shear Strain for First Cycle of Shearing at Various OCR.

amplitudes $\gamma > 0.05\%$, it was observed that for a given shear strain amplitude, the corresponding shear stress in the first quarter of cycle is much higher for overconsolidated samples than for normally consolidated samples. In Fig. 5.13, an average shear modulus is plotted against shear strain amplitude at various OCR values where the shear modulus is calculated for the first quarter of cycle of shear loading. This figure illustrates the increase in shear modulus with increasing OCR. However, since this data is only restricted to $\gamma > 0.06\%$, behaviour of these curves at very small shear strain ($\gamma \simeq .001\%$) is not known. Hence, the increase in G_{mo} due to increasing OCR can not be evaluated from this data.

In the present analysis, the shear modulus and shear strength for sand specimens with OCR were calculated by equations (3.10) and (3.11). For calculating G_{mo} and τ_{mo} the appropriate value of k_o corresponding to OCR was used in equations (3.8) and (3.9).

5.2.4 Pore Pressure Prediction

The ability of the model to predict porewater pressures in overconsolidated sand was tested by predicting the liquefaction strength curves for various OCR and comparing the results with experimental curves. The strength curves, as shown in Fig. 5.14, are plots of the cyclic stress ratio, τ/σ'_{vo} versus the number of cycles to initial liquefaction, N_L; τ being the applied cyclic shear stress. Liquefaction strength curves for OCR = 1,2,3 and 4 are computed using measured volumetric strain characteristics, dynamic rebound characteristics and appropriate G_{mo} and τ_{mo}. As a note of clarification, it should be pointed out that no strain hardening effect has been included. The points in Fig. 5.14 are experimental data from undrained constant volume cyclic simple shear tests. The initial effective vertical pressure, σ'_{vo}, in all tests after the OCR was established

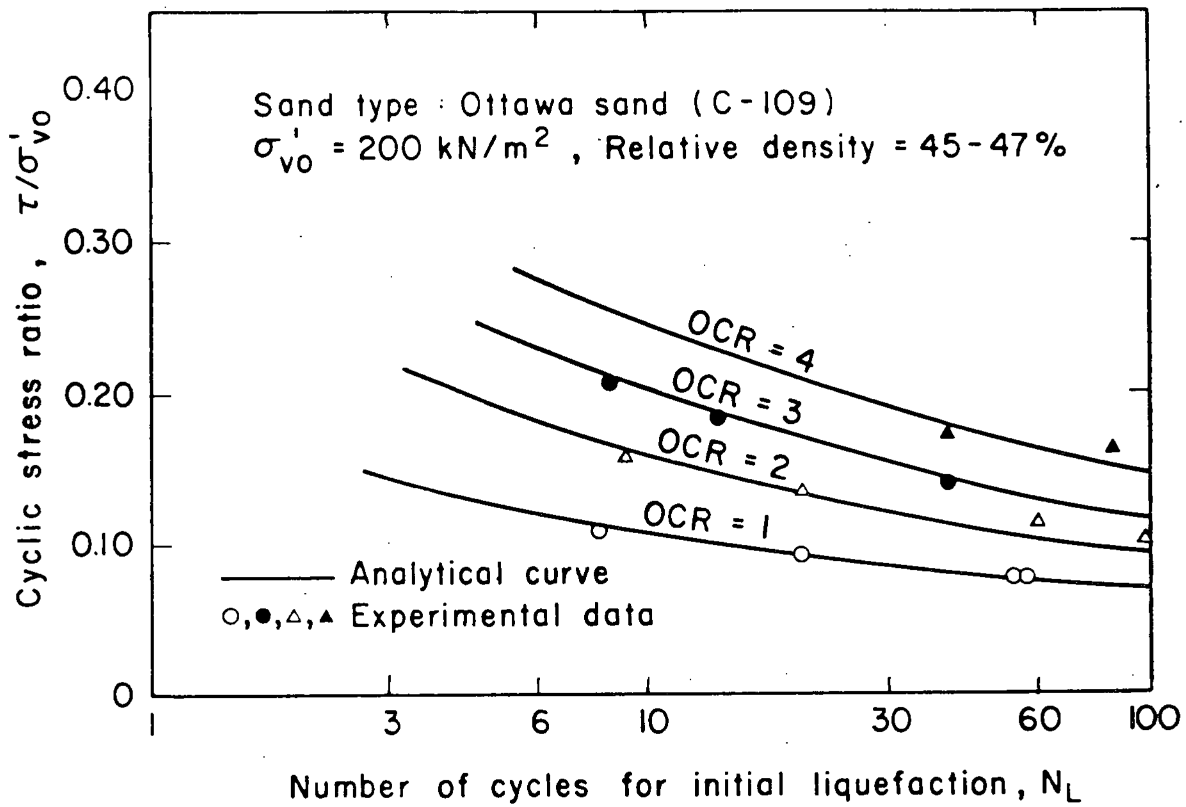

FIG. 5.14 Cyclic Stress Ratio vs. Number of Cycles for Initial Liquefaction for Various OCR Ratios.

as 200 kN/m^2.

The comparison between the computed and measured liquefaction strengths is good, although the performance of the model for overconsolidated samples is not as good as for normally consolidated samples. The difference between analytical and experimental results for higher overconsolidation ratios (OCR = 4) may be due to two reasons - firstly, the inability to account for the correct behaviour of OCR = 4 for the first few cycles; secondly, the unknown increase in shear modulus due to OCR = 4.

5.3 DISCUSSION

It can be concluded that the set of constitutive relationships, both for the pore pressure model and for stress-strain behaviour, developed for normally consolidated sand samples are applicable to overconsolidated sand samples where overconsolidation ratio ranges between 2 to 4. However, it is observed that more research is required to study the effects of overconsolidation on initial shear modulus and shear strength.

CHAPTER 6

POREWATER PRESSURE MODEL BASED ON ENDOCHRONIC THEORY

In Chapters IV and V it has been shown that the constitutive relationships used in effective stress analysis proposed by Finn et al. (1977) can predict realistic pore pressure activity in stress controlled undrained tests. However, the pore pressure model requires the incremental volumetric strain obtained under strain controlled drained conditions given by equation (3.1) and the dynamic rebound modulus as discussed in section 4.2. It is further shown that the rebound modulus cannot be measured with a conventional oedometer as suggested by Martin et al. (1975), because the rebound response of sand under undrained cyclic loading is different from that under static unloading. Thus, measurement of the dynamic rebound modulus requires both undrained and drained cyclic loading tests, a more complicated process than conventional methods of porewater prediction. If a different link could be found between porewater pressure and the dynamic response parameter of the sand-water system, this would obviate the need for measuring the rebound modulus of the sand skeleton under cyclic loading. Such a relationship is found in the endochronic theory proposed by Valanis (1971).

Zienkiewicz et al. (1978) point out that endochronic theory has the capability of relating volumetric strains using a single variable which will account for the dynamic response parameter. In endochronic theory the nonlinearity of soil is represented by a variable which describes the complete sequence of events of loading through successive states of the material. Although for sand endochronic variables are independent of time, they incorporate aspects of the strain history of the sand and are thus termed endochronic[1].

Endochronic variables are mathematical transformations of real physical variables, though they themselves have no direct physical interpretation. For liquefaction it will be seen that these variables are a transformation of deformation increments.

In this chapter pore pressure data obtained from conventional undrained strain controlled and stress controlled tests are related with endochronic variables. The endochronic formulation is a function of a single variable which is uniquely calculated from strain or stress histories. The proposed formulation is verified against irregular strain history data and used to predict the pore pressure response in stress controlled undrained tests. Endochronic formulation of porewater pressure obtained for various relative densities, overconsolidation ratios and types of sands is presented. In addition, the endochronic formulation of volumetric strains obtained in strain controlled drained tests is presented and the predictive capacity of the formulation is checked. Such a formulation can be used to calculate settlement due to irregular loading during earthquakes.

6.1 ENDOCHRONIC THEORY

Valanis (1971) proposes that nonlinearity in a material can be characterized by an independent scalar variable which is a function of deformation and time. The potential of this theory for modelling the liquefaction of sand was first recognised by Bazant and Krizek (1976), who use endochronic variables to represent the densification or volumetric

---

[1]Endochronic: Endo - within; Chronic - related with time.

strains caused by cyclic shearing (cf. Section 2.13). The independent variable, called the rearrangement measure, is related with shear strain in the following relationship (Valanis, 1971):

$$d\xi = (\frac{1}{2}\, de_{ij}\, de_{ij})^{\frac{1}{2}} \tag{6.1}$$

where $d\xi$ is the incremental length of rearrangement measure and de_{ij} is the deviatoric shear strain. To relate volumetric strain or densification with rearrangement measure (ξ), another variable called the damage parameter is proposed. The relationship between the damage parameter and the rearrangement measure takes account of strain hardening[2] and strain softening[3] effects. Note that Bazant and Krizek (1976) do not present a unique relationship between volumetric strains and the damage parameter.

As discussed in section 2.1.3, Zienkiewicz et al. (1978) relate volumetric strain caused by cyclic loading with an endochronic variable and rearrangement measure with damage parameter using the transformation shown in equation 2.8. They observe that volumetric strain can be uniquely related with damage parameter for all levels of shear stress ratio.

In Chapters IV and V above it has been shown emphatically that a relationship exists between volumetric strains in the drained condition and porewater pressure in the undrained condition, when both are subjected to the same strain history. Hence, there is a good possibility that an endochronic formulation which uniquely relates volumetric strains with an endochronic variable can be found for porewater pressure. This endochronic formulation for pore pressure data is derived in the

---

[2]For constant cyclic shear strain the decrease in volumetric strain increment with increasing number of cycles is called strain hardening.
[3]The increase in volumetric strain with increasing amplitude of shear strain is called strain softening.

following section.

6.2 ENDOCHRONIC FORMULATION OF PORE PRESSURE DATA

Data on porewater pressures, u, developed in Ottawa Sand at a relative density D_r = 45% during undrained constant strain cyclic loading tests in simple shear are shown in Fig. 6.1 for four different shear strain amplitudes, γ, ranging from 0.056 to 0.314%. Figure 6.1 shows that the non-dimensional porewater pressure ratio, u/σ'_{vo}, increases with increasing strain amplitude, and incremental change in u/σ'_{vo} per cycle decreases with increasing number of cycles of constant cyclic shear strain amplitude. This behaviour is analogous to the volumetric strain obtained during strain controlled drained tests as discussed in section 3.2.1. Thus, it is clear that the porewater pressure ratio is a function of shear strain amplitude, γ, and the number of cycles, N.

$$u/\sigma'_{vo} = f(\gamma,N) \tag{6.2}$$

An alternative to N in describing the strain history applied to the sample is the length, ξ, of the strain path corresponding to N cycles of γ. As the main source of pore pressure increase is shear strain, it is a likely index for porewater pressure. The variable, ξ[4], is a monotonically increasing and continuous variable. Various definitions of the length of strain path are possible. A definition which equates an increment in the length of strain path with an increment in deviatoric strain, given in equation (6.1) has been chosen.

For the simple shear condition, $\gamma = 2e_{12}$, and equation (6.1) degenerates to:

---

[4]Note that the same variable is called rearrangement measure by Bazant and Krizek (1976).

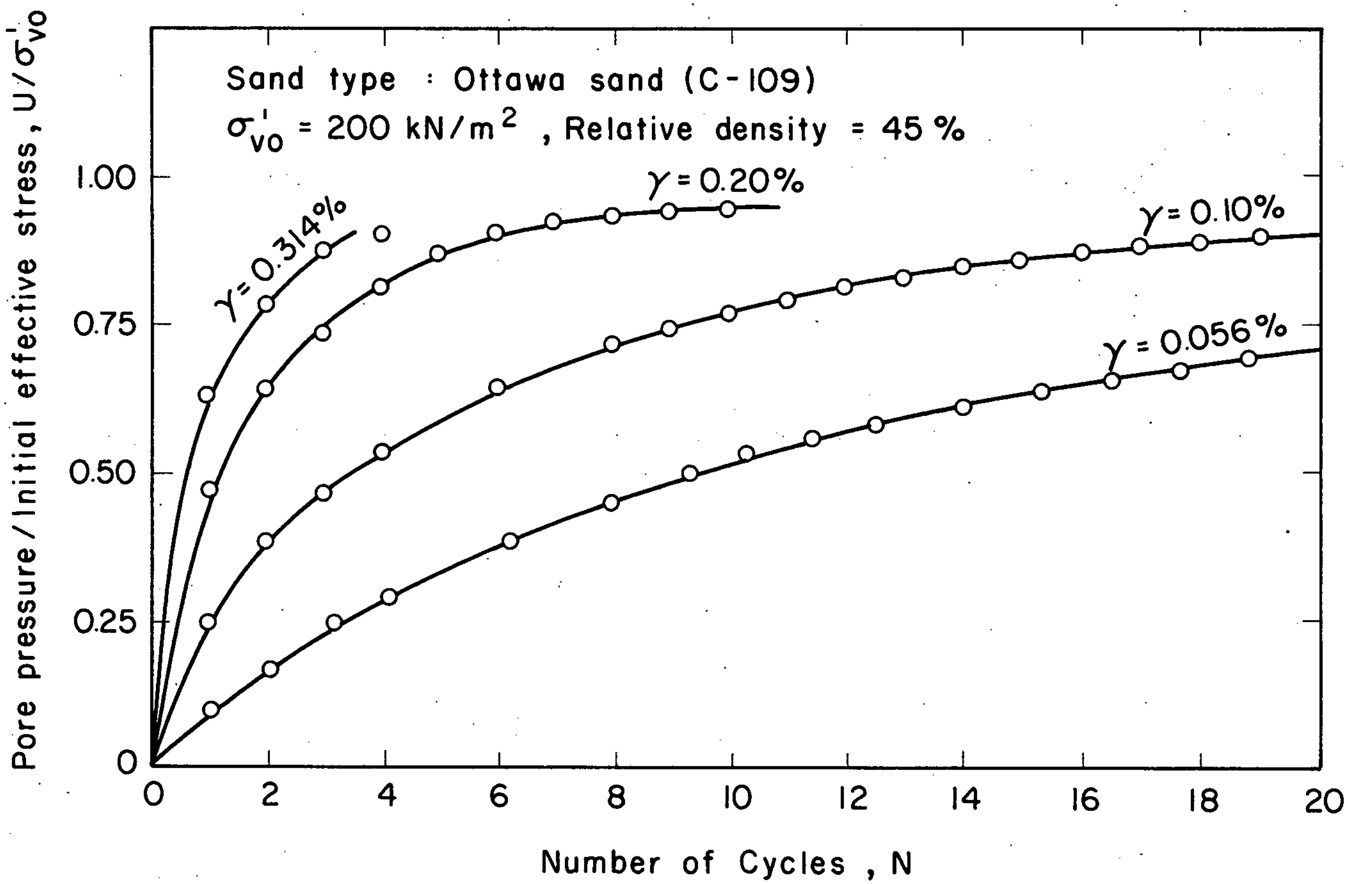

FIG. 6.1 Porewater Pressure Ratio vs. Strain Cycles.

$$d\xi = (de_{12}de_{12} + de_{21}de_{21})^{\frac{1}{2}} / \sqrt{2} = \frac{1}{2}\,|d\gamma| \tag{6.3}$$

When sinusoidal cyclic shear strains are applied and $\gamma = \gamma_o \sin wt$, then ξ at the end of the N^{th} cycle will be:

$$\xi = 2\gamma_o N \tag{6.4}$$

where γ_o is the cyclic shear strain amplitude. From this equation the total length of the strain path is calculated for each cyclic shear strain amplitude as shown in Fig. 6.1. The pore pressure ratio in a constant strain test may now be obtained by

$$u/\sigma'_{vo} = g(\gamma,\xi) \tag{6.5}$$

The data in Fig. 6.1 is shown in Fig. 6.2 with u/σ'_{vo} plotted against the strain length ξ. A natural logarithmic plot is used to expand the plotted path length at small values of ξ. It can be observed from Fig. 6.2 that the pore pressure ratio has a linear relationship with the logarithm of ξ for the range of shear strain amplitude used in testing.

In equation (6.5) the number of cycles, N, of equation (6.2) has been replaced by the continuous variable, ξ. However, before constant shear strain data can be generalised to irregular strain patterns, explicit dependence on the shear strain amplitude, γ, must be removed. For this purpose endochronic variables are used. Our main purpose is to express u/σ'_{vo} as a function of a single monotonically increasing function of a variable, κ, which can be defined for both constant strain and irregular strain histories. Hence, the variable κ must represent all parameters defining the strain history, including varying strain amplitudes and number of cycles. The parameter is called the damage parameter because the effect of shear strain history is to induce pore pressure and weaken the resistance of sand to deformation as discussed by Finn and

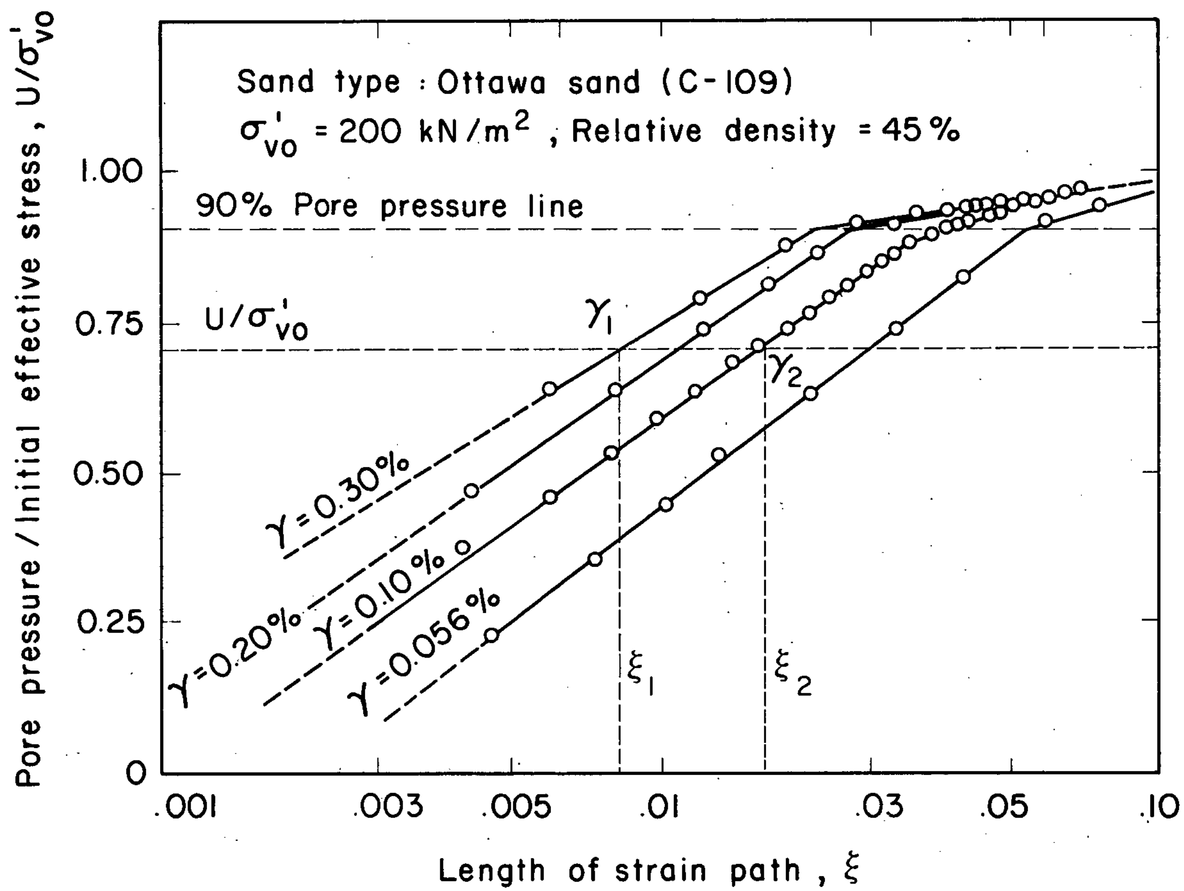

FIG. 6.2 Porewater Pressure Ratio vs. Natural Logarithm of Length of Strain Path.

and Bhatia (1980).

The porewater pressure ratio, u/σ'_{vo}, can be expressed as a function of the damage parameter κ, as given in equation (6.6), where the damage parameter is a transformation of ξ if a transformation T exists so that for $\kappa = T\xi$

$$u/\sigma'_{vo} = G(\kappa) \tag{6.6}$$

The transformation T and the function G are found using the data given in Fig. 6.2. If the pore pressure data is to be explicitly independent of shear strain amplitude then the transformation should be such that all the curves shown in Fig. 6.2 collapse into a single curve giving u/σ'_{vo} as a function of κ, i.e., $u/\sigma'_{vo} = G(\kappa)$. For a particular porewater pressure ratio, u/σ'_{vo}, the length of strain path required to cause this porewater ratio is different for different strain amplitudes. Hence, if the transformation can collapse curves corresponding to different strain amplitudes, the transformation T should be a function of shear strain amplitude, γ.

Referring to Fig. 6.2, consider a particular value of u/σ'_{vo} which occurs at ξ_1 for a shear strain amplitude γ_1, and at ξ_2 for a shear strain amplitude γ_2. The question arises, can this value of u/σ'_{vo} be associated with the value κ_1 of a new variable κ such that

$$\kappa_1 = T\xi_1 = T\xi_2 \tag{6.7}$$

for all (γ_1,ξ_1) and (γ_2,ξ_2)? If so, then all the curves can be collapsed into one curve giving u/σ'_{vo} as a function of κ.

Consider

$$T = e^{\lambda\gamma} \tag{6.8}$$

$$\kappa_1 = \xi_1 e^{\lambda\gamma_1} = \xi_2 e^{\lambda\gamma_2}$$

$$e^{\lambda(\gamma_1-\gamma_2)} = \xi_2/\xi_1$$

or $$\lambda = \ln(\xi_2/\xi_1) / (\gamma_1-\gamma_2) \qquad (6.9)$$

in which λ is called the transformation factor and γ is expressed in percentage. The existence of a unique porewater pressure function $G(\kappa)$ requires a unique value of λ for a given sand at a given relative density. However, when λ is applied to many different data pairs $(\gamma_1, \xi_1; \gamma_2, \xi_2)$ in Fig. 6.2, it is observed that a range of values of λ results. In Fig. 6.3, λ values calculated at various levels of porewater pressure ratio and shear strain amplitudes are shown. About fifty values have been calculated, ranging from 3.0 to 7.0. A weighted average of 4.99 is obtained from these values with values of λ obtained from curves corresponding to shear strains of 0.314% and 0.056% having been weighted most heavily. The calculation of λ values has been restricted to experimental data below a pore pressure ratio, u/σ'_{vo} of 0.90. The experimental data in Fig. 6.2 shows that the pore pressure curves bend at the 0.90 pore pressure ratio and tend to merge into one curve, hence this part of the curves cannot be used for analysis.

Using the average value of λ, each data point $(u/\sigma'_{vo}, \gamma, \xi)$ is converted to a data point $(u/\sigma'_{vo}, \kappa)$ using the following transformation

$$\kappa = \xi \, e^{4.99\gamma} \qquad (6.10)$$

The new data are shown plotted in Fig. 6.4 against the natural logarithm of κ. Because a unique value of λ does not exist, the plotted points define a narrow band rather a single curve. However, despite this range of λ, the use of the mean value of λ for the given sand has consistently yielded data points falling within a narrow band such as shown in Fig. 6.4.

A nonlinear least square curve fitting method has been used to determine the curve shown in Fig. 6.4 describing the relationship between

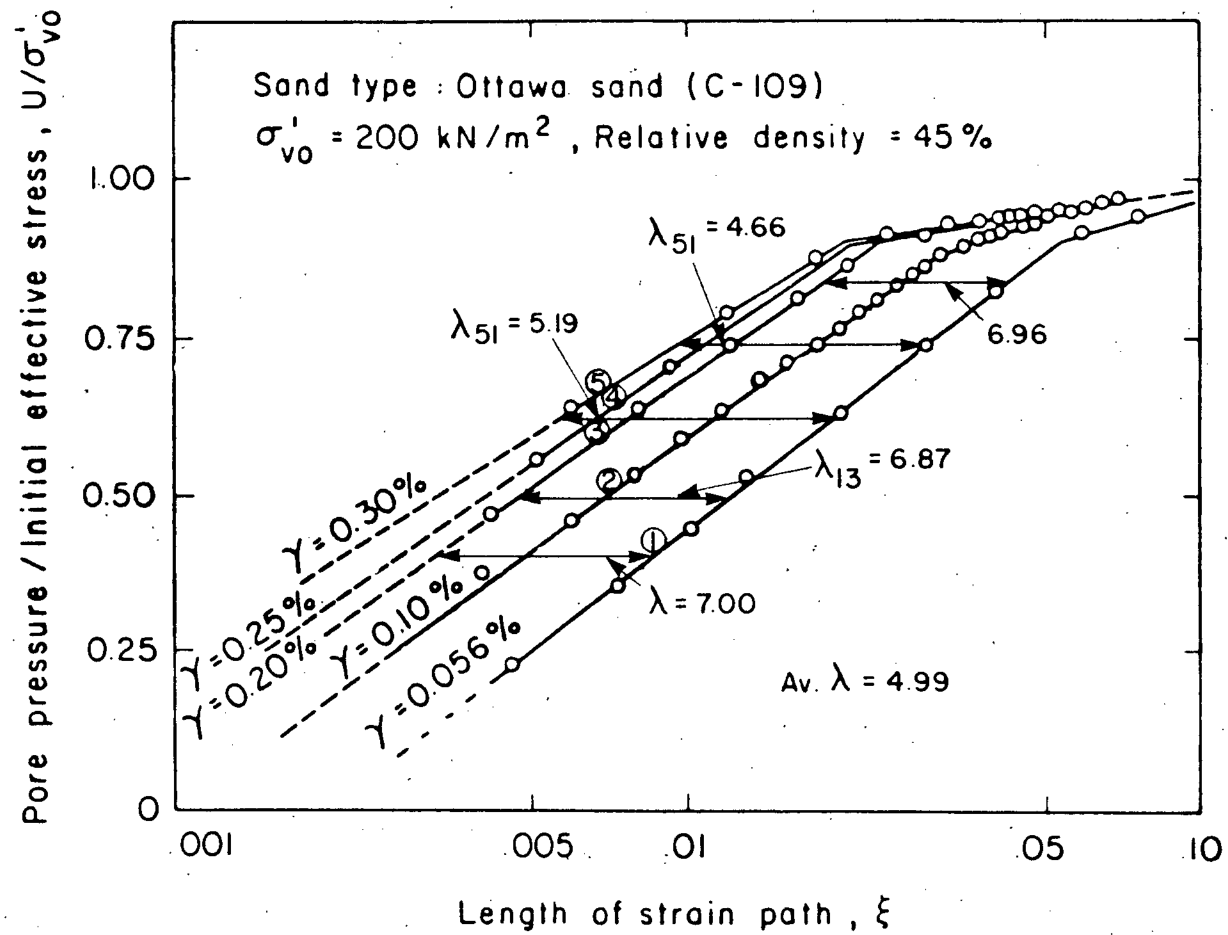

FIG. 6.3 Various Values of Transformation Factor, λ.

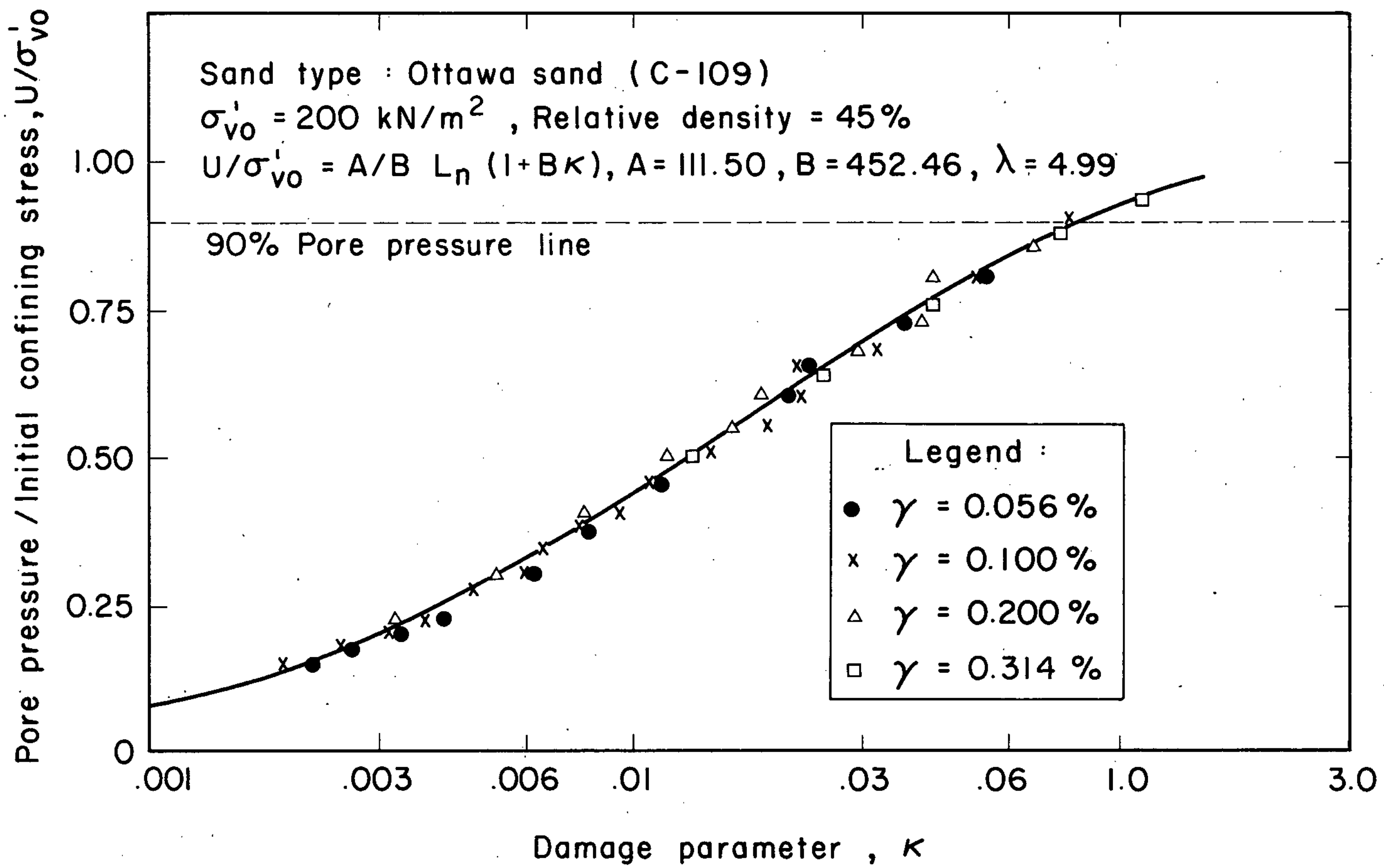

FIG. 6.4 Pore Pressure Ratio vs. Natural Logarithm of Damage Parameter.

u/σ'_{vo} and κ. The equation of this curve is

$$u/\sigma'_{vo} = G(\kappa) = (A/B)\ \mathrm{Ln}(1+B\kappa) \tag{6.11}$$

where A and B, called endochronic constants are 111.5 and 452.5, respectively.

The same data are plotted in Fig. 6.5 on a natural scale. The data shown in Fig. 6.5 have been fitted by the method of nonlinear least squares. The equation of the curve is

$$u/\sigma'_{vo} = \kappa(\bar{D}\kappa+\bar{c}) \ / \ (\bar{A}\kappa+\bar{B}) \tag{6.12}$$

with $\bar{A}$=79.42, $\bar{B}$=0.93, $\bar{C}$=93.58, and $\bar{D}$=71.86.

As is usually the case with least squares fitting procedures, other values of the constants $\bar{A},\bar{B},\bar{C}$ and $\bar{D}$ can be obtained depending on the initial values assumed, however, the relative values of the constants will always be such as to yield the best least square approximation to the data. Therefore, it is possible to relate porewater ratios with a monotonically increasing function of a single variable, κ. The question can be asked, can this formulation be applicable to all levels of initial confining pressure? In Fig. 6.6 the porewater pressure ratio is plotted against constant strain cycles of 0.10 and 0.20 for initial confining stresses, with σ'_{vo} at 1.0, 2.0 and 3.0 kN/m^2. Points corresponding to various initial confining stresses lie on one curve within the range of experimental error. With this supporting evidence in hand it can be assumed that the unique relationship (equation 6.11) between pore pressure ratio and damage parameter is applicable for shear strains in the range of 0.3 to .05% and an initial vertical confining stress, σ'_{vo}, of 1.0 to 3.0 kN/m^2. The range of shear strains and vertical confining pressures are the most useful ranges for liquefaction analysis of saturated sands during earthquakes.

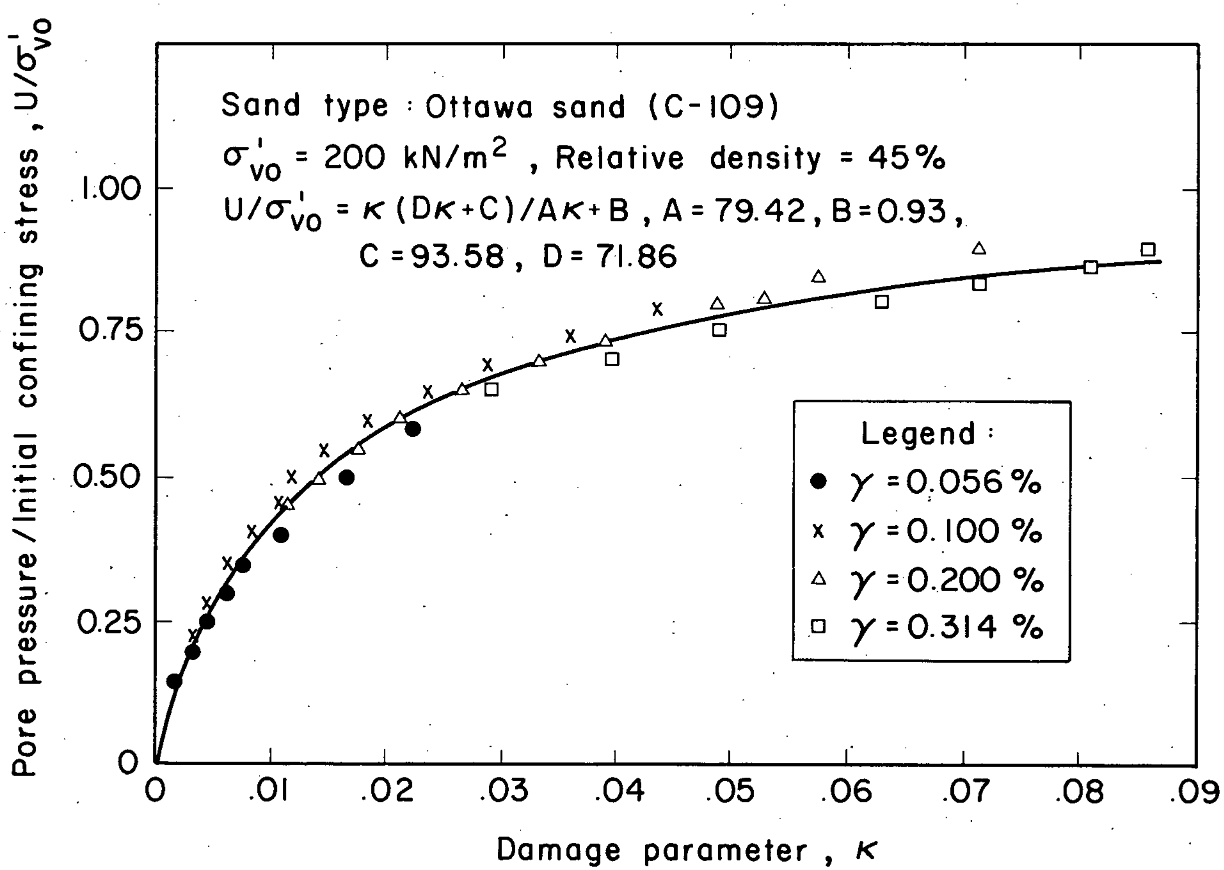

FIG. 6.5 Porewater Pressure Ratio vs. Damage Parameter.

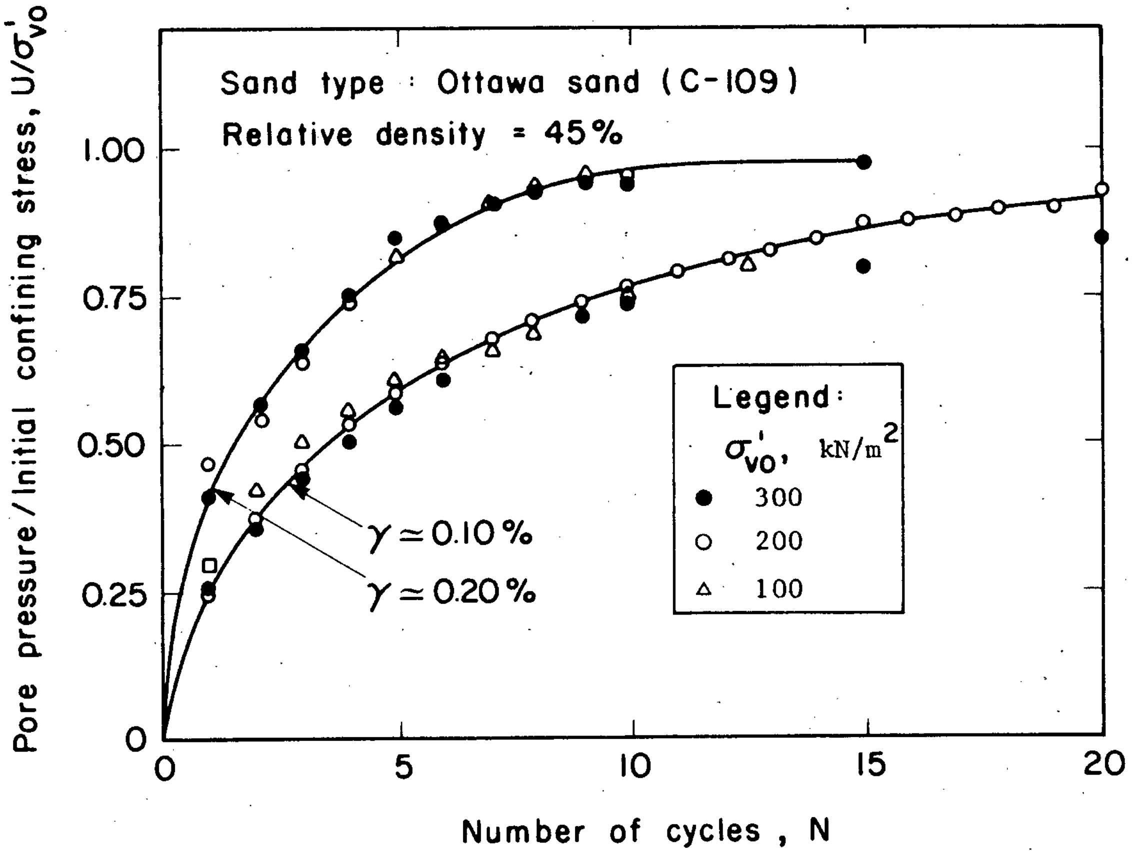

FIG. 6.6 Pore Pressure Ratio vs. Number of Strain Cycles at Various Confining Stresses.

6.2.1 Inverse Transformation

The accuracy with which the basic test data in Fig. 6.1 and 6.2 is represented by equations (6.11) and (6.12) needs to be tested by using the inverse transformation of T to transfer points from curves defined by equations (6.11) and (6.12) back to those of Figs. 6.1 and 6.2 and comparing computed results with the original test data. This process of inverse transformation checks the accuracy of assuming a unique relationship between u/σ'_{vo} and κ.

Analytical and experimental porewater pressure curves are shown in Fig. 6.7 plotted against ξ and in Fig. 6.8 plotted against N. In Fig. 6.8 the dotted curves which represent the analytical inverse transform curve are fairly close to the experimental curves. For a shear strain amplitude of $\gamma = 0.056\%$, the analytical curve overestimates the pore pressure ratio whereas for a shear strain of $\gamma = 0.10\%$, it underestimates the pore pressure ratio by 4 to 5%. It should be noted that the analytical pore pressure curve by inverse transformation was only obtained for values of pore pressure ratio less than 0.90. It is assumed that the analytical function given in equation (6.11) is also applicable for pore pressure ratios greater than 0.90. This assumption may create errors in calculating pore pressure ratios beyond 0.90, however, from a practical point of view pore pressure response beyond 0.90 of initial confining stress is not very important.

Sometimes, the process of converting pore pressure data from ξ-space to κ-space requires two trials. Suppose that with one set of endochronic constants and average value of transformation factor, the representation of pore pressure is not considered satisfactory in a particular strain range, then additional values of λ should be computed in this

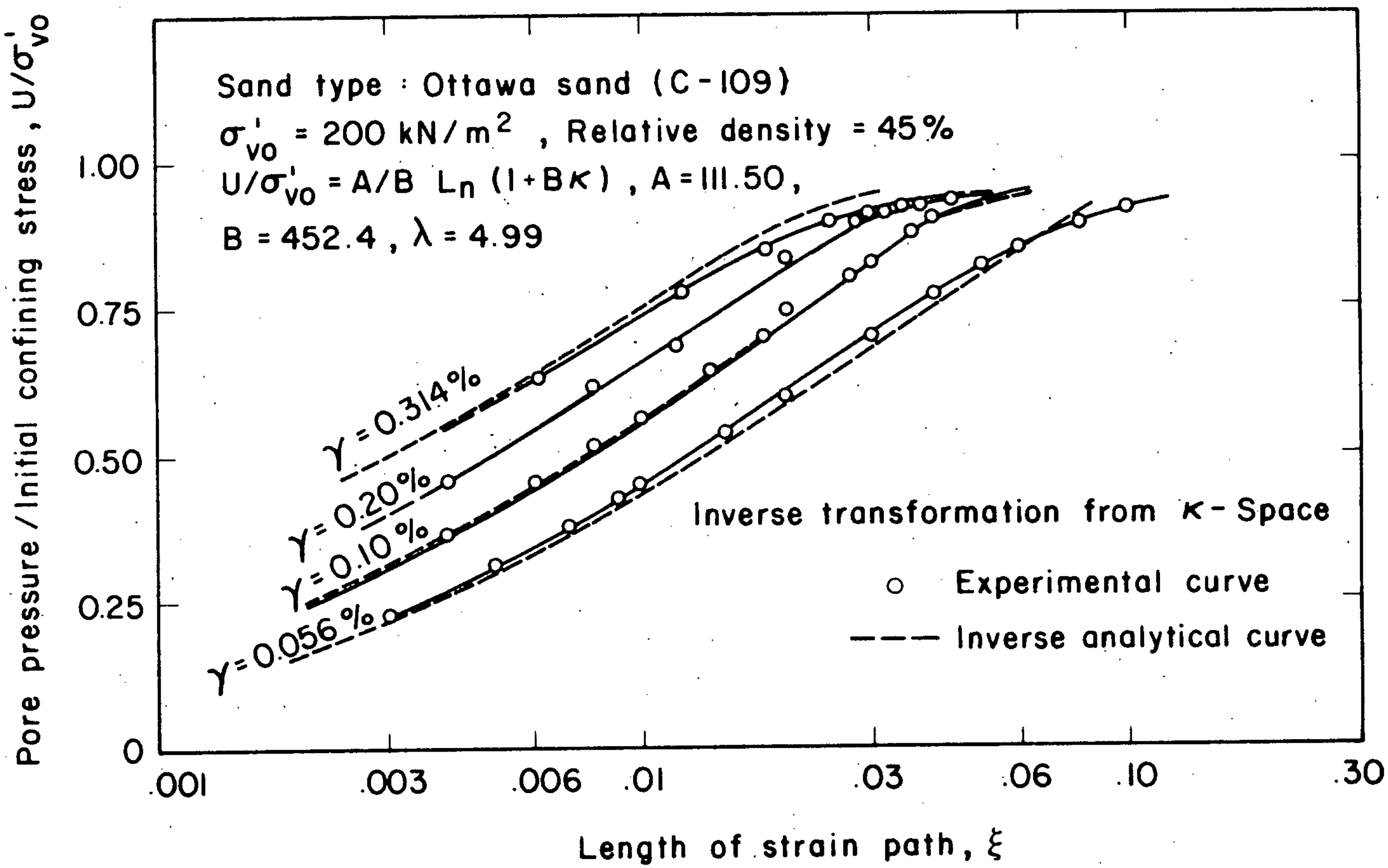

FIG. 6.7 Comparison of Computed and Experimental Porewater Pressure in ξ-plot.

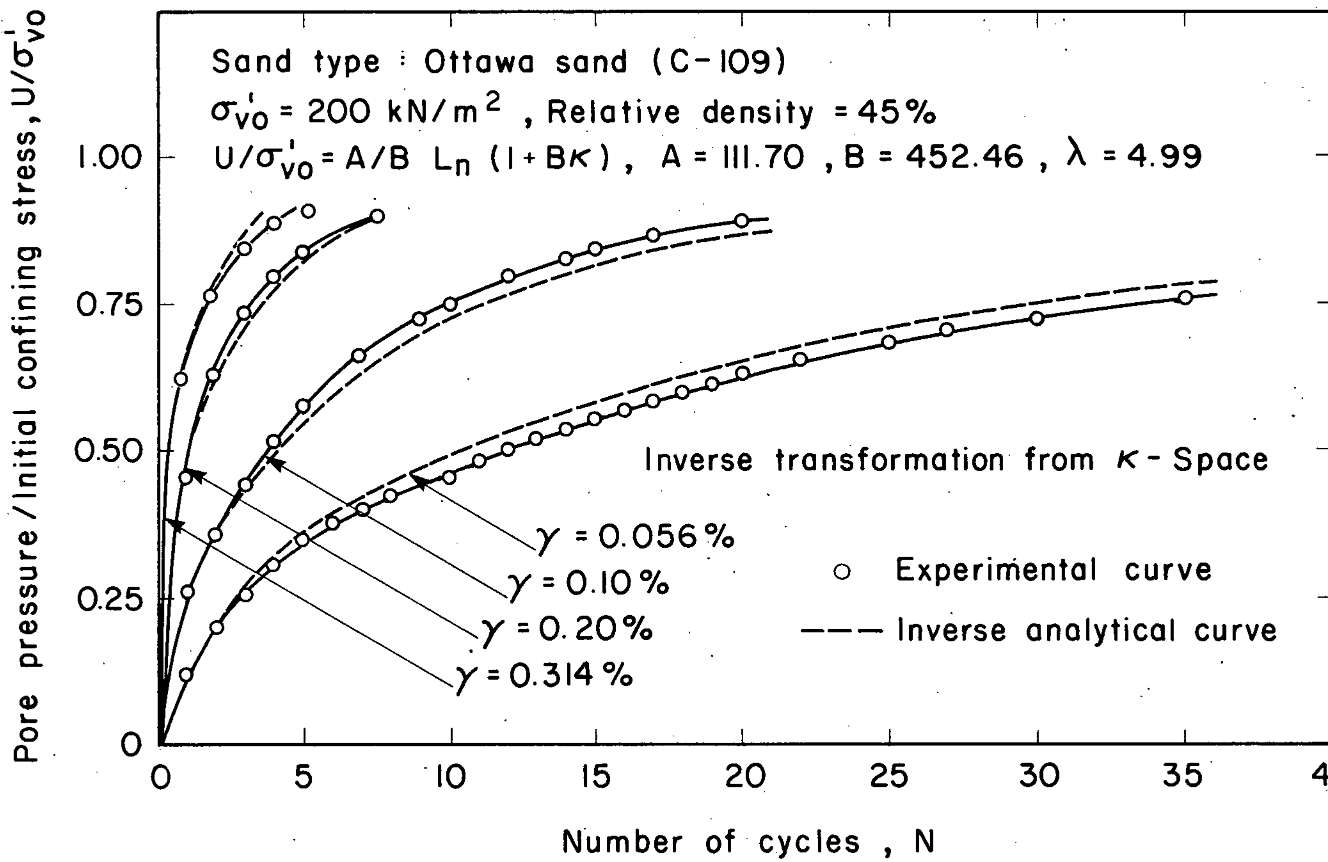

FIG. 6.8 Comparison of Computed and Measured Porewater Pressures in N-plot.

region. These additional values will weight a new mean value of λ towards this strain range and improve the accuracy of data representation in the range. Experience today indicates that, provided a reasonable number of data pairs are used initially in determining the average λ, most of the time no further adjustments are necessary. It should be emphasized that $G(\kappa)$ represents not just the four curves shown in Fig. 6.1 but any test curves that might be determined within the given range. The function $G(\kappa)$ blankets the entire strain amplitude range for which the experimental data used for analysis was obtained. Application of the formulation to strain amplitudes beyond this range, however, should be done only after a preliminary check of the curve for the particular value of shear strain amplitude.

6.2.2 Endochronic Representation of Porewater Pressure Data for Various Relative Densities, Overconsolidation Ratios and Types of Sand

In this section, pore pressure data obtained under strain controlled undrained conditions for various shear strain amplitudes will be presented as a monotonically increasing function of the damage parameter. These data have been obtained for several different conditions, each of which will be discussed separately in the following sections.

6.2.2.1 Various relative densities

A series of tests have been performed on Ottawa Sand at relative densities of 54%, 60% and 68% for shear strain amplitudes $\gamma = 0.10$ to $\gamma = 0.40\%$. A typical plot of porewater ratio, u/σ'_{vo}, against the number of cycles of a shear strain amplitude of $\gamma = 0.20\%$ is shown in Fig. 6.9 for various relative densities. Fig. 6.9 shows that the rate of pore pressure generation decreases with increasing relative density in strain controlled undrained tests.

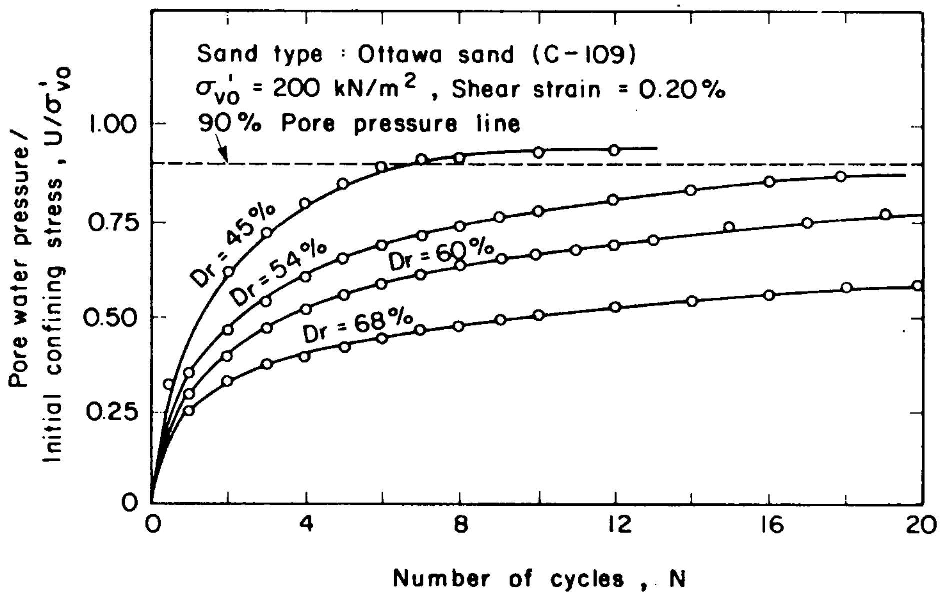

FIG. 6.9 Porewater Pressure Ratio vs. Strain Cycles of 0.20% at Various Relative Densities.

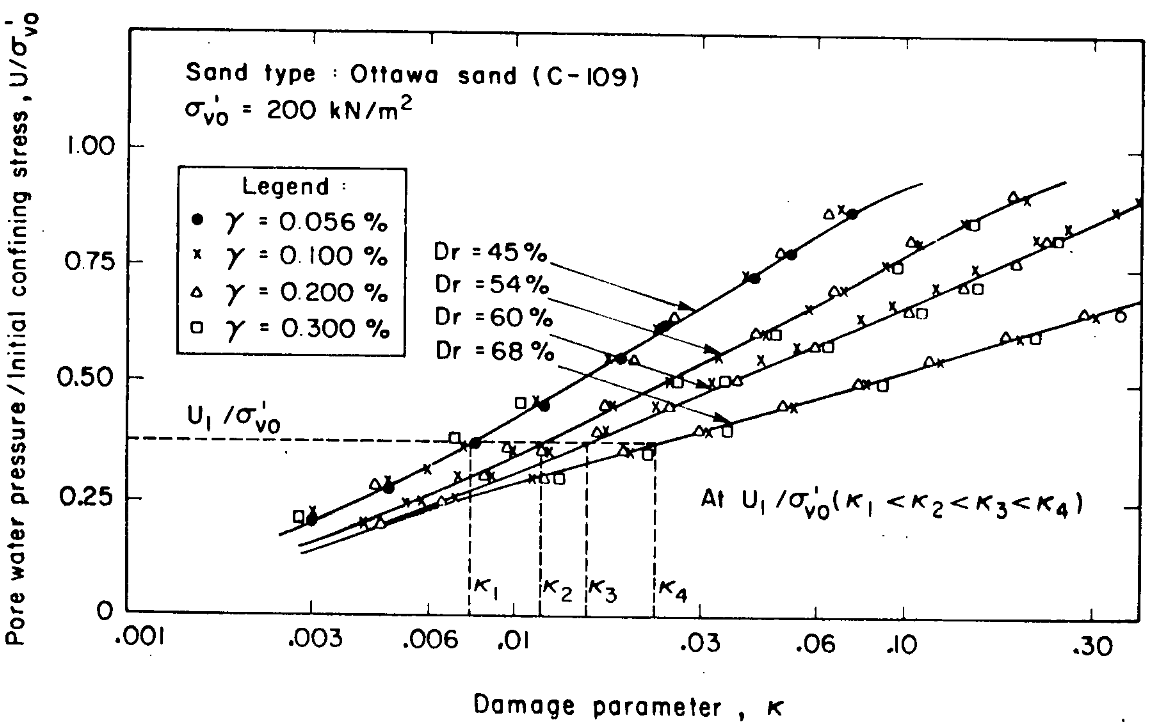

FIG. 6.10 Porewater Pressure Ratio vs. Natural Logarithm of Damage Parameter at Various Relative Densities.

The pore pressure data for various shear strain levels for each relative density are used to calculate the average transformation factor and endochronic constants. For each relative density the final formulation of pore pressure ratio against damage parameter is shown in Fig. 6.10 wherein for each relative density experimental data corresponding to various shear strain amplitudes lie in very narrow bands. The set of endochronic constants and average transformation factor for each relative density is given in Table 6.1. It is apparent that though these sets of constants for the endochronic formulation give good agreement with experimental data, the constants themselves cannot be said to have a uniform tendency with increasing relative density. No concrete conclusions can be drawn about the average transformation factor with various relative densities because in an indirect way, λ also depends on the shape of the porewater pressure curve in ξ-space since pore pressure data when plotted in ξ-space for various relative densities does not always vary linearly with $\mathrm{Ln}(\xi)$.

In general, the tabulated values of average λ for various relative densities indicate that this constant does not differ much for loose to dense Ottawa Sand. Furthermore, Table 6.1 does not indicate any trend in endochronic constants A and B considered alone. However, the ratio A/B decreases with increasing relative density. Since denser sand requires a larger number of cycles of constant shear strain amplitude, compared to loose sand (Fig. 6.9), the length of strain path required to cause a certain level of u/σ'_{vo} will increase with increasing relative density. Even if λ_{ave} as shown in Table 6.1 does not change much with increasing relative density, the damage parameter κ required to create u_l/σ'_{vo} would increase with increasing relative density. This general trend can be seen in Fig. 6.10.

TABLE 6.1

ENDOCHRONIC CONSTANTS FOR VARIOUS RELATIVE DENSITIES

Relative Density D_r%	λ_{ave}	A	B	A/B
45	4.99	111.70	452.46	0.246
54	3.72	100.09	498.40	0.201
60	3.83	92.43	559.11	0.165
68	2.964	148.79	1397.08	0.1065

6.2.2.2 Overconsolidation ratios

As discussed in Chapter V, any increase in overconsolidation ratio causes an increase in the resistance to liquefaction. In Fig. 6.11 pore pressure ratio is plotted against natural logarithm of length of strain path ξ for various overconsolidation ratios and the experimental data shows a considerable reduction in porewater pressure ratio for samples with different overconsolidation ratio at a particular value of ξ. Curves plotted in Fig. 6.11 also indicate that the curvature of the curves becomes more and more pronounced with increasing overconsolidation ratio.

Endochronic transformation has been performed on the porewater pressure data for various shear strain amplitudes and overconsolidation ratios. Results of two such analyses are shown in Fig. 6.12(a) and (b) for overconsolidation ratios of 2 and 4. For both overconsolidation ratios, the data fall in very narrow bands and, again, confirm that pore pressure ratios can be related with damage parameter. The analytical function given by equation (6.11) when fitted to experimental data yields endochronic constants A and B for each overconsolidation ratio. These are presented in Fig. 6.12.

6.2.2.3 Endochronic representation for other sands

In addition to Ottawa Sand, two other types of sands, Crystal Silica Sand and Toyoura Sand were tested. It should be noted that all types of sand are clean sands with quartz particles, though Ottawa Sand has subrounded to rounded particles whereas the other two have subangular to angular particles. In order to make some comparison between the behaviour of all three types of sands, tests on Crystal Silica and Toyoura sands are made at a relative density of 45%. The procedure discussed in section 6.3.1

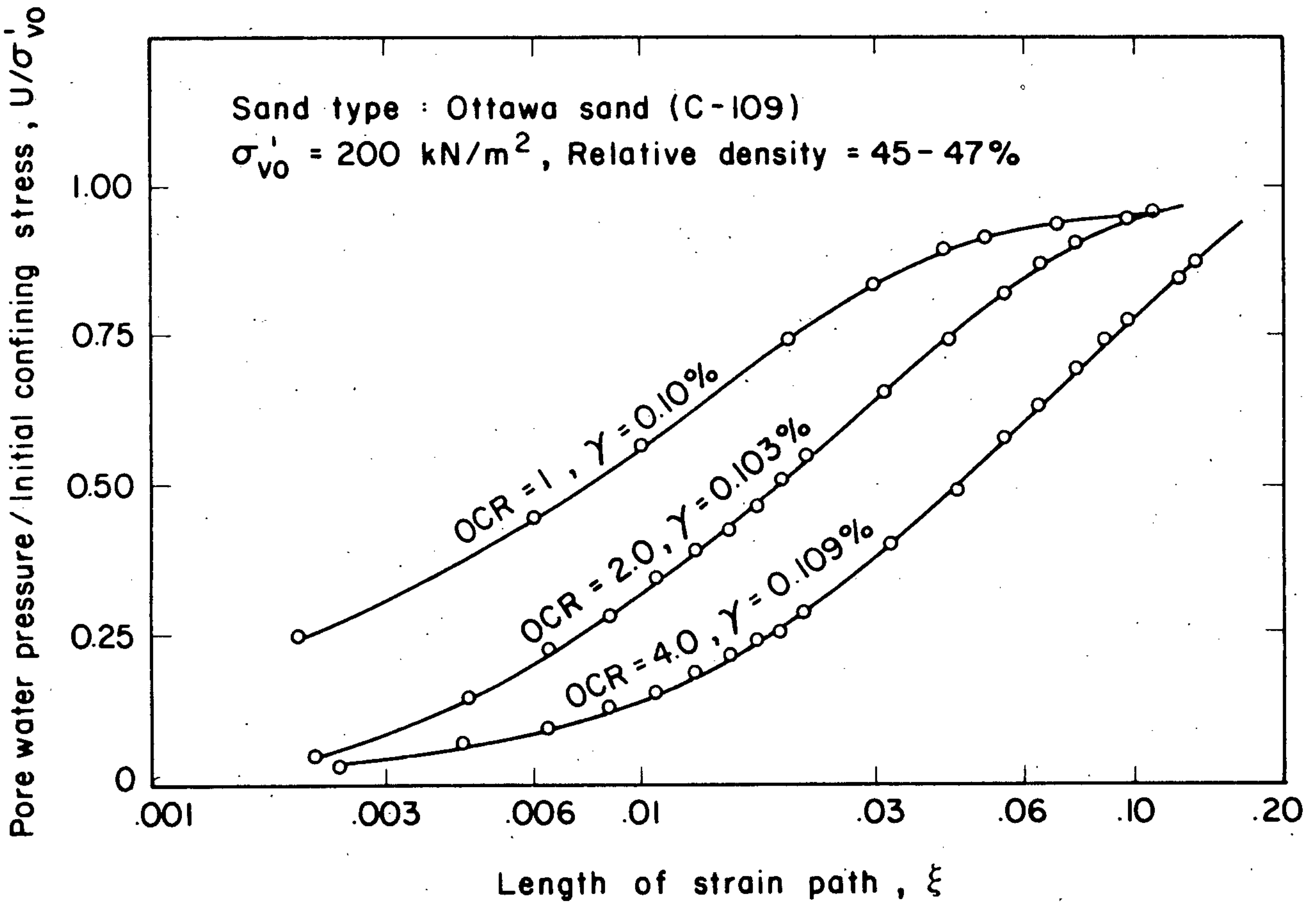

FIG. 6.11 Pore Pressure Ratio vs. Ln (Length of Strain Path) for Various OCR.

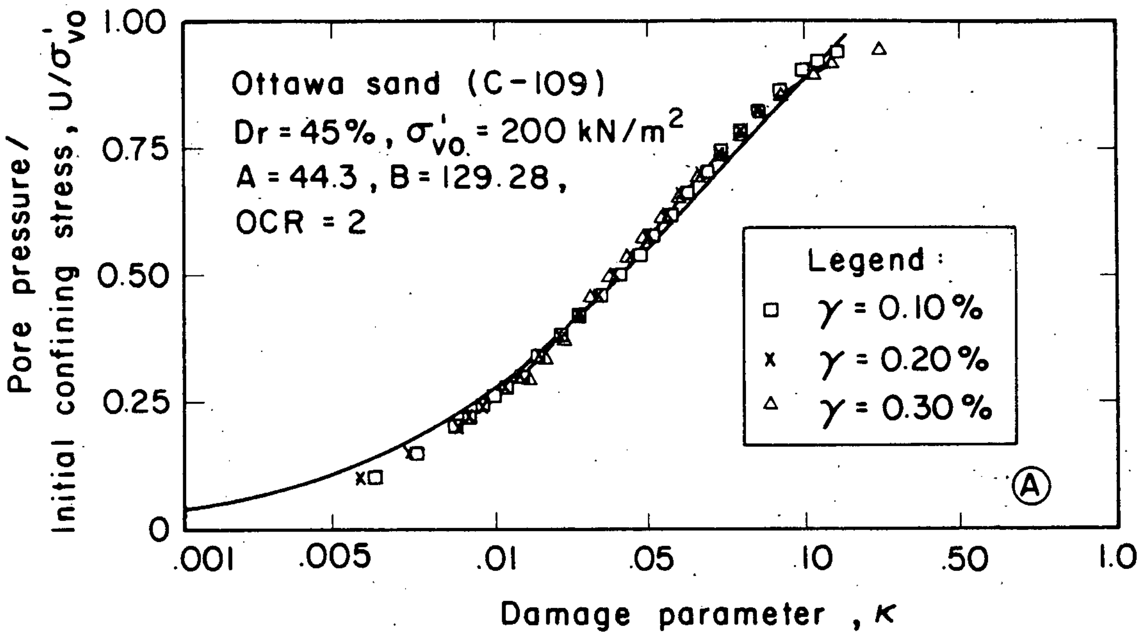

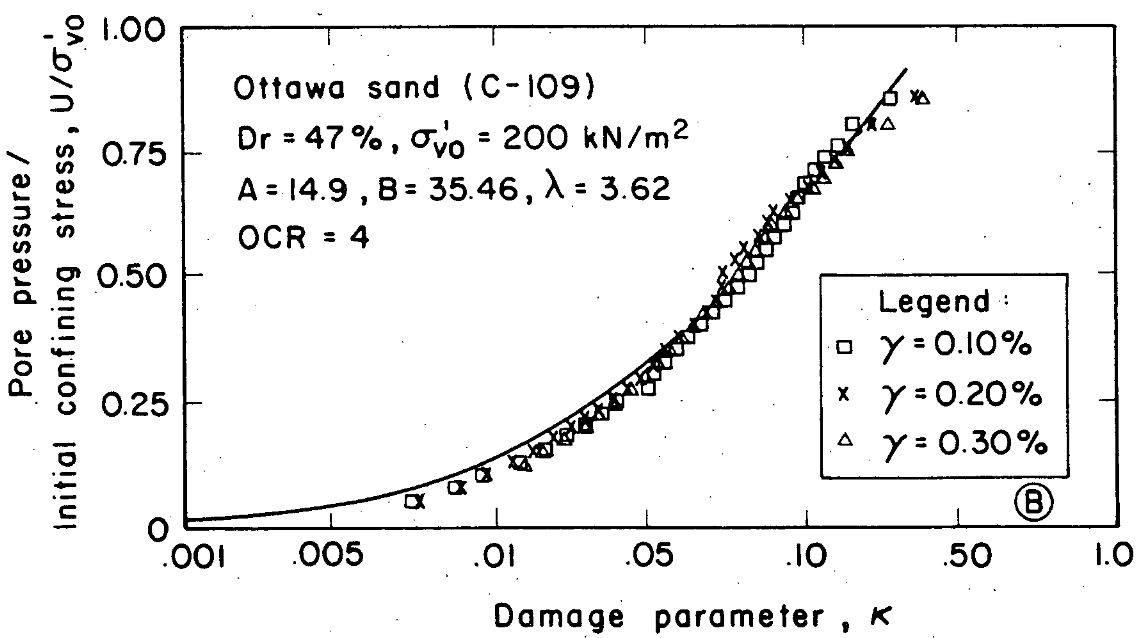

FIG. 6.12 Porewater Pressure Ratio vs. Ln (Damage Parameter) for Overconsolidated Sand.

was again used to obtain a relationship between u/σ'_{vo} and damage parameter, and results of this procedure are shown in Fig. 6.13. The main observation which can be made from this figure is that pore pressure data corresponding to various shear strain amplitudes can be represented by a monotonically increasing function of damage parameter for each type of sand at a particular relative density.

In Fig. 6.14, the pore pressure ratio is plotted against the number of cycles of cyclic shear strain amplitude, $\gamma = 0.20\%$, for all three types of sand at a relative density of 45%. The rate of pore pressure generation is significantly different for each type of sand. Pore pressures generated for Toyoura sand for a given number of cycles are 50% of those for Ottawa sand as shown in Fig. 6.14. Endochronic constants obtained from the analysis of all three types of sands are given in Table 6.2. In Fig. 6.13 curves for Crystal Silica and Toyoura sands shift to the right side or towards the higher values of damage parameter compared to Ottawa sand. This behaviour is justified in two ways, firstly, to generate the same porewater pressure ratio, higher number of cycles of constant strain or a longer strain path is required for Crystal Silica and Toyoura sands compared to Ottawa sand; secondly, the λ_{ave} is greater for Toyoura and Crystal Silica sands. Higher value of the length of strain path and λ_{ave} yields greater values of damage parameter, hence, the pore pressure curve in Fig. 6.13 shifts towards the higher κ-values.

It can be concluded that for each relative density (45,54,60 and 68%) and overconsolidation ratio (OCR = 2,3,4) and different types of sands pore pressure data for each case of various shear strain amplitudes can be represented as a continuously increasing function of damage parameter. Pore pressure curves ($u/\sigma'_{vo} = G(\kappa)$) for various relative densities and types of sands when plotted shows their relative behaviour as shown in

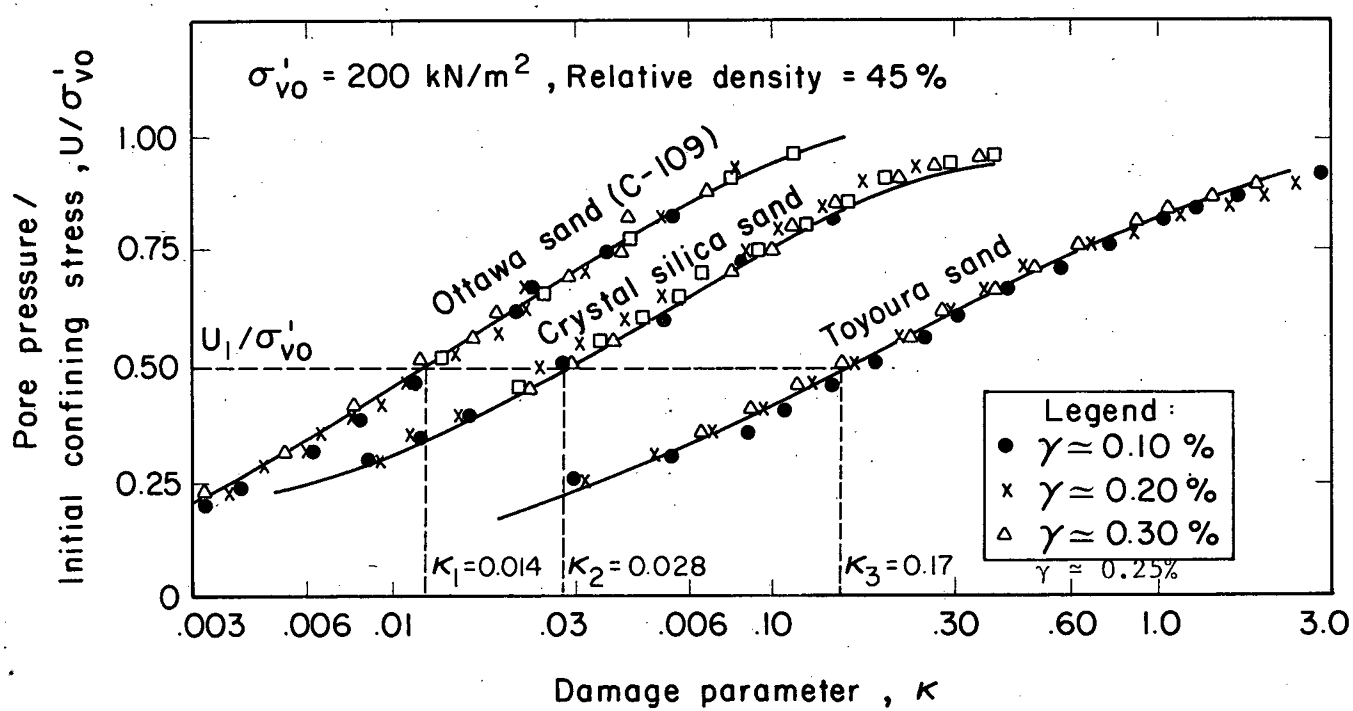

FIG. 6.13 Porewater Pressure Ratio vs. Ln (Damage Parameter) for Various Types of Sands.

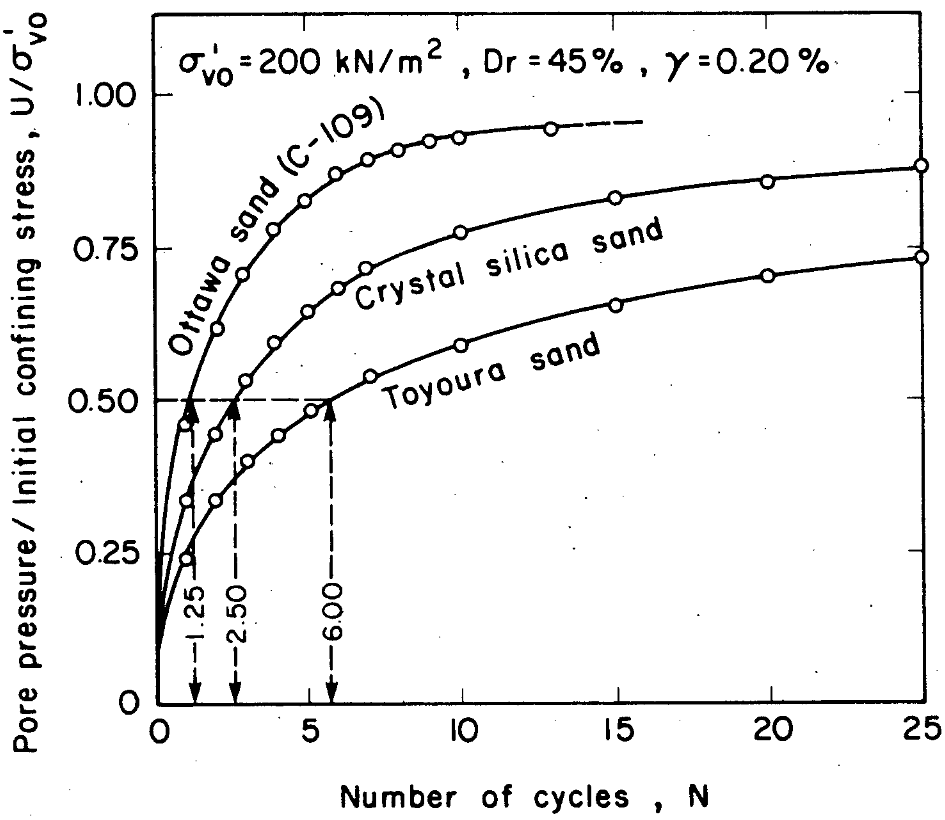

FIG. 6.14 Porewater Pressure Ratio vs. Strain Cycles of γ = 0.20% for Various Types of Sands.

TABLE 6.2

ENDOCHRONIC CONSTANTS FOR VARIOUS TYPES OF SANDS

SAND TYPE	D_r%	λ_{ave}	A	B
Ottawa Sand	45	4.99	111.50	452.46
Toyoura Sand	45	9.36	15.17	82.95
Crystal Silica Sand	45	5.36	99.70	543.60

Figs. 6.10 and 6.13.

6.2.3 Verification of Endochronic Pore Pressure Formulation

Pore pressure generated by a series of symmetrical and unsymmetrical shear strain cycles can readily be computed from the endochronic formulation. However, since the formulation given by equation (6.11) is based on pore pressure data obtained under strain conditions with regular strain cycles, its validity must be checked for irregular strain histories.

For this purpose, the shear strain histories shown in Fig. 6.15(a) and (b) have been used to predict pore pressure ratios. To calculate the pore pressure ratio for each cycle, the incremental length of strain path applied in that cycle is calculated and then converted to the incremental damage parameter. Subsequently, by using the cummulative damage parameter with appropriate values for endochronic constants, pore pressure ratios are calculated using equation (6.11). A typical set of calculations for the strain histories of Fig. 6.15(b) is given in Table 6.3. Calculated and experimental curves for both strain histories are given in Fig. 6.15 showing good agreement.

A more severe check of the endochronic formulation is the calculation of porewater pressure for stress controlled undrained tests. This calculation can use either the shear strain history as recorded experimentally or the constitutive relationships for stress-strain as discussed in Chapter III. Since special care was taken in the undrained stress controlled tests to record the shear strain amplitude, which can fall as low as .03%, the measured shear strain history has been used to calculate the porewater pressure ratio.

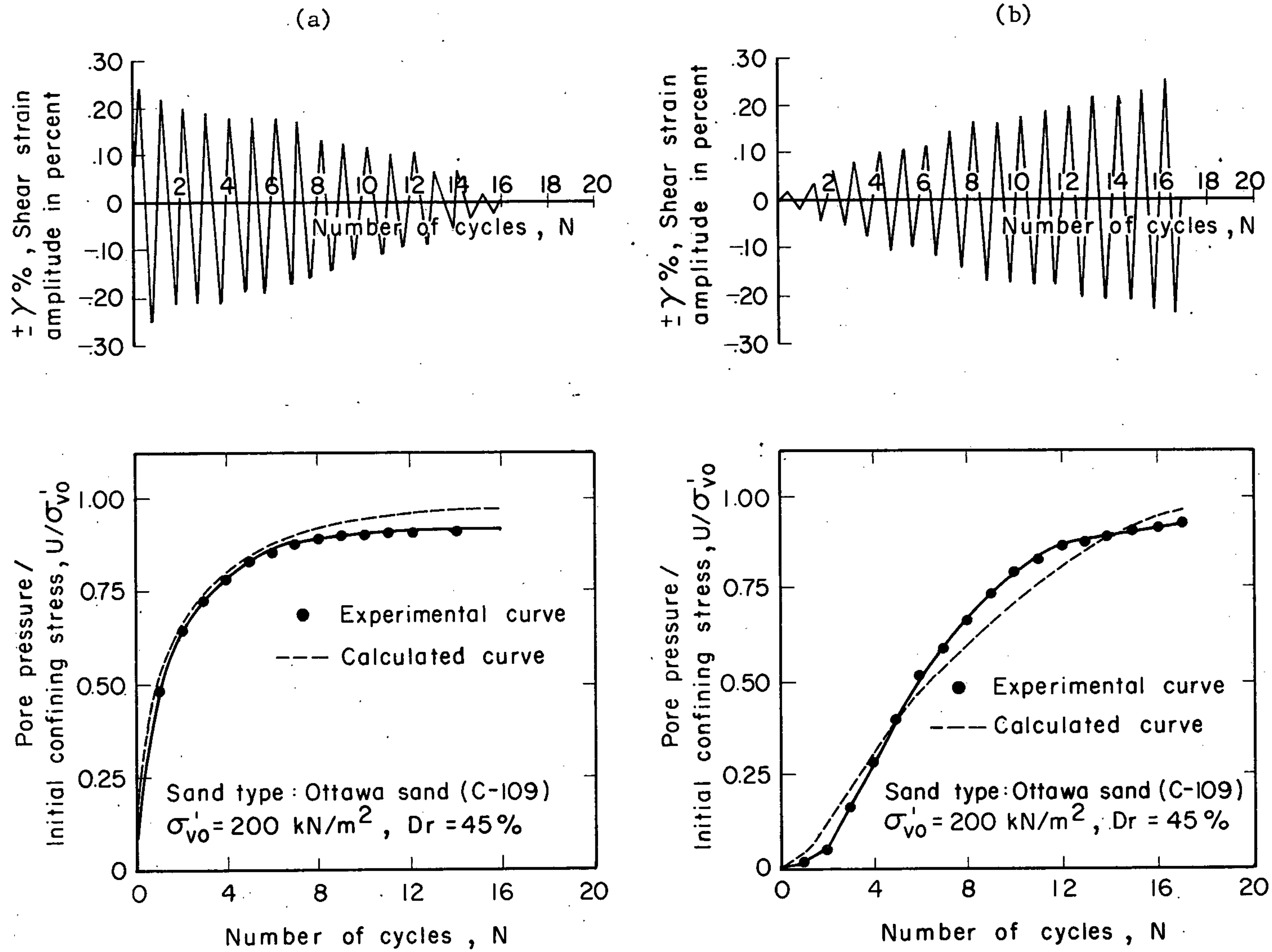

FIG. 6.15 Comparison Between Calculated and Experimental Porewater Pressure Ratios for Irregular Strain History.

TABLE 6.3

PORE PRESSURE CALCULATION FOR IRREGULAR STRAIN HISTORY USING THE ENDOCHRONIC FORMULATION, OTTAWA SAND, D_r=45%

$u/\sigma'_{vo} = A/B \ \mathrm{Ln}(1+B\kappa)$ A = 111.50 B = 452.4 λ = 4.99

N_i	γ%	$\Delta\xi_i$	$e^{\lambda\gamma_i}$	$\Delta\kappa_i$	$\Sigma\ \Delta\kappa_i$	u/σ_{vo} Analytical	u/σ'_{vo} Experimental
1	0.018	.00036	1.093	.000394	.000394	.0404	.0160
2	0.042	.00084	1.233	.00103	.00143	.1220	.058
3	0.06	.00120	1.349	.00106	.00304	.2130	.170
4	0.084	.00168	1.520	.00255	.00559	.3108	.297
5	.108	.00216	1.714	.00370	.00929	.4064	.416
6	.108	.00216	1.714	.00370	.01290	.4754	.523
7	.120	.0024	1.819	.00438	.01728	.5364	.599
8	.144	.00288	2.051	.00590	.0231	.6016	.676
9	.168	.00336	2.312	.00770	.0308	.666	.747
10	.168	.00336	2.312	.0077	.0385	.718	.805
11	.180	.0036	2.455	.0088	.0475	.766	.835
12	.180	.0036	2.455	.0088	.0565	.807	.877
13	.204	.00408	2.768	.01129	.0675	.850	.890
14	.216	.00432	2.938	.01269	.0801	.891	.899
15	.216	.00432	2.938	.01269	.0927	.9266	.917
16	.240	.00480	3.312	.01589	.1087	.9645	.923
17	.240	.00480	3.312	.01589	.1247	.9980	.928

NOTE: γ_i is in percentage.

The calculated and experimental curves for a relative density of 45% are shown in Fig. 6.16, and those for 60% in Fig. 6.17. Both show very good agreement between the experimental and analytical results. A typical calculation is shown in Table 6.4 for a stress ratio of 0.089. It is important to note that the analytical porewater pressure ratio will exceed the value of 1.0 once the cyclic shear strain amplitude reaches 0.8% to 1.0%. However, the porewater pressure ratios corresponding to these shear strains are 0.75 or higher, meaning that the sample requires only one or two more cycles for complete liquefaction, hence this discrepancy is not serious.

Similar analyses have been performed where shear strains calculated using equations (3.10) and (3.14) without hardening produced analytical and experimental curves lying close to each other, though the agreement is not as good as that shown in Fig. 6.16. Pore pressure response has also been calculated for overconsolidated Ottawa sand samples and good agreement between analytical and experimental curves observed.

In conclusion, the proposed endochronic formulation for porewater pressures obtained from experiments performed with constant cyclic shear strain amplitude is capable of predicting porewater pressures for irregular strain histories.

6.2.4 Endochronic Representation of Porewater Pressure from Stress Controlled Undrained Tests

In preceding sections the porewater pressure data used for endochronic formulation has been obtained under constant strain conditions and the verification of the formulation is performed by predicting porewater pressure in stress controlled undrained tests. In this section pore pressure data obtained under stress controlled conditions are used

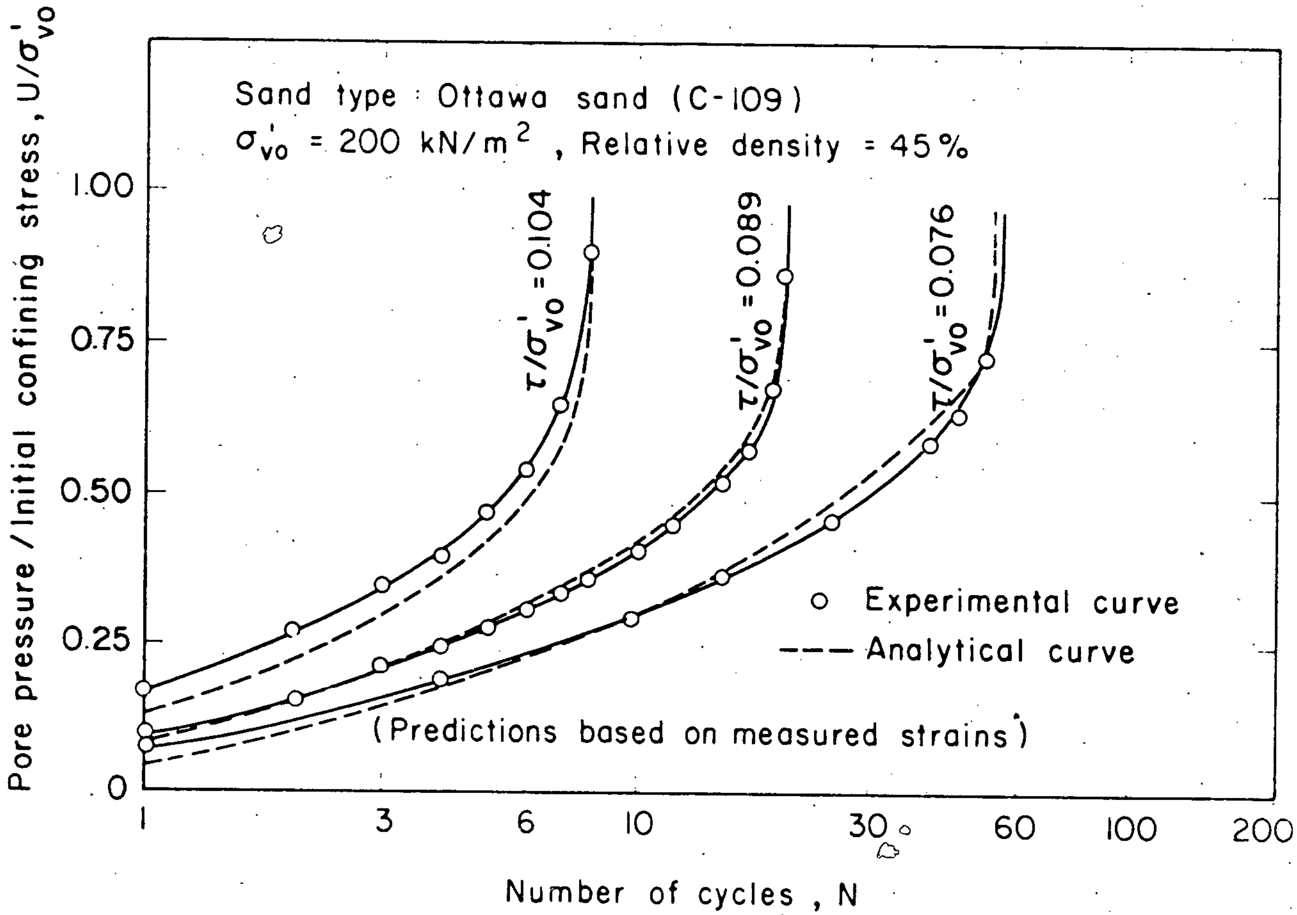

FIG. 6.16 Predicted and Measured Porewater Pressure in Constant Stress Cyclic Simple Shear Tests, D_r = 45%.

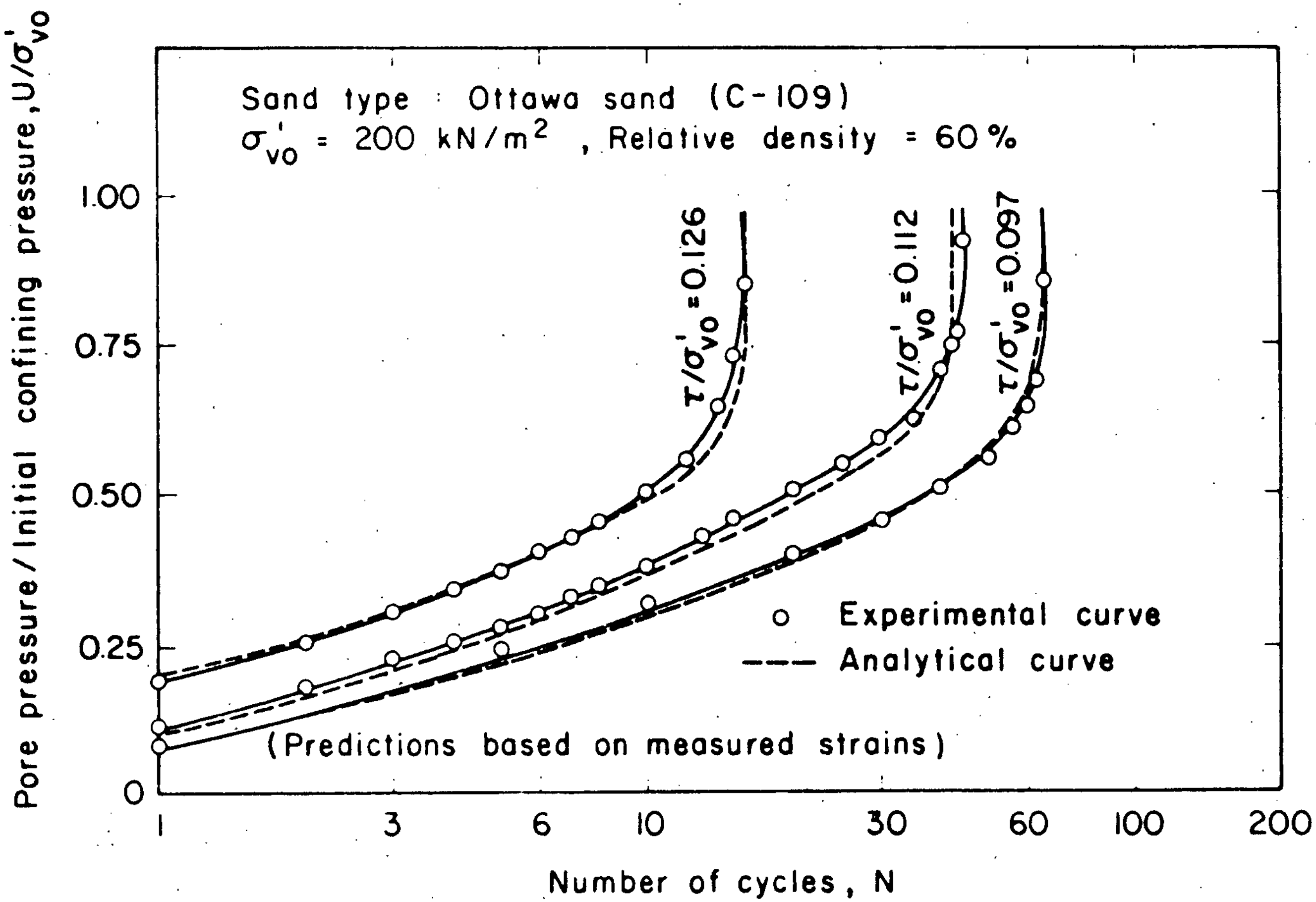

FIG. 6.17 Predicted and Measured Porewater Pressure in Constant Stress Cyclic Simple Shear Tests, D_r = 60%.

TABLE 6.4

CALCULATION OF PORE PRESSURE RATIO FOR STRESS CONTROLLED UNDRAINED TESTS ON OTTAWA SAND AT D_r=45% at τ/σ'_{vo}=0.089

$u/\sigma'_{vo} = A/B \ Ln(1+B\kappa)$ $\qquad$ A = 111.50 $\qquad$ B = 452.4 $\qquad$ λ = 4.99

N	γ%	$\Delta\xi_i$	$e^{\lambda\gamma_i}$	$\Delta\kappa_i$	$\kappa+\Delta\kappa_i$	u/σ'_{vo} Calculated	u/σ'_{vo} Experimental
1	.0409	.000818	1.226	.00103	.00103	.0935	.101
2	.0409	.00818	1.226	.00103	.00206	.163	.166
3	.0409	.000818	1.226	.00103	.00303	.212	.210
4	.0409	.000818	1.226	.00103	.00406	.256	.248
5	.0415	.00083	1.23	.00102	.00508	.294	.281
6	.042	.00084	1.233	.001036	.00611	.326	.312
7	.0431	.000864	1.239	.001069	.00717	.356	.338
8	.0437	.00087	1.243	.00108	.00825	.383	.362
9	.0447	.00089	1.249	.00111	.00936	.407	.386
10	.0464	.00092	1.260	.00117	.0105	.431	.405
11	.0484	.00097	1.273	.00123	.0117	.453	.429
12	.0486	.00103	1.295	.00134	.0130	.476	.450
13	.0519	.00107	1.305	.00139	.0143	.496	.472
14	.0535	.00120	1.349	.00162	.0159	.518	.493
15	.06011	.00125	1.369	.00718	.0176	.540	.514
16	.062	.00144	1.432	.00212	.01970	.565	.544
17	.0801	.00160	1.491	.00271	.0224	.594	.570
18	.1147	.00229	1.772	.00452	.0269	.635	.613
19	0.5247	.01040	13.710	.0324	.0593	.819	.673
20	1.967	.0394	18312.0	128.02	128.07	>1.00	.857

<u>NOTE:</u> γ_i is in percentage.

for the endochronic formulation. The analytical formulations obtained in this section are obtained by two methods:

1. By relating porewater pressure with the length of stress path, and
2. By relating porewater pressure with the length of strain path in which generated shear strain in stress controlled conditions are required to calculate the length of strain path.

6.2.4.1 Pore pressure as a function of stress path

Porewater pressure generated under uniform stress controlled undrained conditions are related with the length of stress path. The definition of length of stress path is chosen as

$$d\eta = \sqrt{d\sigma_{ij} d\sigma_{ij}} \tag{6.13}$$

in which σ_{ij} is deviatoric stress and, for the simple shear condition, $i,j = 1,2$.

For the special case where cyclic shear strain is applied sinusoidally and $\tau = \tau_o \sin wt$, η at the end of the N^{th} cycle will be

$$\eta = 4\tau_o N \tag{6.14}$$

Figure 6.18 shows that porewater pressure ratio is plotted against the natural logarithm of the number of cycles of constant shear stress for various cyclic shear stress ratios, τ/σ'_{vo}. This data was obtained in constant volume simple shear tests performed on Ottawa sand at a relative density of 45%. The pore pressure ratio in constant stress undrained tests may now be defined by

$$u/\sigma'_{vo} = g_1(\tau/\sigma'_{vo}, \eta) \tag{6.15}$$

The general definition of the length of stress path given in equation (6.13) for the simple shear condition will contain the units of shear

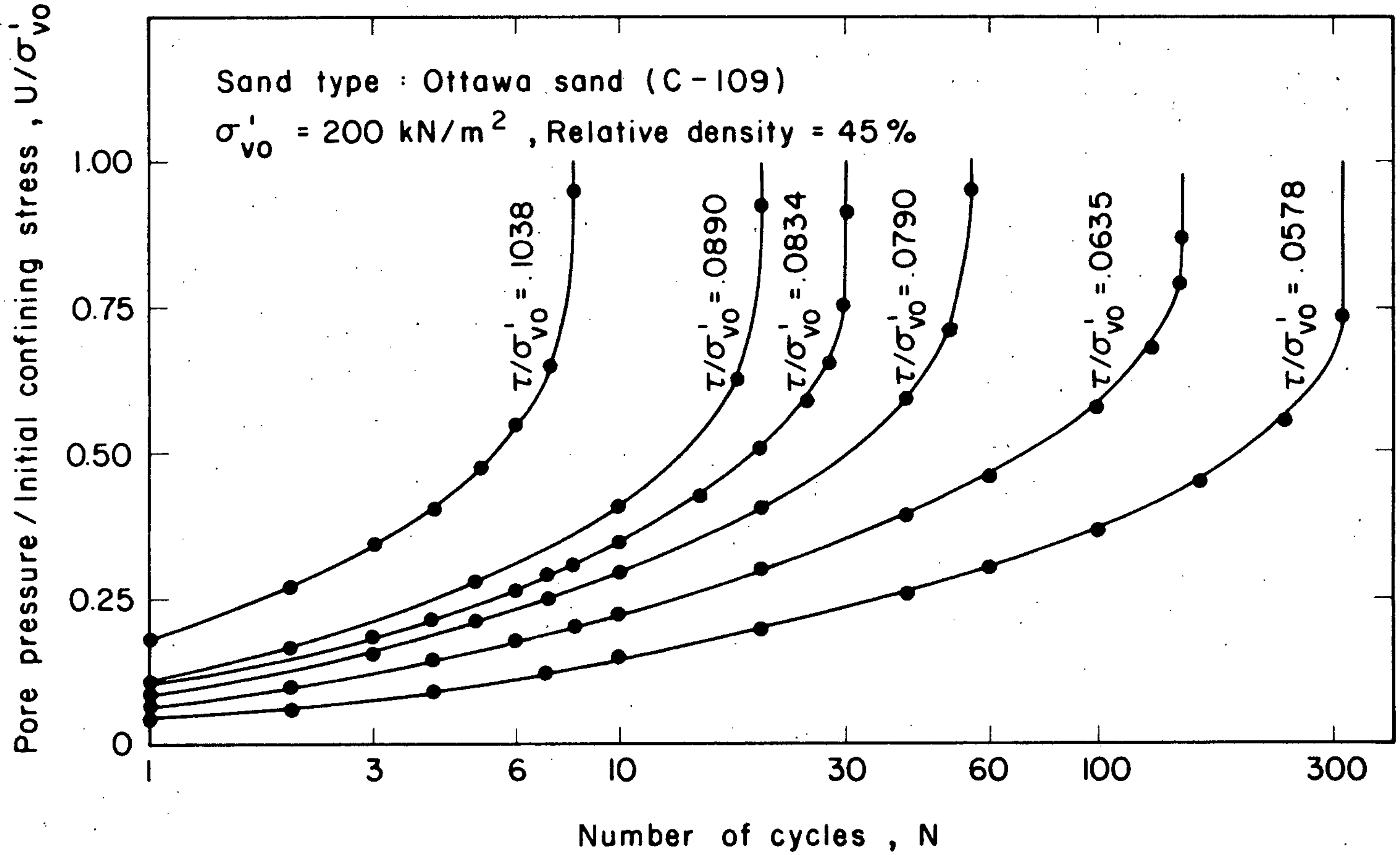

FIG. 6.18 Porewater Pressure Ratio vs. Number of Cycles for Various Cyclic Shear Stress Ratios.

stress. It is considered suitable to define η as given in equation (6.14), where the term, length of stress path, is actually the length of the shear stress ratio

$$\eta = 4 \frac{\tau}{\sigma_v'} N \tag{6.16}$$

The data plotted in Fig. 6.18 is converted in η-space, hence the number of cycles, N, is replaced by the continuous variable η. The transformation T, which is required to convert from stress path space to damage parameter space, is chosen as

$$T = e^{\lambda \tau/\sigma_{vo}'} \tag{6.17}$$

in which τ/σ_{vo}' is the initial cyclic shear stress ratio and λ is the influence factor. In order to evaluate values of λ, experimental data plotted in terms of porewater pressure ratio and length of stress path for various τ/σ_{vo}' have been used. The range of λ value obtained have the mean value of 49.72. Using this average value of λ, the data from η-space has been transformed to κ-space as shown in Fig. 6.19. The experimental points corresponding to various τ/σ_{vo}', as shown in Fig. 6.19, fall in a band that becomes wider after pore pressures have reached 60% of initial confining stress. With the assumed form of transformation given in equation (6.17), the assumption of a unique relationship between u/σ_{vo}' and κ is not very good after the pore pressure ratio has exceeded a value of 0.60. However, for practical purposes this error is not significant.

A nonlinear least squares curve fitting method has been used to determine the curve shown in Fig. 6.19, describing the relationship between u/σ_{vo}' and κ. This equation is of the same form as given in equation (6.11). The values of the endochronic constants A and B are given in Fig. 6.19. Hence, it can be concluded that pore pressure measured

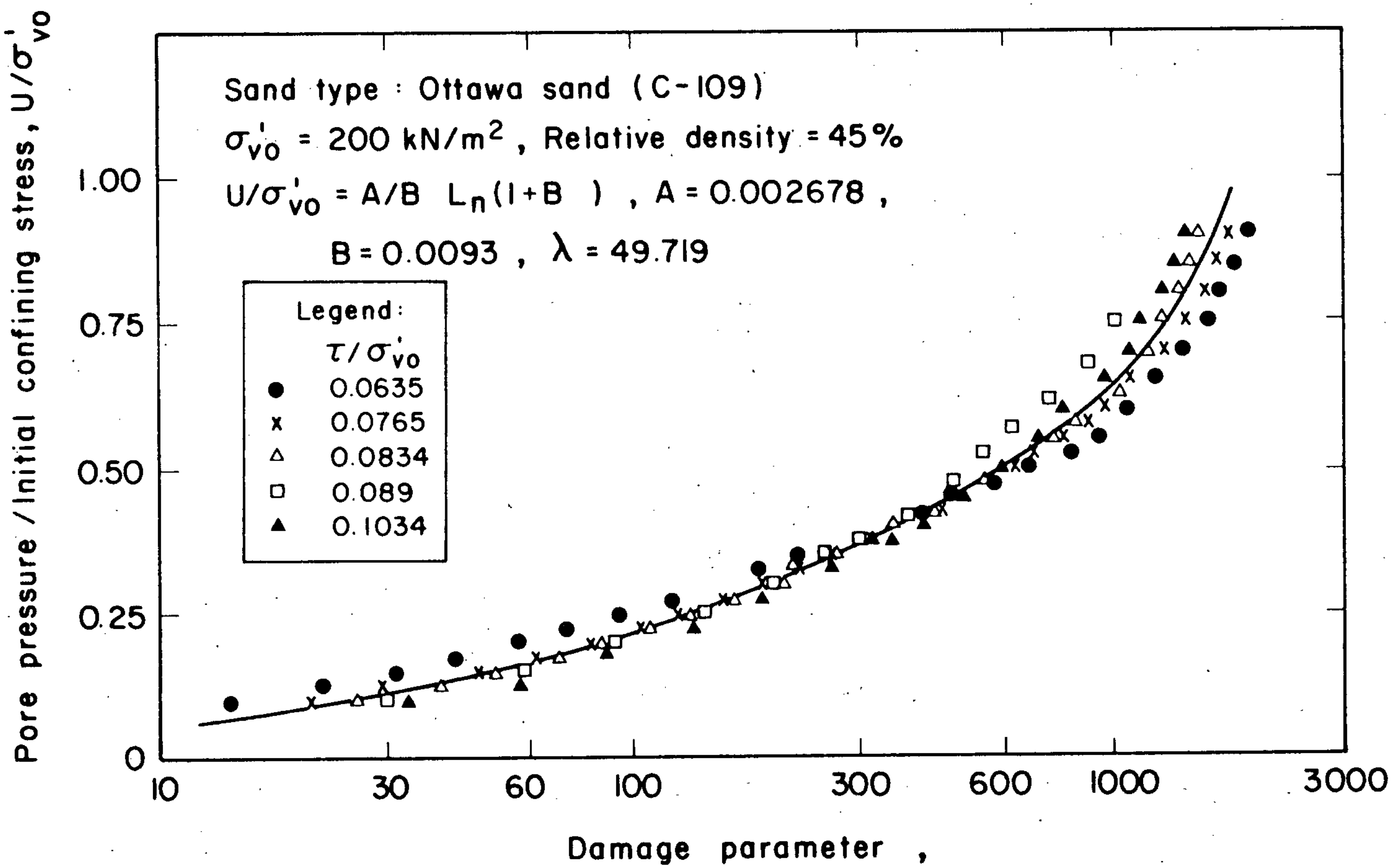

FIG. 6.19 Porewater Pressure Ratio vs. Natural Logarithm of Damage Parameter.

in stress controlled undrained tests for various stress ratios can be represented by a continuous increasing function of the damage parameter. Since, in a general sense, stress controlled tests are a conventional way to study the liquefaction behaviour of sand in cyclic loading, any formulation based on data from these tests is always important. Such formulation obviates the need of performing special tests.

6.2.4.2 Pore pressure as a function of strain path

Porewater pressure ratio measured in stress controlled undrained tests can also be expressed as a function of the length of strain path and the transformation required to convert from strain path to damage parameter can have the form given in equation (6.17).

The shear strains generated during cyclic simple shear tests shown in Fig. 6.18 are plotted in Fig. 6.20(a). The experimental data in this figure show that cyclic shear strains remain almost constant until u/σ'_{vo} is less than 0.30. Beyond this point, shear strain gradually increases with increasing porewater pressure until u/σ'_{vo} reaches a value of 0.65. After this point the sample requires one or two additional cycles to generate shear strains of 5 to 10%. Cyclic shear strains shown in Fig. 6.20(a) are used to calculate the length of strain path where the length of strain path is again given by equation (6.1). Porewater pressure data given in Fig. 6.18 are used in conjunction with the calculated length of strain path and a plot of u/σ'_{vo} and ξ obtained. The transformation of porewater pressure data from ξ-space to κ-space was obtained by assuming the transformation given in equation (6.17). The average value of λ was calculated and final results of this analysis are given in Fig. 6.21, where scatter in data corresponding to various shear stress ratios is significant to conclude the existence of a unique relationship between.

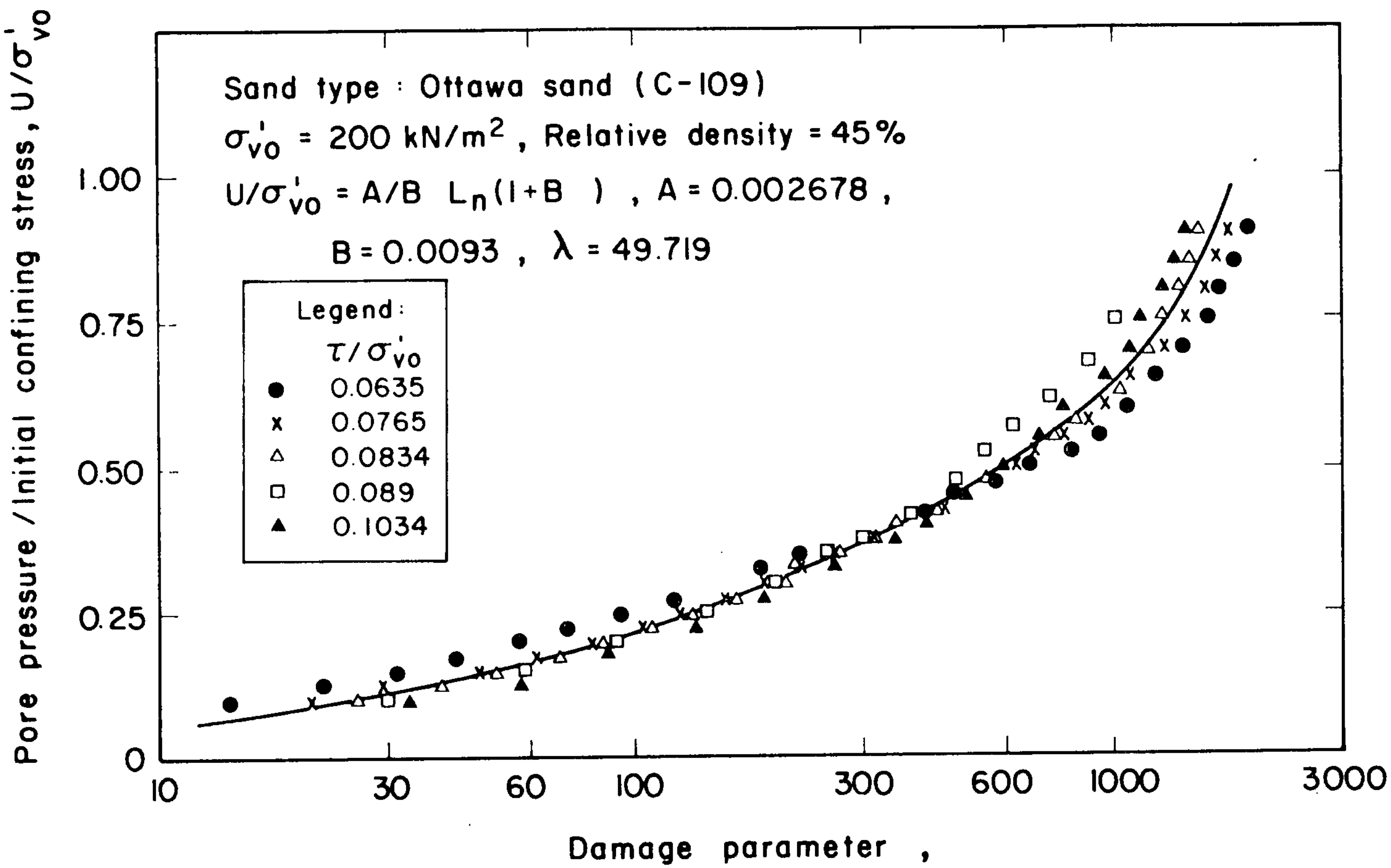

FIG. 6.19 Porewater Pressure Ratio vs. Natural Logarithm of Damage Parameter.

u/σ'_{vo} and κ. A similar analysis is performed by Zienkiewicz et al. (1978) as discussed in section 2.1.2.

In Appendix III, it has been shown that volumetric strains obtained under strain controlled drained conditions can also be presented as a monotonically increasing function of the damage parameter. Such a formulation is capable of predicting volumetric strains for irregular strain histories.

6.3 DISCUSSION

A new method for processing porewater pressure data of a saturated sand at a particular relative density from conventional cyclic simple shear under strain or stress controlled conditions has been presented. Usually, the description of such data involves a curve of the porewater pressure ratio, u/σ'_{vo} vs. the number of uniform load cycles, N, for each shear stress or shear strain amplitude. In the approach presented here all the curves can be replaced by a single curve, $u/\sigma'_{vo} = G(\kappa)$ in which κ is a variable that encompasses the effects of both shear or strain amplitude and cyclic loading. The procedure to obtain this variable κ, is quite simple and uses test data from conventional tests.

In addition, the function $G(\kappa)$ is a super-efficient representation of pore pressure and volumetric strain data, requiring only one curve to describe all the test data at one relative density for the range of cyclic stresses or strains of interest. The variable κ which is easily defined for irregular stress or strain conditions allows the direct use of data from uniform cyclic loading tests to predict the porewater pressure caused by irregular stress or strain histories generated by earthquake loading.

Moreover, the new porewater pressure function, $u/\sigma'_{vo} = G(\kappa)$ simplifies greatly the estimation of porewater pressures in the field. The endochronic formulation of volumetric strains can be used to calculate settlement due to irregular strain or stress cycles.

CHAPTER 7

SUMMARY AND CONCLUSIONS

7.1 SUMMARY

The main purpose of this research is twofold. First, to verify the most crucial assumption made for the constitutive relationships behind the dynamic effective stress analysis by Finn, Lee and Martin (1977). Second, to propose a simple method of porewater pressure prediction based on results from conventional tests.

The dynamic effective stress (Finn, Lee and Martin, 1977) is based on a pore pressure model proposed by Martin et al. (1975) after the incorporation of the realistic constitutive relationships proposed by Lee (1975) for the nonlinear, hysteretic stress-strain behaviour of sand during cyclic loading. In this thesis the performance of these constitutive relationships, both for the pore pressure model and for stress-strain behaviour, is evaluated for normally consolidated and overconsolidated sands.

A simple formulation is proposed that expresses porewater pressure as a monotonically increasing function of a single variable. Data for this formulation are available from conventional constant strain or stress undrained tests. The formulation can be coupled with dynamic response analysis to predict porewater pressures in irregular stress or strain histories such as those that result from earthquakes.

7.2 CONCLUSIONS

After testing under a variety of drained and undrained loading conditions, the porewater pressure model of Martin et al. (1975) appears to be based on sound assumptions. The most crucial questions raised about the model in Chapter III can now be anwered as follows:

1. The experimental data indicates that the potential volumetric strain in undrained conditions is the same as that in drained, when both drained and undrained samples are subjected to the same shear strain history. It has been strongly verified that there is unique relationship between volumetric strain in the drained condition and porewater change in the undrained condition for a given sand and relative density when samples have been subjected to similar strain histories. This observation based on experimental data obtained for Ottawa sand (C-109) at various relative densities and overconsolidation ratios.

2. An important point to emerge from this study is that the rebound modulus used to convert volumetric strains to porewater pressure (equation 3.2) must be measured under cyclic loading conditions. The static rebound modulus used in conjunction with volumetric strain data overestimates porewater in stress controlled undrained conditions. However, it has been found that static rebound modulus can be adjusted towards the dynamic modulus by a factor 3 to 5 and this adjustment can be made in constant k_2.

3. For the application of the model under undrained conditions, the strain hardening effect should not be included for the analysis. However, at the conclusion of such tests, if drainage is allowed to take place, plastic strains are recovered and sands strain-harden.

Provided proper values of the rebound modulus are used and effects of strain-hardening are included whenever drainage occurs, the analysis clearly shows that the set of constitutive relationships can make good predictions of the development of porewater under fairly general loading patterns and drainage conditions in simple shear.

4. The increase in resistance due to overconsolidation cannot be completely attributed to increase in mean effective stress. It may be possible that during the process of overconsolidation, in addition to increased horizontal stress, sands attain more stable structures which would contribute to increased resistance. However, the effective stress pore pressure model can make good prediction of the development of porewater pressure for overconsolidated sand, provided appropriate volumetric strain constants and rebound modulus constants are used.

It is felt that the measurement of volume change constants and dynamic rebound constants require tests which are not considered conventional. In particular, the evaluation of dynamic rebound characteristics is quite time consuming. For this reason a simple and efficient method is proposed by which porewater pressures measured in routine laboratory stress or strain controlled tests can be utilized in dynamic effective stress analysis by a single curve, $u/\sigma'_{vo} = f(\kappa)$. The proposed formulation, based on endochronic theory has been developed from extensive data and its performance thoroughly evaluated. The main conclusions which can be drawn from this study are (cf. Chapter VI):

1. The proposed method for processing porewater pressure data on saturated sand at a particular relative density from conventional cyclic simple shear tests, involves a single curve $u/\sigma'_{vo} = G(\kappa)$ in which κ is a transformed variable that encompasses the effects of both shear stress or strain amplitude and cyclic loading. This observation is based on experimental data for various relative densities, overconsolidation ratios and types of sand.

2. The procedure to obtain the variable κ is simple using conventional test results. The function $G(\kappa)$ is a super-efficient representation of porewater pressure data, requiring only one curve to describe all the test data for the range of cyclic stresses and strains of interest.

3. The variable κ which is easily defined for irregular stress or strain conditions allows the direct use of the data from the uniform cyclic loading tests to predict the porewater pressure caused by irregular strain or stress histories similar to those generated by earthquakes.

4. In addition, it is possible to represent volumetric strains obtained under strain controlled drained conditions as a monotonically increasing function of the damage parameter. Moreover, such a formulation is capable of accurately predicting volumetric strain under irregular strain history or stress controlled conditions.

Finally, for the dynamic effective stress analysis a porewater pressure model based on fundamental properties of the soil skeleton and water is no longer required. During any time increment Δt in the dynamic analysis, the increment in porewater pressure can be determined from the incremental change in κ. The soil properties may now be modified for this change in porewater pressure and the analysis continued for the next time increment Δt. The use of the new procedure means that no special tests are required for dynamic effective stress analysis. Moreover, it is an extremely efficient way of storing large amounts of data. For prediction of seismic settlement, the endochronic formulation of volumetric strain can be used.

7.3 SUGGESTIONS FOR FUTURE RESEARCH WORK

The proposed endochronic formulation should be coupled with dynamic response analysis to perform effective stress analysis. In this way, the performance of this formulation for random and irregular loading patterns can be evaluated. Predictive capacity of the constitutive relationship and proposed endochronic formulation for pore pressure should be checked with field data.

LIST OF REFERENCES

1. Afifi, S.S. and Richart, F.E. (1973), "Stress History Effects on Shear Modulus of Soils", Soils and Foundations, Vol. 13, No. 1, March, pp. 78-95.

2. Bazant, Z.P. and Krizek, R.J. (1976), "Endochronic Constitutive Law for Liquefaction of Sand", Journal of the Engineering Mechanics Division, ASCE, Vol. 102, No. EM2, April, pp. 225-238.

3. Biot, M.A. (1956), "Theory of Propagation of Elastic Waves in Fluid-Saturated Porous Solid-I. Low-Frequency Range", Journal of the Acoustical Society of America, Vol. 28, pp. 168-197.

4. Biot, M.A. (1957), "The Elastic Coefficient of the Theory of Consolidation", Journal of Applied Mechanics, Vol. 24, pp. 594-601.

5. Bjerrum, L. and Landva, A. (1966), "Direct Simple Shear Tests on a Norwegian Quick Clay", Geotechnique 16 1, pp. 1-20.

6. Casagrande, A. (1936), "Characteristics of Cohesionless Soils Affecting the Stability of Earth Fills", Journal of the Boston Society of Civil Engineers, January 1936. Reprinted in "Contributions to Soil Mechanics, 1925-1960", Boston Society of Civil Engineers, October 1940.

7. Castro, G. (1969), "Liquefaction of Sands", Harvard Soil Mechanics Series, No. 81, Cambridge, Mass., January.

8. Cuellar, V. (1977), "A Simple Shear Theory for the One-Dimensional Behaviour of Dry Sand Under Cyclic Loading", Proceedings of DMSR 77, Karlsruhe, Vol. 2, Sept. 5-16, pp. 101-111.

9. Dafalias, Y.F. and Popov, E.P. (1976), "Plastic Internal Variables Formalism of Cyclic Plasticity", Journal of Applied Mechanics, 98(4), pp. 645-650.

10. Finn, W.D. Liam (1979), "Critical Review of Dynamic Effective Stress Analysis", Proceedings, 2nd U.S. National Conference on Earthquake Engineering, Stanford, Calif., August 22-24, pp.

11. Finn, W.D. Liam (1980), "Dynamic Response Analysis of Saturated Sands", State-of-the-Art volume, International Symposium on Soils Under Cyclic and Transient Loading, Swansea, Wales, January 7-11, John Wiley & Sons Ltd., London, (in press).

12. Finn, W.D. Liam and Bhatia, S.K. (1980), "Verification of Non-linear Effective Stress Model in Simple Shear", Accepted for publication, Proceedings, ASCE Special 2-Session Series, Hollywood-by-the-Sea, Florida, October 27-31, (in press).

13. Finn, W.D. Liam, Bhatia, S.K. and Pickering, D.J. (1980), "The Cyclic Simple Shear Test", State-of-the-Art volume, International Symposium on Soils Under Cyclic and Transient Loading, Swansea, Wales, January 7-11, John Wiley & Sons Ltd., London, (in press).

14. Finn, W.D. Liam and Bhatia, S.K. (1980), "Prediction of Seismic Pore-water Pressures", Accepted for publication, Proceedings, 10th International Conference on Soil Mechanics & Foundation Engineering (X.ICSMFE), Stockholm, Sweden, June 15-19, (in press).

15. Finn, W.D. Liam, Bransby, P.L. and Pickering, D.J. (1970), "Effect of Strain History on Liquefaction of Sand", Journal of the Soil Mechanics and Foundations Division, ASCE, Vol. 97, No. SM6, Proc. Paper 7670, November, pp. 1917-1934.

16. Finn, W.D. Liam, Lee, K.W. and Martin, G.R. (1976,1977), "An Effective Stress Model for Liquefaction", ASCE Annual Convention and Exposition, Philadelphia, Pa., Sept. 22-Oct. 1, 1976, Preprint 2752, also in Journal of the Geotechnical Engineering Division, ASCE, Vol. 103, No. GT6, Proc. Paper 13008, June 1977, pp. 517-533.

17. Finn, W.D. Liam and Martin G.R. (1980), "Soil as an Anisotropic Kinematic Hardening Solid", Accepted for publication, Proceedings, ASCE Special 2-Session Series, Hollywood-by-the-Sea, Florida, October 27-31, (in press).

18. Finn, W.D. Liam, Pickering, D.J. and Bransby, P.L. (1971), "Sand Liquefaction in Triaxial and Simple Shear Tests", Journal of the Soil Mechanics and Foundations Division, ASCE, Vol. 97, SM4, pp. 639-659.

19. Finn, W.D. Liam and Vaid, Y.P. (1977), "Liquefaction Potential from Drained Constant Volume Cyclic Simple Shear Tests", Proceedings, 6th World Conference on Earthquake Engineering, New Delhi, India, Session 6, pp. 7-12.

20. Finn, W.D. Liam, Vaid, Y.P. and Bhatia, S.K. (1978), "Constant Volume Cyclic Simple Shear Testing", 2nd International Conference on Microzonation, San Francisco, Calif., Nov. 26-Dec. 1, Vol. 2, pp. 839-851.

21. Florin, V.A. and Ivanov, P.L. (1961), "Liquefaction of Saturated Sandy Soils", Proceedings, 2nd International Conference on Soil Mechanics and Foundation Engineering, Vol. I, pp. 102-111.

22. Ghaboussi, Jamshid and Dikmen, Umit S. (1978), "Liquefaction Analysis of Horizontally Layered Sands", Journal of the Geotechnical Engineering Division, ASCE, Vol. 104, No. GT3, March, pp. 341-357.

23. Hardin, B.O. and Drnevich, V.P. (1972), "Shear Modulus and Damping in Soils" Design Equations and Curves", Journal of the Soil Mechanics and Foundations Division, ASCE, Vol 98, No. SM7, Proc. Paper 9006, July, pp. 667-692.

24. Ishibashi, I. and Sherif, M.A. (1974), "Liquefaction of a Loose Saturated Sand by Torsional Simple Shear Device", Soil Engineering Research Report No. 8, Department of Civil Engineering, University of Washington, Seattle, Washington.

25. Ishibashi, I., Sherif, M.A. and Tsuehiya, C. (1977), "Pore Pressure Rise Mechanism and Soil Liquefaction", Soils and Foundations, Vol. 17, No. 2, June, pp. 17-27.

26. Ishihara, K. and Takatsu, H. (1979), "Effects of Overconsolidation and k_o Conditions on the Liquefaction Characteristics of Sands", Soils and Foundations, Vol. 19, No. 4, pp. 59-68.

27. Ishihara, K., Tatsuoka, F. and Yasuda, S. (1975), "Undrained Deformation and Liquefaction of Sand Under Cyclic Stresses", Soils and Foundations, Vol. 15, No. 1, pp. 29-44.

28. Khosla, V.K. and Wu, T.H. (1976), "Stress-Strain Behaviour of Sand", Journal of the Geotechnical Engineering Division, ASCE, Vol. 102, No. GT4, Proc. Paper 12079, April, pp. 303-322.

29. Kishida, H. (1966), "Damage to Reinforced Concrete Buildings in Niigata Cith With Special Reference to Foundation Engineering", Soils and Foundations, Vol. VII, No. 1.

30. Kolbuszewski, J.J. (1948a), "An Experimental Study of the Maximum and Minimum Porosities of Sands", Proceedings, 2nd International Conference on Soil Mechanics and Foundation Engineering, Rotterdam, Vol. 1, pp. 158-165.

31. Kondner, R.L. and Zelasko, J.S. (1963), "A Hyperbolic Stress-Strain Formulation for Sands", Proceedings, 2nd Pan American Conference on Soil Mechanics and Foundations Engineering, pp. 289-324.

32. Lee, K.L. and Chan, K. (1972), "Number of Equivalent Significant Cycles in Strong Motion Earthquake", Proceedings, International Conference on Microzonation, October, Seattle, Wash., Vol. II, pp. 609-627.

33. Lee, K.W. (1975), "Mechanical Model for the Analysis of Liquefaction of Horizontal Soil Deposits", Ph.D. Thesis, University of British Columbia, Vancouver, Canada.

34. Liou, C.P., Streeter, V.L. and Richart, F.E., Jr. (1977), "Numerical Model for Liquefaction", Journal of the Geotechnical Engineering Division, ASCE, Vol. 103, No. GT6, Proc. Paper 12998, June, pp. 589-606.

35. Lucks, A.S., Christian, J.T., Brandow, G.E. and Hoeg, K. (1972), "Stress Conditions in NGI Simple Shear Test", Proceedings, ASCE 98, SM1, pp. 155-160.

36. Martin, G.R., Finn, W.D. Liam and Seed, H.B. (1974,1975), "Fundamentals of Liquefaction Under Cyclic Loading", Soil Mechanics Series, No. 23, Department of Civil Engineering, University of British Columbia, Vancouver, Canada, 1974, also in Journal of the Geotechnical Engineering Division, ASCE, Vol. 101, No. GT5, Proc. Paper 11284, May 1975, pp. 423-438.

37. Martin, P.P. and Seed, H.B. (1979), "Simplified Procedure for Effective Stress Analysis of Ground Response", Journal of the Geotechnical Engineering Division, ASCE, Vol. 105, No. GT6, Proc. Paper 14659, June, pp. 739-758.

38. Masing, G. (1926), "Eigenspannungen und Verfestigung beim Messing", Proceedings, 2nd International Congress of Applied Mechanics, Zurich, Switzerland.

39. Moussa, A.A. (1975), "Equivalent Drained-Undrained Shearing Resistance of Sand to Cyclic Simple Shear Loading", Geotechnique 25, No. 3, pp. 485-494.

40. Mroz, Z., Norris, V.A. and Zienkiewicz, O.C. (1978), "An Anisotropic Hardening Model for Soils and Its Application to Cyclic Loading", International Journal of Numerical and Analytical Methods in Geomechanics, 2:203-221.

41. Newmark, N.M. and Rosenblueth, E. (1971), Fundamentals of Earthquake Engineering, Prentice-Hall, Inc., Englewood Cliffs, N.J., pp. 162-163.

42. Ohsaki, Yorihiko (1966), "Niigata Earthquakes, 1964, Building Damage and Soil Conditions", Soils and Foundations, Vol. VI, No. 2, pp. 14-37.

43. Peacock, William H. and Seed, H. Bolton (1968), "Sand Liquefaction Under Cyclic Loading Simple Shear Conditions", Journal of the Soil Mechanics and Foundations Division, ASCE, Vol. 94, No. SM3, pp. 689-708.

44. Pickering, D.J. (1969), "A Simple Shear Machine for Soil", Ph.D. Dissertation, University of British Columbia, Vancouver, Canada.

45. Pickering, D.J. (1973), "Drained Liquefaction Testing in Simple Shear", Journal of the Soil Mechanics and Foundation Engineering Division, ASCE, Vol. 99, SM12, pp. 1179-1184.

46. Poorooshasb, H.B. (1971), "Deformation of Sand in Triaxial Compression", Proceedings, 4th Asian Regional Conference on Soil Mechanics and Foundation Engineering, Bangkok, Thailand, Vol. 1, pp. 63-66.

47. Pyke, R.M. (1973), "Settlement and Liquefaction of Sands Under Multidirectional Loading", Ph.D. Thesis, University of California, Berkeley.

48. Roscoe, K.H. (1953), "An Apparatus for the Application of Simple Shear to Soil Samples", Proceedings, 3rd International Conference on Soil Mechanics, Zurich, Switzerland, 1 2, pp. 186-191.

49. Schnabel, P.B., Lysmer, J. and Seed, H.B. (1972), "SHAKE: A Computer Program for Earthquake Response Analysis of Horizontally Layered Sites", Report No. EERC 72-12, Earthquake Engineering Research Center, University of California, Berkeley, December.

50. Schofield, A.N. and Wroth, C.P. (1968), Critical State Soil Mechanics, McGraw-Hill, London.

51. Seed, H.B. (1968), "Landslides During Earthquakes Due to Soil Liquefaction", Journal of the Soil Mechanics and Foundation Division, ASCE, Vol. 94, No. SM5, Proc. Paper 6110, September, pp. 1055-1122.

52. Seed, H.B. (1976), "Evaluation of Soil Liquefaction Effects on Level Ground During Earthquake", ASCE National Convention, Specialty Session, Liquefaction Problems in Geotechnical Engineering, Philadelphia, Pa., September, pp. 1-104.

53. Seed, H.B. and Idriss, I.M. (1967), "Analysis of Soil Liquefaction: Niigata Earthquake", Journal of the Soil Mechanics and Foundations Division, ASCE, Vol. 93, No. SM3, pp. 83-108.

54. Seed, H.B. and Idriss, I.M. (1971), "Simplified Procedure for Evaluating Soil Liquefaction Potential", Journal of the Soil Mechanics and Foundation Division, ASCE, Vol. 97, No. SM9, pp. 1249-1273.

55. Seed, H.B., Idriss, I.M., Makdisi, F. and Banerjee, N. (1975), "Representation of Irregular Stress Time Histories by Equivalent Uniform Stress Series in Liquefaction Analyses", Report No. EERC 75-29, Earthquake Engineering Research Center, University of California, Berkeley, October.

56. Seed, H.B., Mori, K. and Chan, C.K. (1977), "Influence of Seismic History on Liquefaction of Sands", Journal of the Geotechnical Engineering Division, ASCE, Vol. 103, No. GT4, Proc. Paper 12841, April, pp. 246-270.

57. Seed, H.B., Pyke, R.M. and Martin, G.R. (1979), "Effect of Multi-directional Shaking on Pore Pressure Development in Sand", Journal of the Geotechnical Engineering Division, ASCE, Vol. 104, No. GT1, Proc. Paper 13485, January, pp. 27-44.

58. Silver, M.L. and Seed, H.B. (1971), "Deformation Characteristics of Sands Under Cyclic Loading", Journal of the Soil Mechanics and Foundations Division, ASCE, Vol. 97, No. SM8, August, pp. 1081-1098.

59. Silver, M.L. and Seed, H.B. (1971), "Volume Changes in Sands During Cyclic Loading", Journal of the Soil Mechanics and Foundations Division, ASCE, Vol. 97, No. SM9, September, pp. 1171-1182.

60. Streeter, V.L., Wylie, E.B. and Richart, F.E. (1973), "Soil Motion Computations by Characteristics Method", Meeting Preprint 1952, ASCE National Structural Engineering Meeting, San Francisco, Calif., April.

61. Tatsuoka, F. and Ishihara, K. (1974), "Yielding of Sand in Triaxial Compression", Soils and Foundations, Vol. 14, No. 2, pp. 63-76.

62. Toki, S. and Kitago, S. (1974), "Effect of Repeated Loading on Deformation Behaviour of Dry Sand", Journal of the Japanese Society of Soil Mechanics and Foundation Engineering, Vol. 14, No. 1, pp. 95-103 (in Japanese).

63. Vaid, Y.P. and Finn, W.D. Liam (1979), "Effect of Static Shear on Liquefaction Potential", Journal of the Geotechnical Engineering Division, ASCE, Vol. 105, GT10, Proc. Paper 14909, pp. 1233-1246.

64. Valanis, K.C. (1971), "A Theory of Viscoplasticity Without a Yield Surface", Archivum Mechaniki Stosowanej, Vol. 23, No. 4, pp. 517-533.

65. Wood, D.M. and Budhu, M. (1980), "The Behaviour of Leighton Buzzard Sand in Cyclic Simple Shear Test", International Symposium on Soils Under Cyclic and Transient Loading, Swansea, Wales, January 7-11, Vol. 1, pp. 9-21.

66. Wood, D.M., Drescher, A. and Budhu, M. (1979), "On the Determination of the Stress State in the Simple Shear Apparatus", Submitted for publication.

67. Youd, T.L. (1972), "Compaction of Sands by Repeated Shear Straining", Journal of the Soil Mechanics and Foundations Division, ASCE, Vol. 98, No. SM7, July, pp. 709-725.

68. Youd, T.L. and Craven, T.N. (1975), "Lateral Stress in Sands During Cyclic Loading", Journal of the Geotechnical Engineering Division, ASCE, Vol. 100, GT2, Technical Note, February, pp. 217-223.

69. Zienkiewicz, O.C., Chang, C.T. and Hinton, E. (1978), "Non-linear Seismic Response and Liquefaction", International Journal for Numerical and Analytical Methods in Geomechanics, Vol. 2, pp. 381-404.

APPENDIX I

DESCRIPTION OF THE CYCLIC SIMPLE SHEAR APPARATUS AND SAMPLE PREPARATION

Description of the Cyclic Simple Shear Apparatus

The University of British Columbia's (UBC) simple shear apparatus is an improved version of the apparatus originally designed by Roscoe (1953). The simple shear apparatus consists of horizontal carriage, vertical carriage and body frame with a sample of dimensions, 5.08 x 5.08 x 2.78 cm. The UBC simple shear apparatus was designed by Pickering (1969) and detailed description of components are given by Finn et al. (1970). In Plate I-1, the UBC cyclic simple shear apparatus is shown.

The most recent advances in the cyclic simple shear apparatus is the development of the constant volume cyclic simple shear test by Finn and Vaid (1977). In evaluating the results of cyclic loading tests on saturated sands carried out under undrained conditions, it is assumed that no volume changes occur during the test. However, compliance in the test system allows volume expansion to occur in the supposedly constant volume saturated sample. This volume change, having the same effect as partial drainage, decreases the tendency for the porewater pressure to rise during cyclic loading. Therefore, undrained tests overestimate the resistance to liquefaction. Finn and Vaid (1977) showed that the error due to system compliance are always on the unsafe side and may range up to 100%.

During this study, an alternative procedure for determining

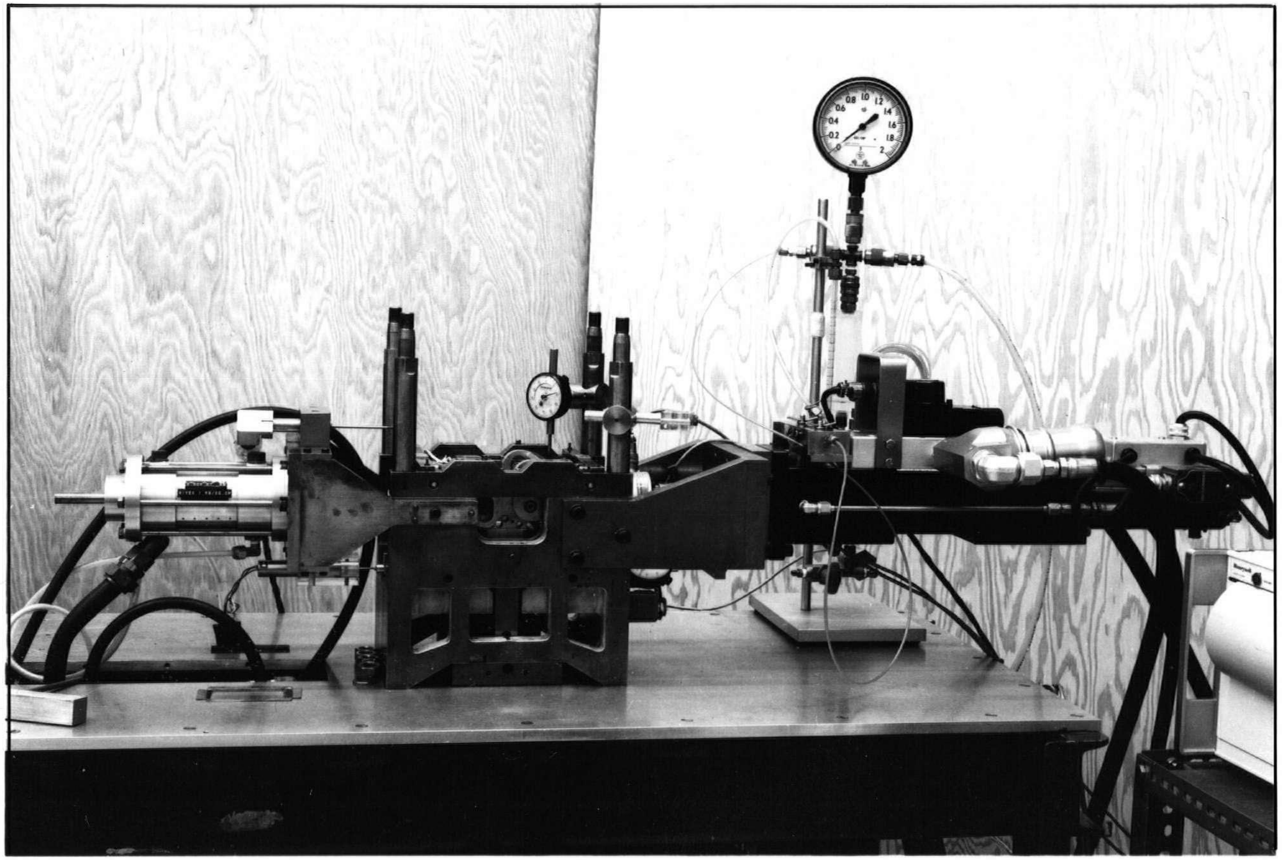

Plate I-1 Cyclic simple shear apparatus

the undrained behaviour of sand, ie., constant volume tests on dry sands are performed. In these tests, the change in confining pressure to maintain constant volume are equivalent to the changes in porewater pressure in the corresponding test. Finn et al. (1978) have shown that tests performed on dry and saturated sands gave exactly the same results, hence, in this research all tests were performed on dry sands.

The modified apparatus is shown in Fig. I-1 and Plate I-2. The two components of linear horizontal strain are identically zero in this simple shear apparatus. Thus, a constant volume condition is achieved by clamping the loading head to prevent vertical strain. A horizontal reaction plate is clamped to four vertical posts which are threaded into the body of the simple shear apparatus. Thus, a constant volume condition is achieved by clamping the loading head and carrying on its upper side a heavy loading bolt which passes through a central hole in the reaction plate.

The desired vertical pressure on the sample is applied by tightening the loading bolt nut on the underside of the reaction plate. Simultaneously, the loading head is clamped in position by tightening the loading bolt nut on the top side of the reaction plate. Another important innovation was the incorporation of two small stiff pressure transducers (350 kPa capacity and full scale deflection of 0.0015 cm) on one of the moveable lateral boundaries in order to monitor the lateral stresses during cyclic loading.

Maximum gross volume change introduced at the onset of liquefaction in this so called constant volume test is very small and arises as a result of the recovery of elastic deformation in the vertical loading components when the load on the clamped loading head is reduced to zero.

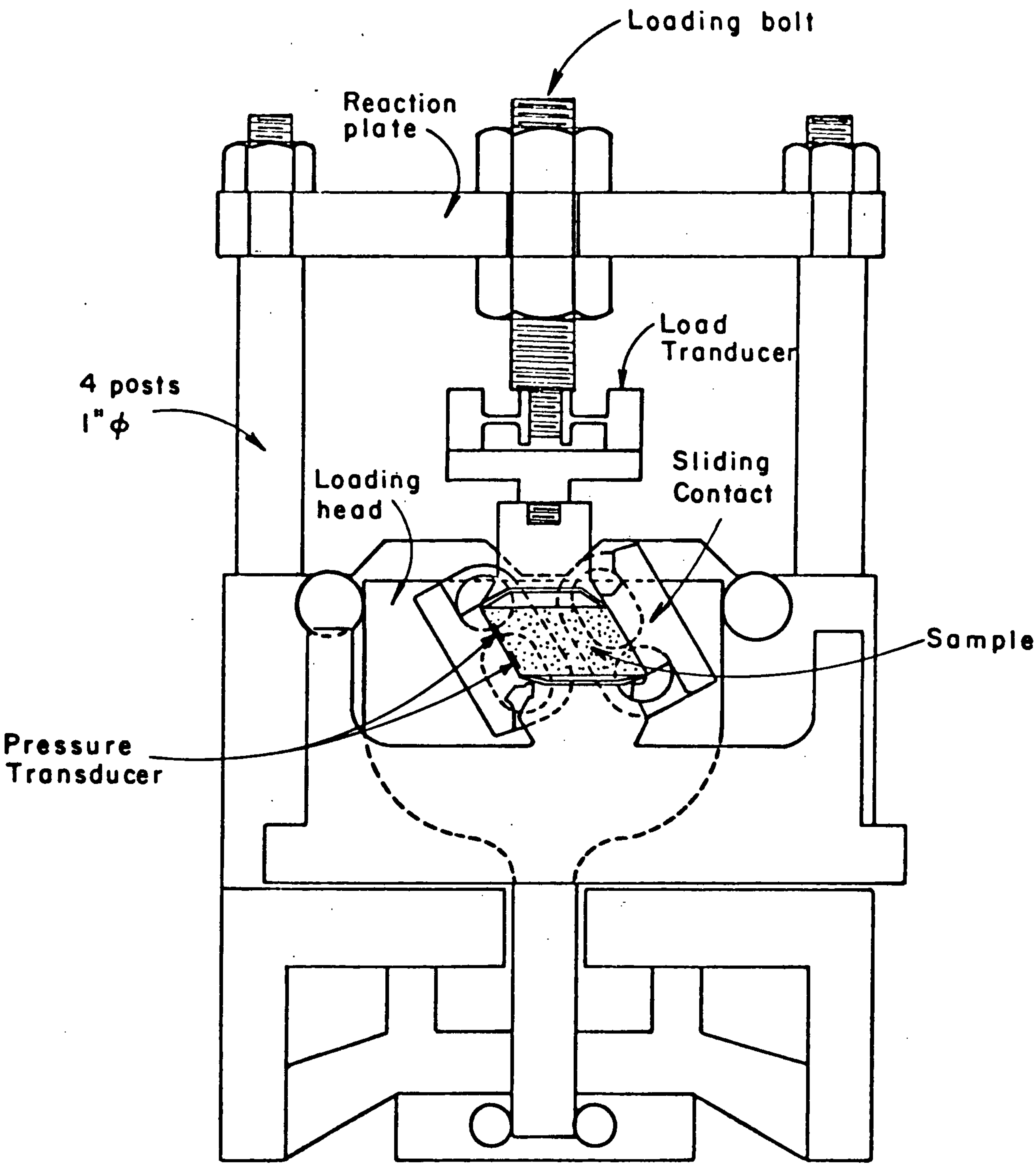

FIG. I-1 Constant Volume Cyclic Simple Shear Apparatus.

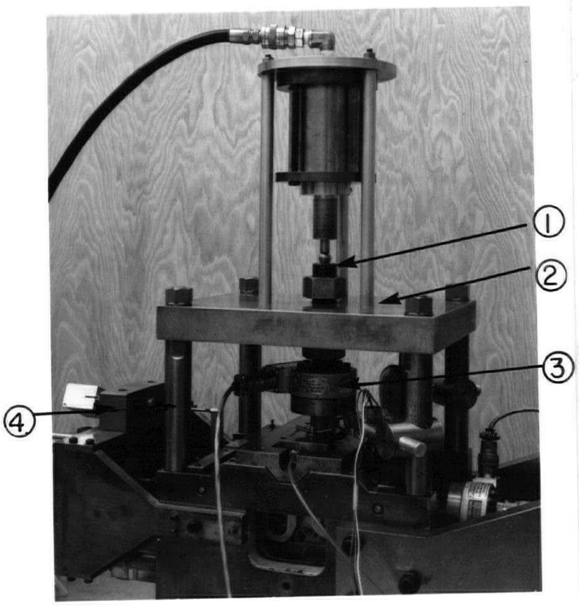

Plate I-2 Constant Volume Simple

① Loading Bolt

② Reaction Plate

③ Load Transducer

④ 4 Posts on 7"x 9" Rectangle

The use of a thick reaction plate, heavy vertical posts and loading bolt, and a very stiff load transducer reduces the vertical movement of the clamped head to a negligible amount. For liquefaction tests with initial σ'_{vo} = 196 kN/m^2 this movement amounted to a maximum of 5 x 10^{-4} cm which was only 5% of the movement of the floating head due to the system compliance in liquefaction tests on saturated undrained samples in the same equipment and is equivalent to a total vertical strain of the order of 0.02%.

Recently, Finn, Bhatia and Pickering (1980) presented a complete analysis of the UBC simple shear apparatus including the effect of the boundary conditions on the test results.

Method of Sample Preparation

The tests conducted for this research were performed on dry sand samples. To prepare a sample with the cyclic simple shear apparatus, the membrane mounted was clamped to the pedestal by the bottom plate (which was inside the membrane) and the rubber membrane was held wide open by metal hooks as shown in Plate I-3. A weighted amount of dry sand was deposited within the membrane in the apparatus through a funnel top permitting a freefall. However, to achieve very loose samples, the height of fall of the sand particles was kept at 1 cm and the funnel was gradually raised as the sand was poured within the membrane. The funnel was transformed across the plane area of the sample so that the sand surface remained almost level. Kolbuszewski (1948) has shown that the density achieved by pluvial compaction such as this depends on the intensity of the rain of sand particles, higher intensities yielding lower densities. Since the aim was to make identical and loose samples for each specimen the total pouring time was one minute. By this process, it was possible

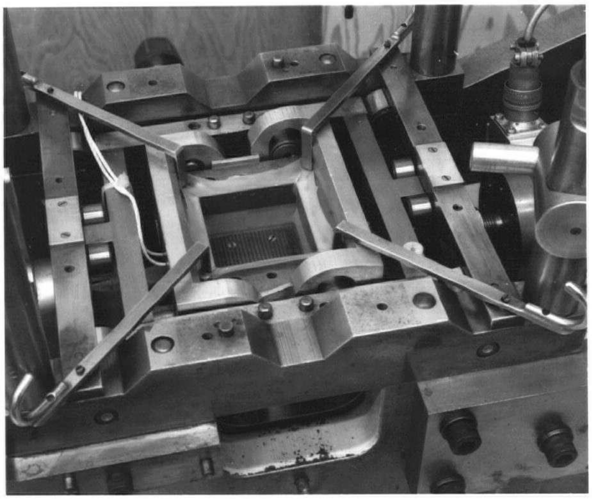

Plate I-3 Membrane streched out

Plate I-4 Placing top plate on sand sample

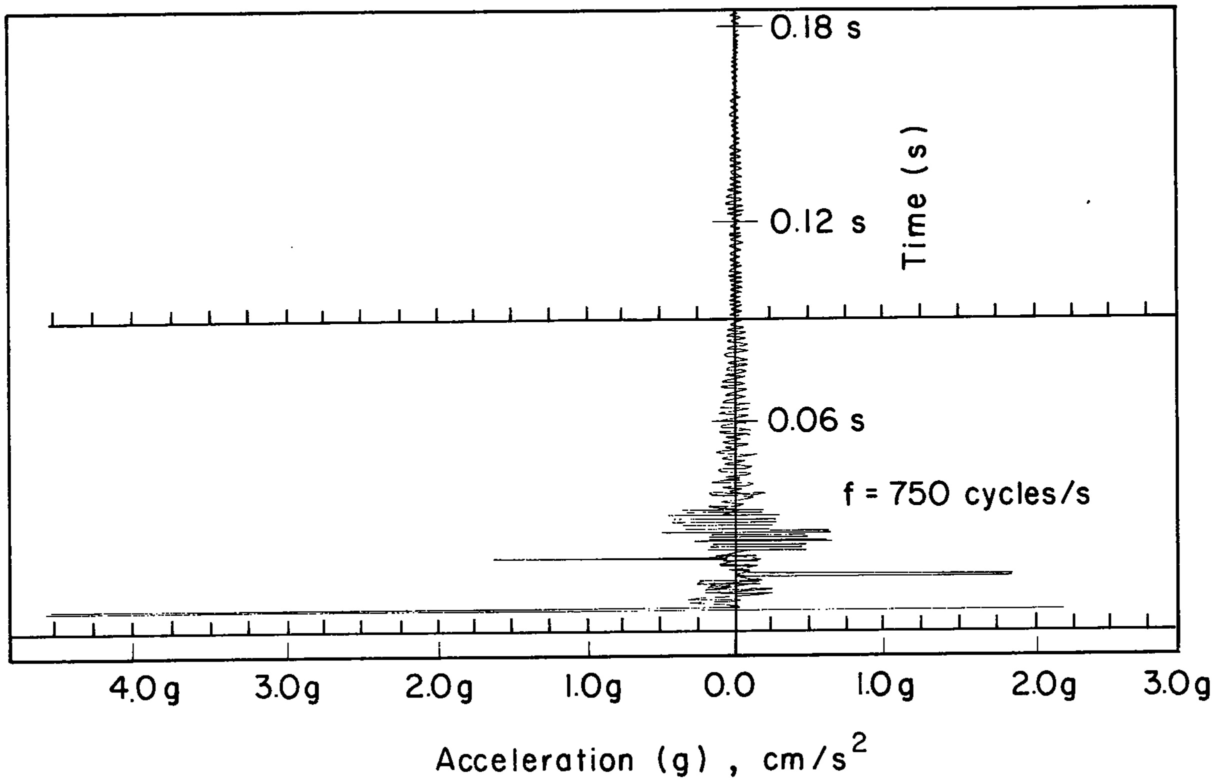

FIG. I-2 Vibrations Applied to Sand Sample.

to prepare a sample of relative density of 32 to 35% for Ottawa sand.

Once the sand had been poured, the excess sand over the final elevation was siphoned off using a small vacuum. The top ribbed plate was then placed on the sand surface (Plate I-4) and extra sand particles sandwiched between the plate and rubber membrane were sucked in. Then, the rubber membrane was closed over it and sealed to the loading head. The desired final relative density was then obtained by hitting the simple shear apparatus bed with a plastic hammer. By this method, the sample was subjected to high frequency vibrations (Fig. I-2) and these vibrations were applied when the sample was kept under a seating pressure of approximately 0.2 kg/cm^2.

The top ribbed plate resting on top of the sand sample thus follows the settlement of the sand surface and resumes a proper seating, while the entire sample gets uniformly densified without development of a loose thin layer at the top of the sample. Finn, Vaid and Bhatia (1978) showed that the development of a thin layer on top of the sample underestimates the liquefaction potential for sand samples.

The vertical confining pressure was then increased to the required value of the overburden pressure and during consolidation lateral stresses (pressure transducers from top and bottom) were recorded.

Tests Performed

For this research the following types of tests were performed:

1. Drained test under cyclic strain controlled and cyclic stress controlled conditions;
2. Constant volume test under cyclic strain controlled and cyclic stress controlled conditions;

3. Static unloading tests in simple shear apparatus and consolidation equipment.

For cyclic loading tests, both for drained and undrained tests, cyclic stress and strains were applied by an MTS servo-controlled electro-hydraulic piston using a sinusoidal waveform at a frequency of 0.2 Hz. During each test vertical stress, lateral, stress, cyclic shear stress and cyclic shear strain were continuously monitored with electronic transducers and records obtained on chart recorders. In Plate I-5, the cyclic simple shear appartus is shown with all recording equipments.

To measure the static unloading curve for the sand sample consolidated to initial vertical confining stress, vertical was decreased in small increments and recovered volumetric strains were measured. To completely unload the sample in the simple shear apparatus (since wt. of the loading frame was 0.396 kg/cm^2), a double-acting piston was used (Plate I-6).

Most of the tests were on Ottawa sand at relative densities of D_r = 45,54,60 and 68%. Tests were on Crystal Silica and Toyoura sands at D_r = 45%. In most of the tests, the samples were consolidated to initial vertical confining pressure σ'_{vo} = 200 kN/m^2 but a few tests were also performed at σ'_{vo} = 100 kN/m^2 and 300 kN/m^2.

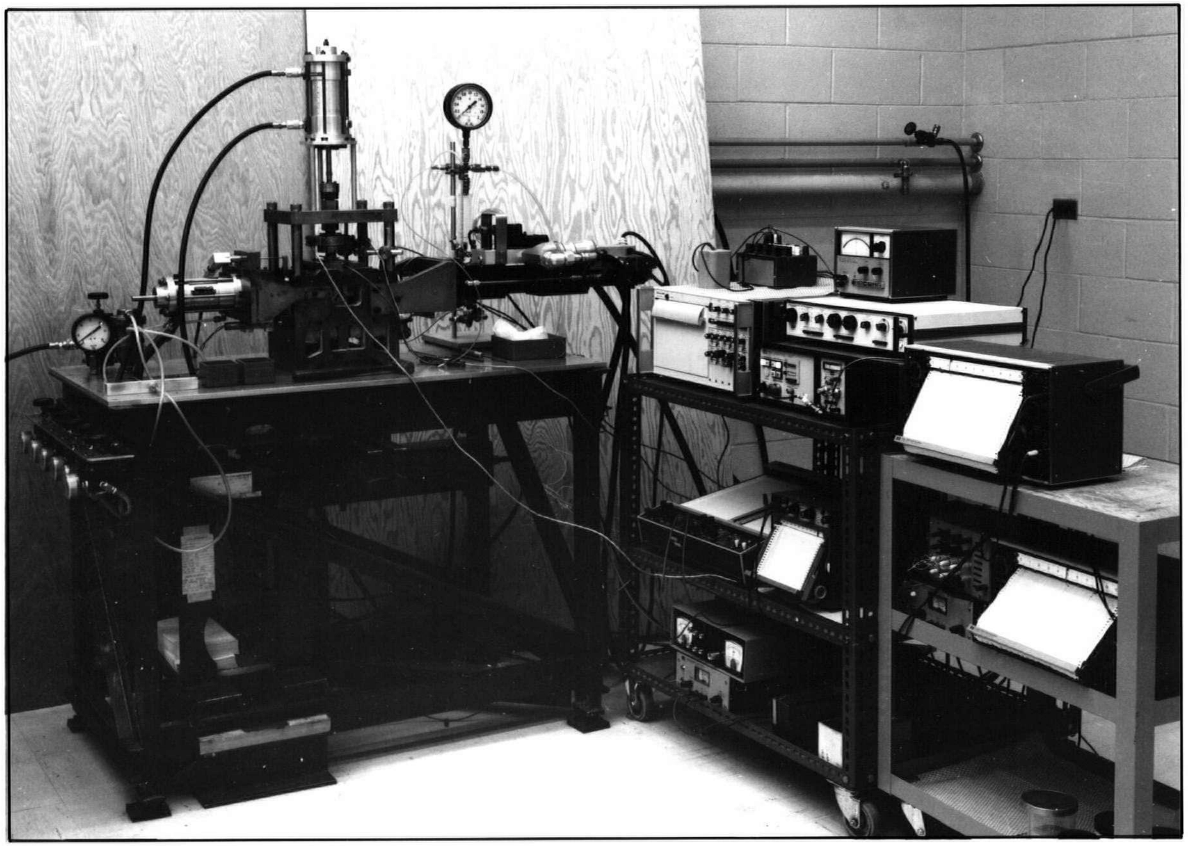

Plate I-5 Cyclic simple shear apparatus with recording equipments

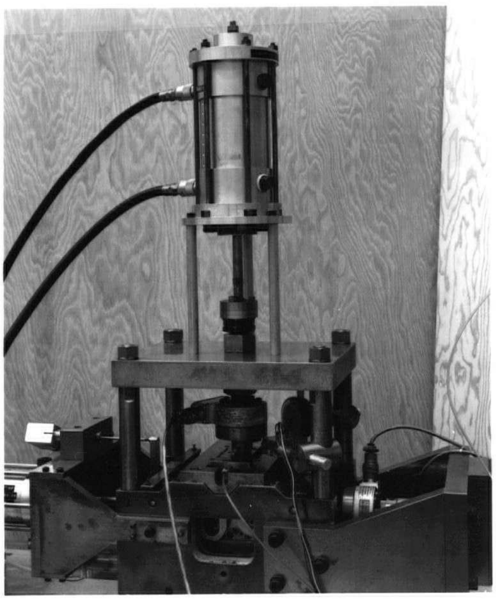

Plate I-6 Set up with double acting piston to measure static rebound modulus

APPENDIX II

PHYSICAL PROPERTIES OF OTTAWA SAND (C-109), CRYSTAL SILICA SAND (NO. 20) AND TOYOURA SAND

Most of the tests were performed on Ottawa Sand (C-109). This is a natural Silica Sand consisting of round to subround particles as shown in Plate II-1. Grain size distribution curve and physical properties of the sand are given in Fig. II-1 and Table II, respectively. This sand has been tested by Finn et al. (1971) to relate behaviour of saturated sand in cyclic simple shear and cyclic triaxial. Finn and Vaid (1977) used it for constant volume simple shear tests.

The maximum void ratio was determined in accordance with ASTM D2049-69 and minimum void ratio was obtained by the Kolbuszewski (1948) method.

Crystal Silica Sand (No. 20) is a uniform angular quartz sand. Silver and Seed (1971) used this sand and physical properties listed in Table II-a were obtained from that reference.

Toyoura Sand is the most widely used sand in Japan for research purposes. This sand consists of quartz (80%), chert (30%) and feldspar (17%) and particles are subangular to angular (Plate II-1).

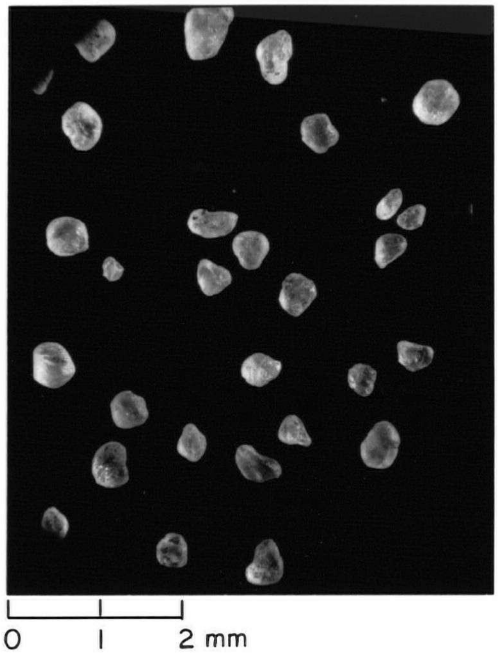

Ottawa sand (C-109)

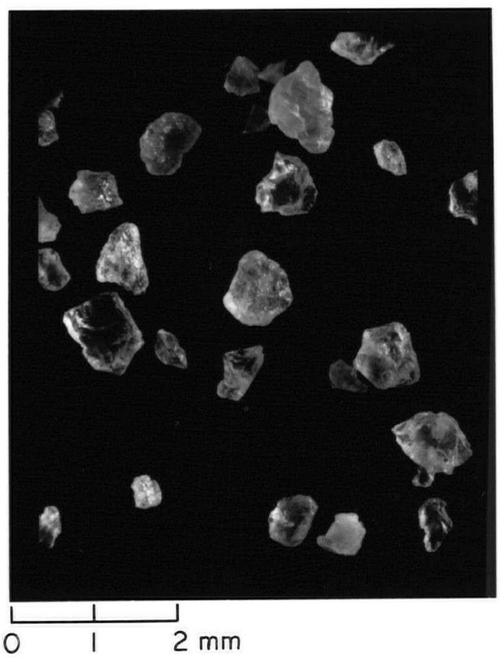

Crystal silica sand No. 20

Plate II-1

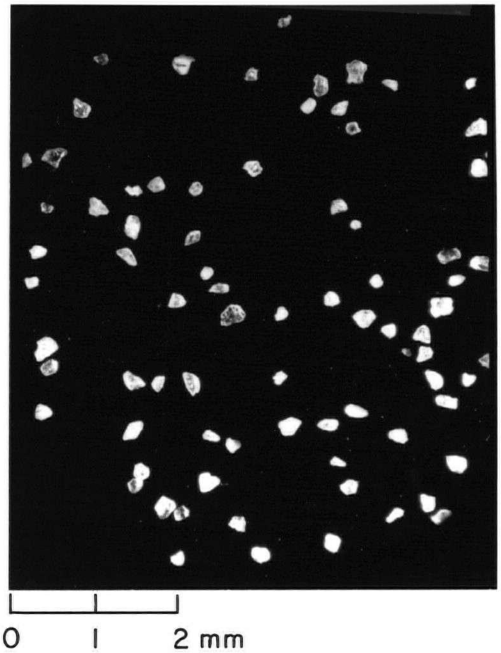

Toyoura sand

GRAIN SHAPE

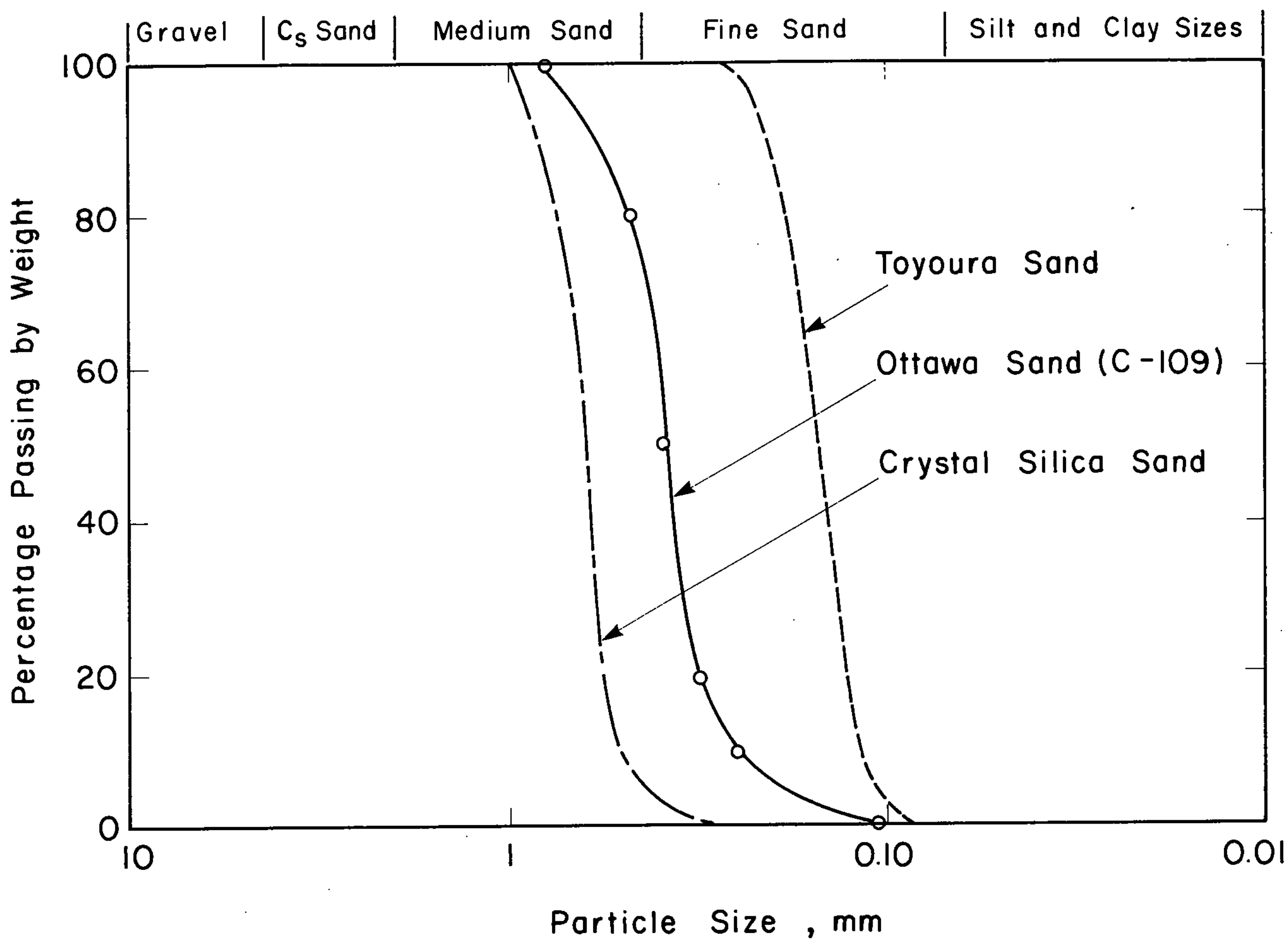

FIG. II-1 Particle Size Distribution of Soils Used in the Tests.

TABLE II-1

PROPERTIES OF SANDS

SAND TYPE	OTTAWA (ASTM C-109)	CRYSTAL SILICA SAND	TOYOURA SAND
GRAIN SIZE	D_{60} = 0.40 mm D_{10} = 0.19 mm	D_{60} = 0.65 mm D_{10} = 0.52 mm	D_{60} = 0.16 mm D_{10} = 0.11 mm
GRAIN SHAPE	Subround to Round	Subangular to Angular	Subangular
UNIFORMITY COEFFICIENT, c_u	2.10	1.25	1.44
SPECIFIC GRAVITY, G_s	2.67	2.65	2.65
MAXIMUM VOID RATIO, e_{max}	0.82*	0.973	0.960
MINIMUM VOID RATIO, e_{min}	0.50	0.636	0.64

*Ishibashi and Sherif (1974) reported e_{max} = 0.76 for the same sand.

APPENDIX III

ENDOCHRONIC REPRESENTATION OF VOLUMETRIC STRAINS

In this appendix volumetric strain, ε_{vd}, obtained under constant strain cyclic loading in the simple shear condition for loose Ottawa sand will formulate in endochronic form. The purpose of this formulation is two-fold: firstly, to check whether volumetric strain can also be presented as a continuous function of the drainage parameter; secondly, if so, to check whether this simple formulation can be used to calculate volumetric strain, hence settlement for the irregular strain history encountered by soil during an earthquake.

III-1 Endochronic Formulation of Volumetric Strains

The volumetric strains generated in cyclic simple shear at various constant strain amplitudes ranging from $\gamma = 0.056\%$ to $\gamma = 0.314\%$ are shown in Fig. III-1 versus the number of load cycles N. Definition of length of strain path, ξ, is again assumed as given in equation (6.1). Thus, for simple shear conditions, $d\xi$ is given by equation (6.2). The data shown in Fig. III-2 is plotted against the length of the strain path, ξ. We again seek a transformation, exactly of the same form as equation (6.8), where the transformation factor, λ, is defined by equation (6.9). When equation (6.9) is applied to the data shown in Fig. III-1, a range of values for λ results with a mean value of 5.71. Using this average value of λ, the data in Fig. III-2 is transformed to ζ*-space, where ζ is again called the damage parameter, and transformed results are plotted in

*For the pore pressure transformation, the symbol used for damage parameter is κ. In order to differentiate the numerical values of damage parameter for volumetric strain to that of porewater pressure for the same sand at the same relative density, the symbol ζ is referred to as damage parameter in section 6.3.

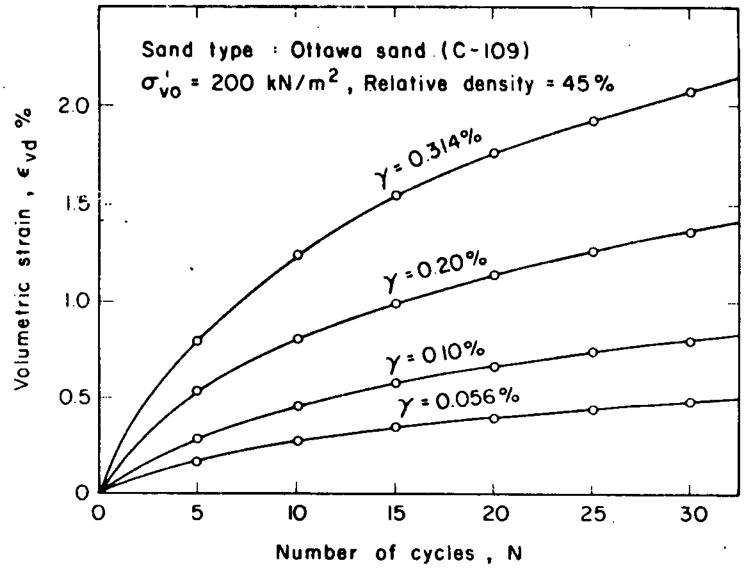

FIG. III-1 Volumetric Strain vs. Strain Cycles for Ottawa Sand.

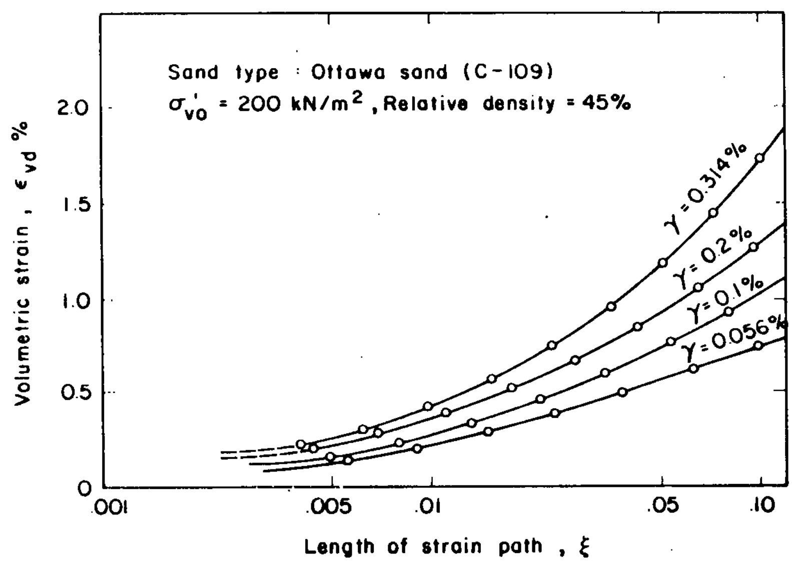

FIG. III-2 Volumetric Strain vs. Natural Logarithm of Length of Strain Path for Ottawa Sand.

Fig. III-3. Experimental data plotted in Fig. III-4 for various shear strain amplitudes lie in a very narrow band. The same data are plotted on a natural scale where a nonlinear least square curve fitting method has been used to define the analytical curve

$$\varepsilon_{vd} = \zeta(D_1\zeta + CD) \; / \; (A_1\zeta + B_1) \qquad \text{(III-1)}$$

with $A_1 = 0.078$, $B_1 = 0.0038$, $C_1 = 0.0716$ and $D_1 = 0.138$. Although it is quite evident that volumetric strain obtained for a type of sand and relative density under constant cyclic strain can be represented as a unique function of damage parameter, ζ, it seem appropriate that the inverse transformation as discussed in section 6.2.2 should again be applied. Hence, the inverse transformation is performed to transfer points back as shown in Figs. III-1 and III-2. In Figs. III-5 and III-6 both analytical and experimental volumetric curves are shown in ξ-space and N-space which show that the unique relationship between volumetric strain and damage parameter ζ as given in equation (III-1) represents experimental data correctly.

It should be emphasized that the relationship given in equation (III-1) represents not just the four curves shown in Fig. III-1 but any test curve that might be determined within the same range. Finn (1979) presents an endochronic formulation of volumetric strain obtained for Nakashima sand and some details about the endochronic formulation of volumetric strain data are discussed by Finn and Bhatia (1980).

III-2 Verification of the Endochronic Representation of Volumetric Strain

In order to check the validity of volumetric strain given by equation (III-1), the formulation is used to calculate volumetric strains in drained stress controlled tests on Ottawa sand. In drained stress controlled tests with a continuous application of cyclic shear stress, shear

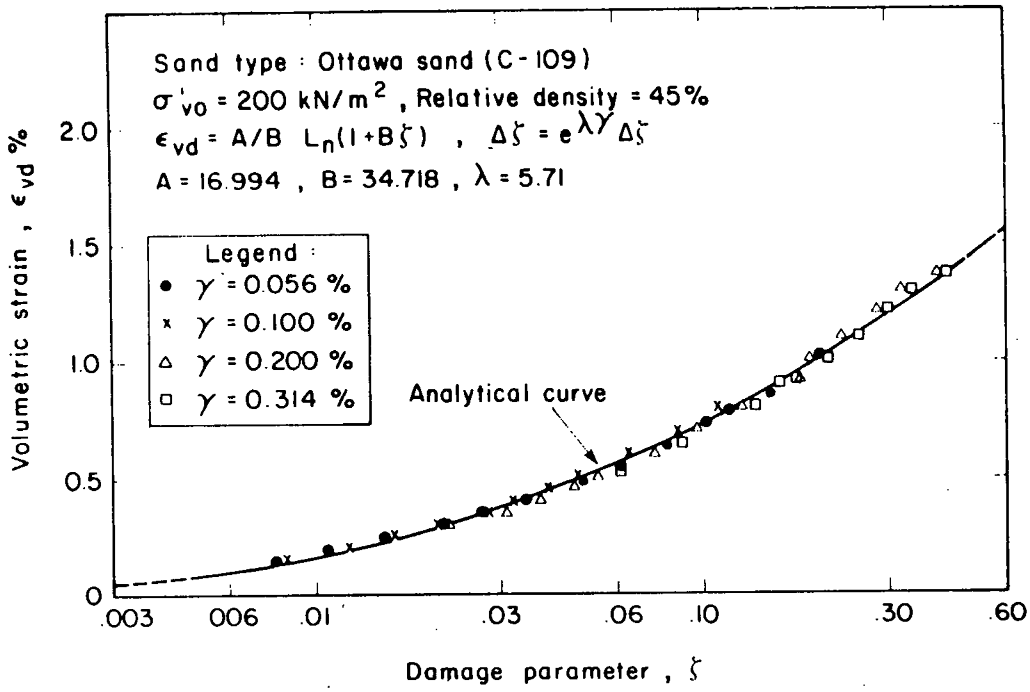

FIG. III-3 Volumetric Strain vs. Ln (Damage Parameter) for Ottawa Sand.

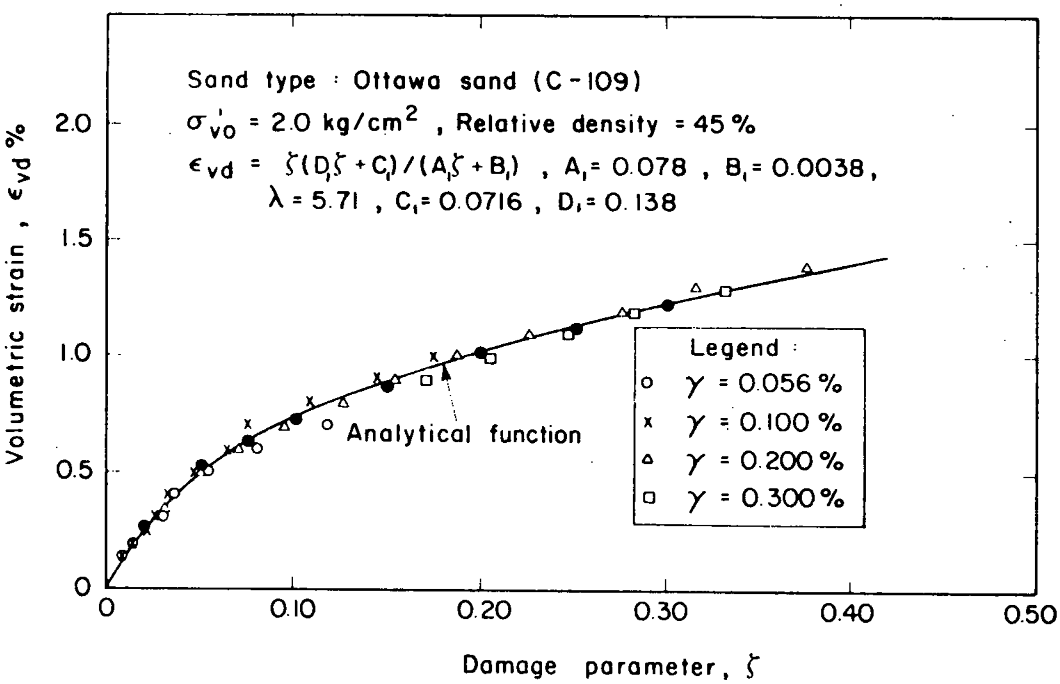

FIG. III-4 Volumetric Strain vs. Damage Parameter for Ottawa Sand.

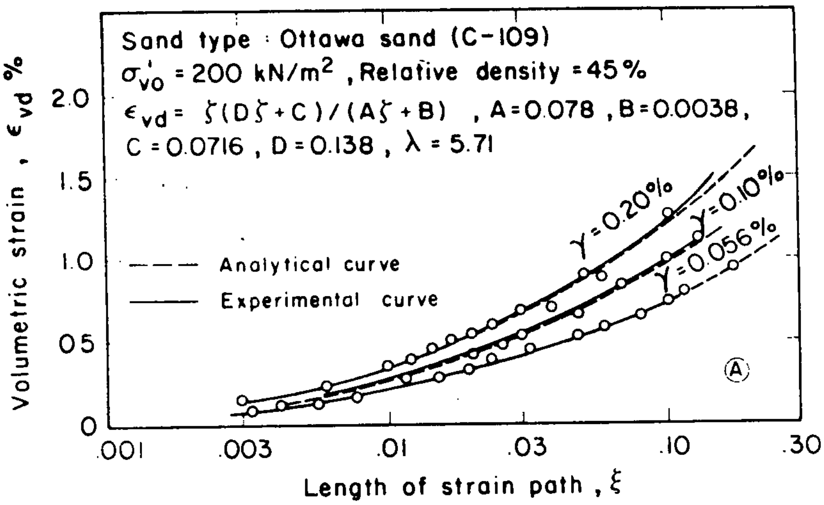

FIG. III-5 Comparison of Computed and Experimental Volumetric Strains in ξ-plot.

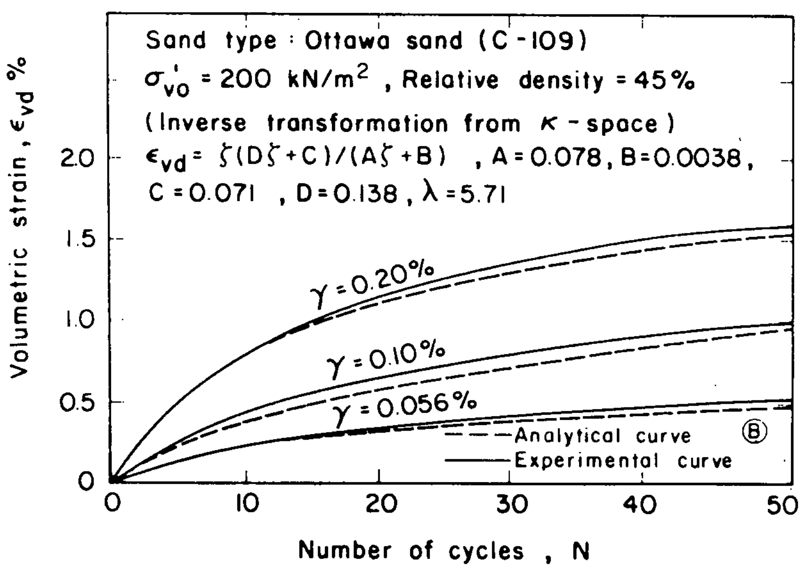

FIG. III-6 Comparison of Computed and Experimental Volumetric Strains in N-plot.

strain decreases as shown in Fig. III-7 for two stress ratios, τ/σ'_{vo} = 0.146 and τ/σ'_{vo} = 0.119. This condition is obviously different from the original test condition that supplied the data for the endochronic formulation.

For the present analysis, average shear strains are calculated for each cycle as shear strains generated in each half cycle are different. Shear strain for each cycle is converted to incremental length of strain path and the incremental damage parameter generated for the cycle is calculated. The cumulative damage parameter is used in equation (III-1) with the set of constants given for Ottawa sand to calculate the total volumetric strain. The analytical and experimental volumetric strains plotted in Fig. III-8 for two cyclic stress ratios show that fairly good predictions of volumetric strains can be made by the endochronic formulation of volumetric strain data. Some discrepancy in the experimental and analytical results in Fig. III-8 may be attributed to the fact that the endochronic formulation used for an analysis corresponding to D_r = 45% whereas the stress controlled tests have been performed at D_r = 47%.

The volumetric strains represented in endochronic form can be used in conjunction with dynamic rebound modulus for the pore pressure prediction. In addition, such a formulation can be used to calculate settlements.

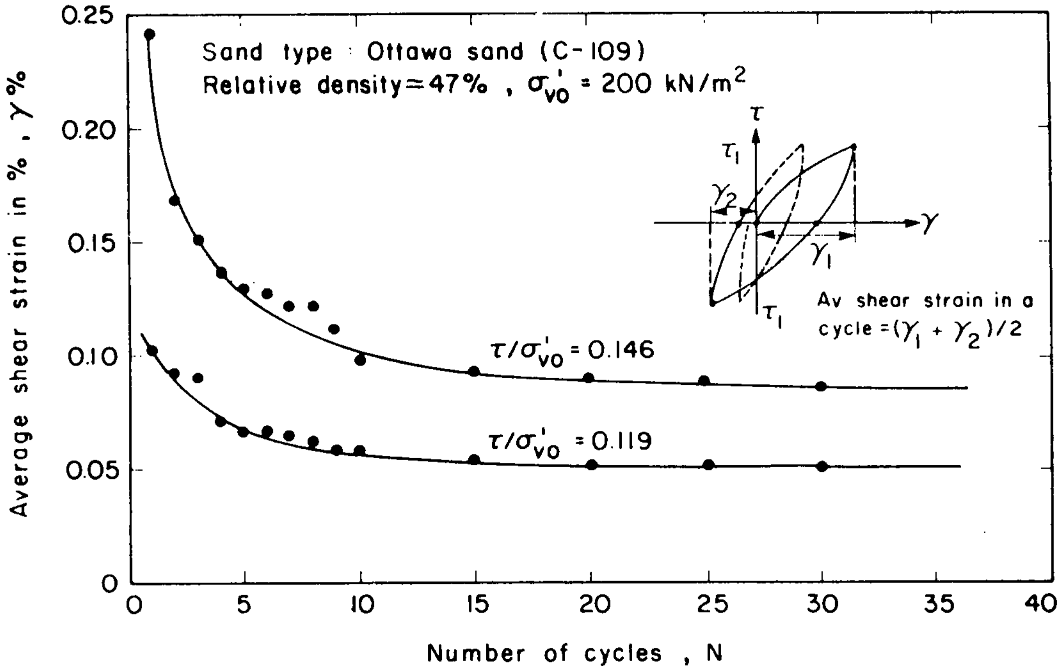

FIG. III-7 Av. Shear Stress vs. Number of Cycles for Constant Stress Drained Test.

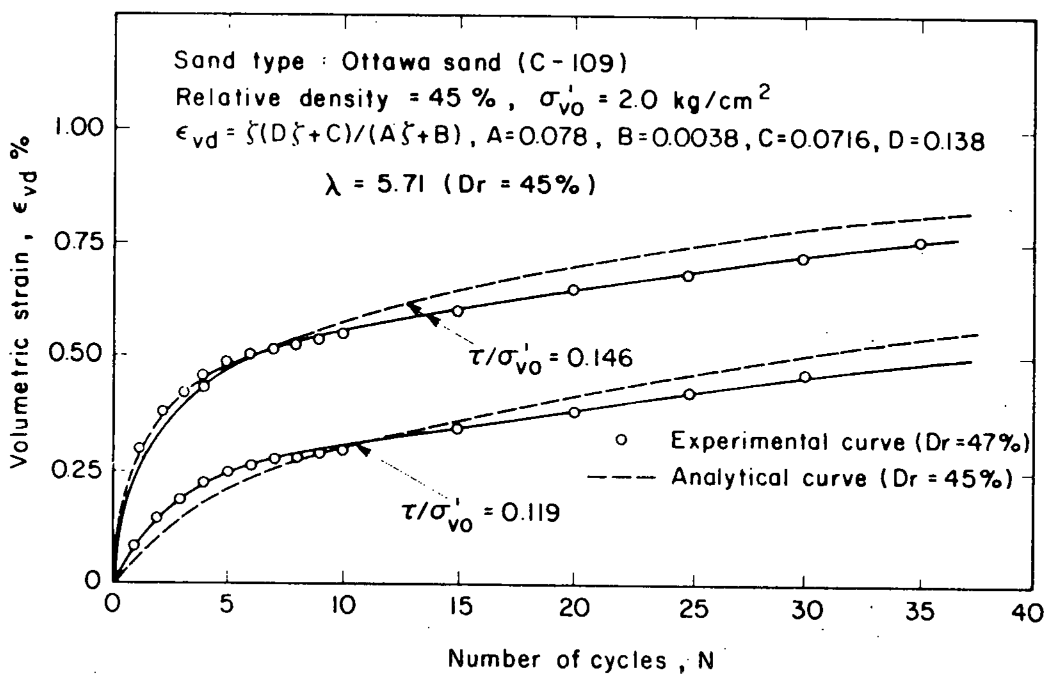

FIG. III-8 Comparison of Calculated and Experimental Volumetric Strains.